Eliashberg Theory in the weak-coupling limit:
Results on the real frequency axis

by

Sepideh Mirabi

A thesis submitted in partial fulfillment of the requirements for the degree of

Master of Science

Department of Physics

University of Alberta

ABSTRACT

One of the theoretical mechanisms for accurately describing superconductivity is the electron-phonon interaction. This attractive interaction occurs between two electrons near the Fermi surface and leads to gapped quasi-particle states. The equations describing the mean-field properties are called the Eliashberg equations. By accounting for the frequency of phonons, it follows that the interaction within Eliashberg theory is retarded in time and local in space. In the BCS theory of superconductivity, however, the nature of the interaction is instantaneous in time.

The dynamical nature of the order parameter in Eliashberg theory is the foremost difference with the order parameter in the BCS counterpart. The motivation for this thesis is to explore this disparity, with a particular emphasis on the nature of the weak-coupling limits of the two variant theories. In this thesis, both the numerical solution and analytical approximation for the Eliashberg theory on the real frequency axis are evaluated in the weak electron-phonon coupling limit. To first order in the weak-coupling limit, the analytical solution is shown to agree well with the numerical result. Previous literature has shown that the weak-coupling limit of the BCS and Eliashberg theories do not converge to the same result, and moreover there exists a difference of $1/\sqrt{e}$ between the critical temperatures of the two theories. Here, we have extended this result further to investigate the behaviour of the zero-temperature gap edge on the real frequency axis. This quantity is analytically solved on the real axis under certain approximations, and it is found that there exists the same pre-factor of $1/\sqrt{e}$ in the zero-temperature gap edge as observed in the critical temperature in the Eliashberg theory. Remarkably, in the weak-coupling limit, the ratio of these two quantities therefore approaches the same universal value as obtained in the BCS theory.

In chapter one, a brief development of the history of the BCS and Eliashberg theories is given. In chapter two, a full derivation of the Eliashberg equations is included, based on solving the time development of the Green's functions. The Green's function can be evaluated on either the imaginary or real frequency axes. It is much more convenient to use the Matsubara formalism, especially when performing the numerical calculations. However, most of the dynamical and physical properties are determined on the real axis. By implementing the correct analytical continuation procedure on the real axis, we recover the results on the imaginary frequency axis.

In chapter three, the imaginary axis Eliashberg equations are considered, first in the case where the renormalization factor is included, and then in the case where it is neglected. The critical temperature is calculated using the linearized gap function. Also, the analytical solution using digamma expressions for the gap function is provided both on the real and imaginary frequency axes.

In chapter four, the numerical solutions on the real and imaginary axes in the zero-temperature, finite-

temperature, and critical-temperature limits are studied.

Finally, in chapter five the thermodynamic properties of superconductors are studied. The free energy, heat capacity and the critical magnetic field are considered using both BCS and Eliashberg theories. It is shown that the heat capacity ratio at the critical temperature of both theories are identical, and in the zero-temperature limit in the Eliashberg theory the free energy has a correction factor of $(1/\sqrt{e})^2$ compared to its BCS counterpart.

ACKNOWLEDGMENT

CONTENTS

LIST OF FIGURES

vii

LIST OF TABLES

I. INTRODUCTION

The superconducting state is a macroscopic quantum phenomenon observed in many conductors in the low-temperature limit. In 1950, two separate experiments with an isotope of mercury provided evidence that the electron-phonon interaction plays a significant role in superconductivity [1]. The critical temperature depends on the average isotope mass as $M^{-\beta}$, where $\beta = -d(\ln T_c)/d(\ln M)$ [2, 3]. In 1957, Bardeen, Cooper, and Schrieffer [4] gave the first theoretical explanation for superconductivity that agreed with experiment and it is now commonly known as BCS theory. This phenomenon occurs due to the presence of an attractive interaction of the spin-up and spin-down electrons on the opposite sides of the Fermi surface, which bind together to form a zero-momentum bound state known as a Cooper pair. These Cooper pairs open up a gap in the excitation spectrum. The BCS theory describes the phenomenology of superconductivity, however, it does not account for the retardation of the electron-phonon interaction.

When an electron moves in a crystal lattice, a deformation of the ions ensues; the electronic polarization will then be created as a result of the attraction between the positive ions and the electron, after which the electron scatters away. A second electron will be attracted to this region, and since the ions are more massive, it takes a longer time for them to return to their equilibrium position. Therefore, the time scale[1] of the electronic Coulomb interaction is of the order of ϵ_F^{-1} whereas the electron-phonon interaction is of the order of ω_{ph}^{-1} [5]. This retardation effect is tantamount to the first electron being attracted to the second one. The finite time it takes for the ions to be displaced from their equilibrium positions is proportional to the inverse of the phonon frequency. As a matter of fact, the lower the phonon frequency value is, the longer the time it takes for the ions to reach their equilibrium position. Taking into account the frequencies of phonons in the superconducting system shows that the interaction is not static but dynamical and retarded. The most natural way of satisfactorily dealing with the retardation is to invoke a field-theoretical description of the phonons in the Hamiltonian [1, 6].

The electron-phonon interaction in superconductors leads to a mass enhancement of the electrons near the Fermi level and a short lifetime for the quasi-particle. In several metals these effects are robust and the quasi-particle damping effect is comparable to their energies [7]. As a result, the well-described quasi-particle does not exist anymore.

In 1958, Migdal [8] applied the Feynman-Dyson perturbation theory to derive an approximate solution for the problem of electron-phonon interaction. Migdal's rationalization is based on the fact that the higher-order vertex corrections are of the order of $\omega_{ph}/\epsilon_F \sim \sqrt{m/M} \sim 10^{-2}$, where M is the mass of the ions and m is the mass of the electron. In 1960, Nambu [9] and Eliashberg [10] derived a formalism that leads to an appropriate solution when phonons are present in the Hamiltonian. Eliashberg derived a pair of coupled integral equations for the complex gap function and mass renormalization function for the superconducting state in the zero-temperature limit [1]. The finite-temperature case was also considered by Eliashberg.

In 1964, Ambegaokar and Tewordt [11], and then subsequently in 1965 Scalapino et al. [12], developed a formalism for the finite-temperature gap function $\Delta(\omega; T)$. In 1968, McMillan [13] found the superconducting transition temperature by constructing an approximate equation which is given as

$$T_c = \frac{\omega_D}{1.45} \exp\left[-\frac{1.04(1 + \lambda)}{\lambda - \mu^*(1 + 0.62\lambda)} \right]. \tag{1.1}$$

Equation (1.1) makes a connection between the transition temperature, the electron-phonon coupling and Coulomb coupling constants. This is one of the most useful relations for practical purposes and has been highly cited. Also, in 1975, Allen and Dynes [14] improved McMillan's formula by replacing $\omega_D/1.45$ with $\omega_{\ln}/1.2$. Here, ω_D is the Debye frequency of phonons, λ is the electron-phonon coupling constant which is calculated based on the phonon frequency distribution function $\alpha^2 F(\omega)$ to get a better fit for the critical temperature. Here, α^2 which is the strength of coupling between electrons is frequency-dependant and it is squared because of the coupling between two electrons. Also, μ^* is the Coulomb pseudopotential of

---

[1]In this thesis, k_B and $\hbar$ are set to unity, which means that the temperature and frequency have units of energy.

Morel and Anderson [15]:

$$\mu^*(\omega_c) = \frac{\mu(\epsilon_F)}{[1 + \mu(\epsilon_F)\ln(\epsilon_F/\omega_c)]}, \tag{1.2}$$

which tends to vary between 0 to 0.25. The Coulomb interaction is frequency independent, however, it depends on the cut-off frequency ω_c which is of the order of the Fermi energy, ϵ_F. The electron-phonon coupling parameter λ is defined as

$$\lambda = 2 \int_0^\infty d\omega \frac{\alpha^2 F(\omega)}{\omega}. \tag{1.3}$$

Here, $\alpha^2 F(\omega)$ is the Eliashberg coupling function which is modelled by

$$\alpha^2 F(\omega) = A\delta(\omega - \omega_E), \tag{1.4}$$

where $A = \lambda\omega_E/2$. The logarithmic average phonon frequency is defined by

$$\omega_{\ln} = \exp\left[\frac{2}{\lambda}\int_0^\infty d\omega \ln\omega \frac{\alpha^2 F(\omega)}{\omega}\right].$$

For the model with an Einstein mode, we obtain

$$\begin{aligned}
\omega_{\ln} &= \exp\left[\frac{2}{\lambda}\int_0^\infty d\omega \ln\omega \frac{\lambda\omega_E\delta(\omega - \omega_E)}{2\omega}\right] \\
&= \exp(\ln\omega_E) \\
&= \omega_E.
\end{aligned} \tag{1.5}$$

Therefore, the Einstein mode with frequency ω_E is the logarithmic average phonon frequency. The BCS solution for the critical temperature is

$$T_c = 1.13\omega_E \exp\left(-\frac{1}{\lambda}\right). \tag{1.6}$$

Here, $\lambda = N(0)|V|$ is the electron-phonon coupling constant, $N(0)$ is the single-spin density of states at the Fermi surface and $|V|$ is the strength of the electron-phonon interaction. The numerical pre-factor 1.13 is an approximation to $2e^\gamma/\pi$. Here, $\gamma \approx 0.5772$ is the Euler-Mascheroni constant. However, the Eliashberg solution for T_c in the weak-coupling limit, has a correction to this result, which is shown as follows:

$$T_c = \frac{1.13}{\sqrt{e}}\omega_E \exp\left(-\frac{1}{\lambda}\right). \tag{1.7}$$

There exists the pre-factor $1/\sqrt{e}$ in the transition temperature of Eliashberg theory, which is significantly different from the BCS result [16].

Eliashberg theory describe some of the properties of superconductors like Pb and Hg in the strong-coupling limit [5]. These equations are expressed in terms of the Green's functions, which can be solved along the imaginary or the real frequency axes [17]. The imaginary-axis Eliashberg equations are computationally efficient because they include a summation over the Matsubara frequencies that are sufficient for the calculation of the critical temperature T_c and superconducting gap. To obtain information of the spectral properties, such as the single-particle excitation spectrum or the quasi-particle density of states, solving the real-axis Eliashberg equations is required. However, solution of the Eliashberg equations on the real frequency axis includes the calculation of principal-value integrals and square-root singularities which is challenging computationally [17–19].

Alternatively, the solution can be found using analytical continuation along the real frequency axis. The analytical continuation can be performed using Padé approximation, which was constructed by

Vidberg and Serene [20], or by employing the numerical iterative procedure which is called Marsiglio, Schossomann, and Carbotte method [17].

In this thesis, we have considered the weak-coupling limit of Eliashberg theory. We have obtained the frequency-dependent weak-coupling gap function on the real axis using an analytical continuation technique, including the renormalization factor and without the renormalization factor. One of the most striking facets of this work is to show that the weak-coupling Eliashberg theory does not reduce to BCS theory. It was tacitly assumed (in early literature) that in the weak-coupling limit, BCS theory and Eliashberg theory coincide, but here we investigate this further for the real frequency axis extending Marsiglio's work [21] on the imaginary axis. In chapter two, the Eliashberg equations are derived using Green's function and the equation of motion method. The electron self energy on the real and imaginary axes is calculated as well. In chapter three, a full derivation of the gap equation in the weak-coupling limit is given both on the imaginary and real frequency axes. Also, the zero-temperature limit of the gap equation is solved by converting the Matsubara frequency summation into an integral. We also calculate the gap edge on the real frequency axis. In chapter four, we present our numerical results both on the imaginary and real frequency axes. In chapter five, some of the thermodynamic properties, like the free energy, heat capacity and the critical magnetic field of superconductors are studied.

II. THE ELIASHBERG THEORY OF ELECTRON-PHONON INTERACTIONS IN THE SUPERCONDUCTING STATE

A. Derivation of the equations of motion in Eliashberg theory

In this section we follow Rickayzen's derivation of the Eliashberg equations [1]. We consider the following Hamiltonian which is defined as

$$H = \sum_{\mathbf{k},\boldsymbol{\sigma}} \xi_{\mathbf{k}} c^{\dagger}_{\mathbf{k}\boldsymbol{\sigma}} c_{\mathbf{k}\boldsymbol{\sigma}} + \sum_{\mathbf{k},\mathbf{k}'} g_{\mathbf{k}-\mathbf{k}'} (b^{\dagger}_{\mathbf{k},\mathbf{k}'} + b_{\mathbf{k}',\mathbf{k}})(c^{\dagger}_{\mathbf{k}\uparrow} c_{\mathbf{k}'\uparrow} + c^{\dagger}_{-\mathbf{k}'\downarrow} c_{-\mathbf{k}\downarrow}) + \sum_{\mathbf{k},\mathbf{k}'} \hbar\omega_{\mathbf{k}-\mathbf{k}'} b^{\dagger}_{\mathbf{k},\mathbf{k}'} b_{\mathbf{k},\mathbf{k}'}. \tag{2.1}$$

Here, $\boldsymbol{\sigma}$ is the spin and $\mathbf{k}$ is the momentum. The interaction between electrons and phonons is represented by $g_{\mathbf{k}-\mathbf{k}'}$ such that $g_{\mathbf{k}'-\mathbf{k}} = g^{\dagger}_{\mathbf{k}-\mathbf{k}'}$. The shifted electron dispersion $\xi_{\mathbf{k}}$ is

$$\xi_{\mathbf{k}} = \varepsilon_{\mathbf{k}} - \mu, \tag{2.2}$$

where μ is the chemical potential and $\varepsilon_{\mathbf{k}} = \mathbf{k}^2/(2m)$. The phonon dispersion is $\omega_{\mathbf{k}-\mathbf{k}'}$. The time evolution of the fermionic creation and annihilation operators is

$$c^{\dagger}_{\mathbf{k}\boldsymbol{\sigma}}(\tau) \equiv e^{H\tau} c^{\dagger}_{\mathbf{k}\boldsymbol{\sigma}} e^{-H\tau}, \tag{2.3}$$

$$c_{\mathbf{k}\boldsymbol{\sigma}}(\tau) \equiv e^{H\tau} c_{\mathbf{k}\boldsymbol{\sigma}} e^{-H\tau}, \tag{2.4}$$

where $\tau = it$. The operator $b^{\dagger}_{\mathbf{k},\mathbf{k}'}$ and $b_{\mathbf{k}',\mathbf{k}}$ are the phonon creation and annihilation operators. When an electron is scattered from $\mathbf{k}' \uparrow$ to $\mathbf{k} \uparrow$ it can emit a phonon, then another electron will be scattered from $-\mathbf{k}' \downarrow$ to $-\mathbf{k} \downarrow$ by absorbing this phonon. The exchange of a virtual phonon between two electrons is depicted in Fig.(1). The perturbative solution of the Hamiltonian is given in terms of the single-particle Green's function $G_{\boldsymbol{\sigma}}(\mathbf{k}, \tau - \tau')$ in momentum space. The Green's function is introduced as a sum of infinite terms of a perturbation series which incorporate phonons in the calculations. The poles of the Green's function provide us with the excitation energies of the system [1]. We use the equation of motion method to find the Matsubara single-particle Green's function, which involves differentiating the Matsubara Green's function with respect to time [1]. The Green's function is defined in terms of creation and annihilation operators by

$$G_{\boldsymbol{\sigma}}(\mathbf{k}, \tau - \tau') \equiv -\langle T_{\tau} c_{\mathbf{k}\boldsymbol{\sigma}}(\tau) c^{\dagger}_{\mathbf{k}\boldsymbol{\sigma}}(\tau')\rangle. \tag{2.5}$$

3
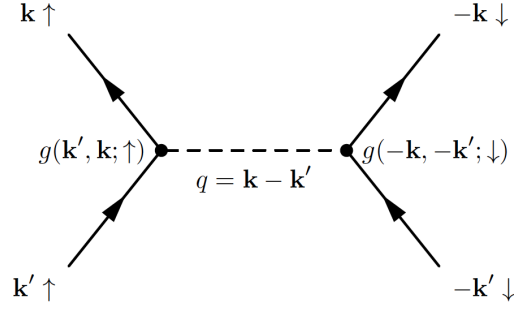
Figure 1. Exchange of a virtual phonon between electron states (the dashed line shows the virtual phonon).

The angular bracket $\langle \cdots \rangle$ denotes thermal averaging. The phonon propagator is defined as [1]

$$D(\mathbf{k} - \mathbf{k}', \tau - \tau') \equiv \langle T_\tau A_{\mathbf{k},\mathbf{k}'}(\tau) A_{-\mathbf{k},-\mathbf{k}'}(\tau') \rangle, \tag{2.6}$$

where $A_{\mathbf{k},\mathbf{k}'} \equiv b_{\mathbf{k},\mathbf{k}'}(\tau) + b^\dagger_{-\mathbf{k},-\mathbf{k}'}(\tau)$. Note that here D is in principle the fully interacting phonon propagator. However, we will ignore the phonon self energy and then we use the non-interacting phonon propagator. We now consider the Green's function with $\boldsymbol{\sigma} = \uparrow$. The time derivative of $G_\uparrow(\mathbf{k}, \tau - \tau')$ is [1]

$$-\frac{\partial}{\partial \tau} G_\uparrow(\mathbf{k}, \tau - \tau') = \frac{\partial}{\partial \tau} \left[\theta(\tau - \tau') \langle c_{\mathbf{k}\uparrow}(\tau) c^\dagger_{\mathbf{k}\uparrow}(\tau') \rangle - \theta(\tau' - \tau) \langle c^\dagger_{\mathbf{k}\uparrow}(\tau') c_{\mathbf{k}\uparrow}(\tau) \rangle \right]$$

$$= \delta(\tau - \tau') \left(\langle c_{\mathbf{k}\uparrow}(\tau) c^\dagger_{\mathbf{k}\uparrow}(\tau') \rangle + \langle c^\dagger_{\mathbf{k}\uparrow}(\tau') c_{\mathbf{k}\uparrow}(\tau) \rangle \right)$$

$$+ \theta(\tau - \tau') \langle [H, c_{\mathbf{k}\uparrow}(\tau)] c^\dagger_{\mathbf{k}\uparrow}(\tau') \rangle - \theta(\tau' - \tau) \langle c^\dagger_{\mathbf{k}\uparrow}(\tau') [H, c_{\mathbf{k}\uparrow}(\tau)] \rangle. \tag{2.7}$$

We use the fact that $\frac{\partial}{\partial \tau} \theta(\tau - \tau') = \delta(\tau - \tau')$. Simplifying then gives

$$-\frac{\partial}{\partial \tau} G_\uparrow(\mathbf{k}, \tau - \tau') = \delta(\tau - \tau') \langle \{ c_{\mathbf{k}\uparrow}(\tau), c^\dagger_{\mathbf{k}\uparrow}(\tau) \} \rangle + \langle T_\tau [H, c_{\mathbf{k}\uparrow}(\tau)] c^\dagger_{\mathbf{k}\uparrow}(\tau') \rangle. \tag{2.8}$$

To find the commutator in the second term of Eq.(2.8) we write the Hamiltonian as follows

$$H = \sum_{\mathbf{q},\sigma} \xi_\mathbf{q} c^\dagger_{\mathbf{q}\sigma} c_{\mathbf{q}\sigma} + \sum_{\mathbf{q},\mathbf{q}'} g_{\mathbf{q}-\mathbf{q}'} (b^\dagger_{\mathbf{q},\mathbf{q}'} + b_{\mathbf{q}',\mathbf{q}})(c^\dagger_{\mathbf{q}\uparrow} c_{\mathbf{q}'\uparrow} + c^\dagger_{-\mathbf{q}'\downarrow} c_{-\mathbf{q}\downarrow}) + \sum_{\mathbf{q},\mathbf{q}'} \hbar \omega_{\mathbf{q}-\mathbf{q}'} b^\dagger_{\mathbf{q},\mathbf{q}'} b_{\mathbf{q},\mathbf{q}'}. \tag{2.9}$$

Using the Hamiltonian, the commutator in Eq.(2.8) is then [2]

$$[H, c_{\mathbf{k}\uparrow}(\tau)] = [\sum_{\mathbf{q},\sigma} \xi_\mathbf{q} c^\dagger_{\mathbf{q}\sigma} c_{\mathbf{q}\sigma}, c_{\mathbf{k}\uparrow}(\tau)] + \sum_{\mathbf{q},\mathbf{q}'} g_{\mathbf{q}-\mathbf{q}'} (b^\dagger_{\mathbf{q},\mathbf{q}'} + b_{\mathbf{q}',\mathbf{q}})[c^\dagger_{\mathbf{q}\uparrow} c_{\mathbf{q}'\uparrow} + c^\dagger_{-\mathbf{q}'\downarrow} c_{-\mathbf{q}\downarrow}, c_{\mathbf{k}\uparrow}(\tau)]$$

$$= -\sum_{\mathbf{q},\sigma} \delta_{\mathbf{q},\mathbf{k}} \delta_{\sigma\uparrow} \xi_\mathbf{q} c_{\mathbf{q}\sigma} - \sum_{\mathbf{q},\mathbf{q}'} g_{\mathbf{q}-\mathbf{q}'} (b^\dagger_{\mathbf{q},\mathbf{q}'} + b_{\mathbf{q}',\mathbf{q}}) \delta_{\mathbf{k},\mathbf{q}} c_{\mathbf{q}'\uparrow}$$

$$= -\xi_\mathbf{k} c_{\mathbf{k}\uparrow} - \sum_{\mathbf{k}'} g_{\mathbf{k}-\mathbf{k}'} (b^\dagger_{\mathbf{k},\mathbf{k}'} + b_{\mathbf{k}',\mathbf{k}}) c_{\mathbf{k}'\uparrow}. \tag{2.10}$$

—————

[2] Applying the identity

$$[AB, C] = ABC - CAB = ABC + ACB - ACB - CAB = A\{B, C\} - \{A, C\}B.$$

Substituting the result of Eq.(2.10) in Eq.(2.8) we obtain

$$-\left(\frac{\partial}{\partial\tau}+\xi_{\mathbf{k}}\right)G_\uparrow(\mathbf{k},\tau-\tau')=\delta(\tau-\tau')-\sum_{\mathbf{k}'}g_{\mathbf{k}-\mathbf{k}'}\langle T_\tau[b_{\mathbf{k},\mathbf{k}'}^\dagger(\tau)+b_{\mathbf{k}',\mathbf{k}}(\tau)]c_{\mathbf{k}'\uparrow}(\tau)c_{\mathbf{k}\uparrow}^\dagger(\tau')\rangle. \qquad (2.11)$$

The two-particle Green's function equation is defined as [1]

$$G(\mathbf{k}_1\boldsymbol{\sigma}_1\tau_1,\mathbf{k}_2\boldsymbol{\sigma}_2\tau_2;\mathbf{k}_3\boldsymbol{\sigma}_3\tau_3,\mathbf{k}_4\boldsymbol{\sigma}_4\tau_4)\equiv\langle T_\tau c_{\mathbf{k}_1\boldsymbol{\sigma}_1}(\tau_1)c_{\mathbf{k}_2\boldsymbol{\sigma}_2}(\tau_2)c_{\mathbf{k}_4\boldsymbol{\sigma}_4}^\dagger(\tau_4)c_{\mathbf{k}_3\boldsymbol{\sigma}_3}^\dagger(\tau_3)\rangle. \qquad (2.12)$$

The (imaginary) time derivative acting on the two particle Green's function gives

$$\left(\frac{\partial}{\partial\tau_1}+\xi_{\mathbf{k}_1}\right)G(\mathbf{k}_1\uparrow\tau_1,\mathbf{k}_2\boldsymbol{\sigma}_2\tau_2;\mathbf{k}_3\boldsymbol{\sigma}_3\tau_3,\mathbf{k}_4\boldsymbol{\sigma}_4\tau_4)$$
$$=-\delta(\tau_1-\tau_3)G_{\boldsymbol{\sigma}_2}(\mathbf{k}_2,\tau_2-\tau_4)\delta_{\mathbf{k}_2\mathbf{k}_4}\delta_{\boldsymbol{\sigma}_2\boldsymbol{\sigma}_4}\delta_{\mathbf{k}_1\mathbf{k}_3}\delta_{\uparrow\boldsymbol{\sigma}_3}+\delta(\tau_1-\tau_4)G_{\boldsymbol{\sigma}_2}(\mathbf{k}_2,\tau_2-\tau_3)\delta_{\mathbf{k}_2\mathbf{k}_3}\delta_{\boldsymbol{\sigma}_2\boldsymbol{\sigma}_3}\delta_{\mathbf{k}_1\mathbf{k}_4}\delta_{\uparrow\boldsymbol{\sigma}_4}$$
$$-\sum_{\mathbf{k}'}g_{\mathbf{k}_1-\mathbf{k}'}\langle T_\tau[b_{\mathbf{k}_1,\mathbf{k}'}^\dagger(\tau_1)+b_{\mathbf{k}',\mathbf{k}_1}(\tau_1)]c_{\mathbf{k}'\uparrow}(\tau_1)c_{\mathbf{k}_2\boldsymbol{\sigma}_2}(\tau_2)c_{\mathbf{k}_4\boldsymbol{\sigma}_4}^\dagger(\tau_4)c_{\mathbf{k}_3\boldsymbol{\sigma}_3}^\dagger(\tau_3)\rangle. \qquad (2.13)$$

The time derivative of an n-particle G functions includes $2n$ operators for the electrons and one operator for the phonon. One can build higher-order equations following the same approach [1]. Now, one can write the one and two particle Green's function equation of motion as[3]

$$-\left(\frac{\partial}{\partial\tau_1}+\xi_{\mathbf{k}}\right)G_\uparrow(\mathbf{k},\tau_1-\tau_2)=\delta(\tau_1-\tau_2)+\sum_{\mathbf{k}'}\left|g_{\mathbf{k}-\mathbf{k}'}\right|^2\int_0^\beta d\tau'D(\mathbf{k}-\mathbf{k}',\tau_1-\tau')\times$$
$$\{G(\mathbf{k}\uparrow\tau',\mathbf{k}'\uparrow\tau_1;\mathbf{k}\uparrow\tau_2,\mathbf{k}'\uparrow\tau')+G(-\mathbf{k}'\downarrow\tau',\mathbf{k}'\uparrow\tau_1;\mathbf{k}\uparrow\tau_2,-\mathbf{k}\downarrow\tau')\}, \qquad (2.14)$$

and

$$\left(\frac{\partial}{\partial\tau_1}+\xi_{\mathbf{k}_1}\right)G(\mathbf{k}_1\uparrow\tau_1,\mathbf{k}_2\boldsymbol{\sigma}_2\tau_2;\mathbf{k}_3\boldsymbol{\sigma}_3\tau_3,\mathbf{k}_4\boldsymbol{\sigma}_4\tau_4)=-\delta(\tau_1-\tau_3)G_{\boldsymbol{\sigma}_2}(\mathbf{k}_2,\tau_2-\tau_4)\delta_{\mathbf{k}_2\mathbf{k}_4}\delta_{\boldsymbol{\sigma}_2\boldsymbol{\sigma}_4}\delta_{\mathbf{k}_1\mathbf{k}_3}\delta_{\uparrow\boldsymbol{\sigma}_3}$$

$$+\delta(\tau_1-\tau_4)G_{\boldsymbol{\sigma}_2}(\mathbf{k}_2,\tau_2-\tau_3)\delta_{\mathbf{k}_2\mathbf{k}_3}\delta_{\boldsymbol{\sigma}_2\boldsymbol{\sigma}_3}\delta_{\mathbf{k}_1\mathbf{k}_4}\delta_{\uparrow\boldsymbol{\sigma}_4}+\sum_{\mathbf{k}'}\left|g_{\mathbf{k}_1-\mathbf{k}'}\right|^2\int_0^\beta d\tau'D(\mathbf{k}_1-\mathbf{k}',\tau_1-\tau')\times$$

$$\langle[c_{\mathbf{k}'\uparrow}^\dagger(\tau')c_{\mathbf{k}_1\uparrow}(\tau')+c_{-\mathbf{k}_1\downarrow}^\dagger(\tau')c_{-\mathbf{k}'\downarrow}(\tau')]c_{\mathbf{k}'\uparrow}(\tau_1)c_{\mathbf{k}_2\boldsymbol{\sigma}_2}(\tau_2)c_{\mathbf{k}_4\boldsymbol{\sigma}_4}^\dagger(\tau_4)c_{\mathbf{k}_3\boldsymbol{\sigma}_3}^\dagger(\tau_3)\rangle. \qquad (2.15)$$

In this case, we define the correlation functions C such that the second-order correlation function is zero for particles with parallel spins. Furthermore, the complete third-order correlation function is assumed to be zero [1]. In general,

$$G(\alpha_1\tau_1,\alpha_2\tau_2;\alpha_3\tau_3,\alpha_4\tau_4)=G(\alpha_1,\tau_1-\tau_3)G(\alpha_2,\tau_2-\tau_4)\delta_{\alpha_1\alpha_3}\delta_{\alpha_2\alpha_4}$$
$$-G(\alpha_1,\tau_1-\tau_4)G(\alpha_2,\tau_2-\tau_3)\delta_{\alpha_1\alpha_4}\delta_{\alpha_2\alpha_3}$$
$$+C(\alpha_1\tau_1,\alpha_2\tau_2;\alpha_3\tau_3,\alpha_4\tau_4). \qquad (2.16)$$

In addition,

$$G(\alpha_1\tau_1,\alpha_2\tau_2,\alpha_3\tau_3;\alpha_4\tau_4,\alpha_5\tau_5,\alpha_6\tau_6)=\sum_{i,j,k=4}^6 G(\alpha_1,\tau_1-\tau_i)G(\alpha_2,\tau_2-\tau_j)G(\alpha_3,\tau_3-\tau_k)\delta_{\alpha_1\alpha_i}\delta_{\alpha_2\alpha_j}\delta_{\alpha_3\alpha_k}\varepsilon_{ijk}$$

$$+(1/2)\sum_{i,j,k=4}^6 G(\alpha_1,\tau_1-\tau_i)C(\alpha_2\tau_2,\alpha_3\tau_3;\alpha_j\tau_j,\alpha_k\tau_k)\delta_{\alpha_1\alpha_i}\varepsilon_{ijk}$$

$$+C(\alpha_1\tau_1,\alpha_2\tau_2,\alpha_3\tau_3;\alpha_4\tau_4,\alpha_5\tau_5,\alpha_6\tau_6), \qquad (2.17)$$

————

[3]Eq.(2.14) and Eq.(2.15) are proved in Appendix (A 1) and Appendix (A 2).

where ε_{ijk} is the antisymmetric tensor of third-order which is defined as $\varepsilon_{456} = 1$. Thus, the equations simplify to [4]

$$-\left(\frac{\partial}{\partial \tau_1} + \xi_{\mathbf{k}}\right) G_\uparrow(\mathbf{k}, \tau_1 - \tau_2) = \delta(\tau_1 - \tau_2) + \sum_{\mathbf{k}'}|g_{\mathbf{k}-\mathbf{k}'}|^2 \int d\tau' D(\mathbf{k} - \mathbf{k}', \tau_1 - \tau') \times$$
$$[G_\uparrow(\mathbf{k}, \tau_1 - \tau')G_\uparrow(\mathbf{k}', \tau' - \tau_2) + C(-\mathbf{k}' \downarrow \tau', \mathbf{k}' \uparrow \tau_1; \mathbf{k} \uparrow \tau_2, -\mathbf{k} \downarrow \tau')],$$
(2.18)

and

$$\left(\frac{\partial}{\partial \tau_1} + \xi_{\mathbf{k}_1}\right) C(\mathbf{k}_1 \uparrow \tau_1, -\mathbf{k}_1 \downarrow \tau_2; \mathbf{k}_2 \uparrow \tau_3, -\mathbf{k}_2 \downarrow \tau_4)$$
$$= \sum_{\mathbf{k}'}|g_{\mathbf{k}_1-\mathbf{k}'}|^2 \int d\tau' D(\mathbf{k}_1 - \mathbf{k}', \tau_1 - \tau')\{G_\uparrow(\mathbf{k}', \tau_1 - \tau')C(\mathbf{k}_1 \uparrow \tau', -\mathbf{k}_1 \downarrow \tau_2; \mathbf{k}_2 \uparrow \tau_3, -\mathbf{k}_2 \downarrow \tau_4)$$
$$+ G_\downarrow(-\mathbf{k}_1, \tau_2 - \tau')C(\mathbf{k}' \uparrow \tau_1, -\mathbf{k}' \downarrow \tau'; \mathbf{k}_2 \uparrow \tau_3, -\mathbf{k}_2 \downarrow \tau_4)\}.$$
(2.19)

The equations for time development of C to (imaginary) time τ_2 and τ_3 are as follows [1]

$$\left(\frac{\partial}{\partial \tau_2} + \xi_{\mathbf{k}_1}\right) C(\mathbf{k}_1 \uparrow \tau_1, -\mathbf{k}_1 \downarrow \tau_2; \mathbf{k}_2 \uparrow \tau_3, -\mathbf{k}_2 \downarrow \tau_4)$$
$$= \sum_{\mathbf{k}}|g_{\mathbf{k}-\mathbf{k}_1}|^2 \int d\tau D(\mathbf{k} - \mathbf{k}_1, \tau_2 - \tau)\{G_\uparrow(\mathbf{k}, \tau_1 - \tau)C(\mathbf{k} \uparrow \tau, -\mathbf{k} \downarrow \tau_2; \mathbf{k}_2 \uparrow \tau_3, -\mathbf{k}_2 \downarrow \tau_4)$$
$$+ G_\downarrow(-\mathbf{k}, \tau_2 - \tau)C(\mathbf{k}_1 \uparrow \tau_1, -\mathbf{k}_1 \downarrow \tau; \mathbf{k}_2 \uparrow \tau_3, -\mathbf{k}_2 \downarrow \tau_4)\},$$
(2.20)

and

$$\left(\frac{\partial}{\partial \tau_3} - \xi_{\mathbf{k}_3}\right) C(\mathbf{k}_1 \uparrow \tau_1, -\mathbf{k}_1 \downarrow \tau_2; \mathbf{k}_2 \uparrow \tau_3, -\mathbf{k}_2 \downarrow \tau_4)$$
$$= -\sum_{\mathbf{k}}|g_{\mathbf{k}-\mathbf{k}_2}|^2 \int d\tau D(\mathbf{k} - \mathbf{k}_2, \tau_3 - \tau)\{G_\uparrow(\mathbf{k}, \tau - \tau_3)C(\mathbf{k}_1 \uparrow \tau_1, -\mathbf{k}_1 \downarrow \tau_2; \mathbf{k}_2 \uparrow \tau, -\mathbf{k}_2 \downarrow \tau_4)$$
$$+ G_\downarrow(-\mathbf{k}_2, \tau - \tau_4)C(\mathbf{k}_1 \uparrow \tau_1, -\mathbf{k}_1 \downarrow \tau_2; \mathbf{k} \uparrow \tau_3, -\mathbf{k} \downarrow \tau)\}.$$
(2.21)

These equations can be solved utilizing the relation

$$C(\mathbf{k}_1 \uparrow \tau_1, -\mathbf{k}_1 \downarrow \tau_2; \mathbf{k}_2 \uparrow \tau_3, -\mathbf{k}_2 \downarrow \tau_4) = F(\mathbf{k}_1, \tau_1 - \tau_2)\bar{F}(\mathbf{k}_2, \tau_3 - \tau_4).$$
(2.22)

In the superconducting phase, there exists non-vanishing expectation values referred to as anomalous amplitudes. F and $\bar{F}$ respectively destroy and create a Cooper pair in the superconducting ground state. These functions are defined as [1]

$$F(\mathbf{k}, \tau - \tau') \equiv -\langle T_\tau c_{\mathbf{k}\uparrow}(\tau)c_{-\mathbf{k}\downarrow}(\tau')\rangle.$$
(2.23)

$$\bar{F}(\mathbf{k}, \tau - \tau') \equiv -\langle T_\tau c^\dagger_{-\mathbf{k}\downarrow}(\tau)c^\dagger_{\mathbf{k}\uparrow}(\tau')\rangle.$$
(2.24)

Since we are considering the case where there is time reversal symmetry, then these two functions are even in time so they are even in frequency [1].

$$F(\mathbf{k}, \tau) = F(\mathbf{k}, -\tau), \quad \bar{F}(\mathbf{k}, \tau) = \bar{F}(\mathbf{k}, -\tau).$$
(2.25)

———

[4]Eq.(2.19) is proved in Appendix (A 3).

$$F(\mathbf{k}, i\omega_n) = F(\mathbf{k}, -i\omega_n), \quad \bar{F}(\mathbf{k}, i\omega_n) = \bar{F}(\mathbf{k}, -i\omega_n). \tag{2.26}$$

Using these definitions in the equation of motion, we obtain [1]

$$-\left(\frac{\partial}{\partial\tau_1} + \xi_\mathbf{k}\right) G(\mathbf{k}, \tau_1 - \tau_2) = \delta(\tau_1 - \tau_2) - \sum_{\mathbf{k}'} \left|g_{\mathbf{k}-\mathbf{k}'}\right|^2 \int_0^\beta d\tau D(\mathbf{k} - \mathbf{k}', \tau_1 - \tau) \times$$
$$[G(\mathbf{k}, \tau - \tau_2)G(\mathbf{k}', \tau_1 - \tau) - F(\mathbf{k}', \tau - \tau_1)\bar{F}(\mathbf{k}, \tau_2 - \tau)], \tag{2.27}$$

and

$$\left(\frac{\partial}{\partial\tau_1} + \xi_\mathbf{k}\right) F(\mathbf{k}, \tau_1 - \tau_2) = \sum_{\mathbf{k}'} \left|g_{\mathbf{k}-\mathbf{k}'}\right|^2 \int_0^\beta d\tau D(\mathbf{k} - \mathbf{k}', \tau_1 - \tau) \times$$
$$[G(\mathbf{k}', \tau_1 - \tau)F(\mathbf{k}, \tau - \tau_2) + G(\mathbf{k}, \tau_2 - \tau)F(\mathbf{k}', \tau_1 - \tau)], \tag{2.28}$$

$$\left(\frac{\partial}{\partial\tau_1} - \xi_\mathbf{k}\right) \bar{F}(\mathbf{k}, \tau_1 - \tau_2) = -\sum_{\mathbf{k}'} \left|g_{\mathbf{k}-\mathbf{k}'}\right|^2 \int_0^\beta d\tau D(\mathbf{k}' - \mathbf{k}, \tau_1 - \tau) \times$$
$$[G(\mathbf{k}', \tau - \tau_1)\bar{F}(\mathbf{k}, \tau - \tau_2) + G(\mathbf{k}, \tau - \tau_2)\bar{F}(\mathbf{k}', \tau_1 - \tau)]. \tag{2.29}$$

The Fourier transform of Green's function in (imaginary) frequency is [1][5]

$$G(\mathbf{k}, \tau_1 - \tau_2) = \frac{1}{\beta} \sum_n G(\mathbf{k}, i\omega_n) e^{-i\omega_n(\tau_1 - \tau_2)}. \tag{2.31}$$

The imaginary time τ is restricted to one period $[0, \beta]$ where $\beta = \frac{1}{k_B T}$. Now, we define the self energy and the pairing function as follows [1]

$$\Sigma(\mathbf{k}, i\omega_n) = -\sum_{\mathbf{k}',n'} \left|g_{\mathbf{k}-\mathbf{k}'}\right|^2 D(\mathbf{k} - \mathbf{k}', i\omega_n - i\omega_{n'}) G(\mathbf{k}', i\omega_{n'}). \tag{2.32}$$

$$\phi(\mathbf{k}, i\omega_n) = -\sum_{\mathbf{k}',n'} \left|g_{\mathbf{k}-\mathbf{k}'}\right|^2 D(\mathbf{k} - \mathbf{k}', i\omega_n - i\omega_{n'}) F(\mathbf{k}', i\omega_{n'}). \tag{2.33}$$

The self energy $\Sigma(\mathbf{k}, i\omega_n)$ and the pairing function $\phi(\mathbf{k}, i\omega_n)$ of the variable $\mathbf{k}$ and $i\omega_n$ are both complex functions. The Fourier transform of Eq.(2.27) and Eq.(2.29) are [1]

$$-(-i\omega_n + \xi_\mathbf{k})G(\mathbf{k}, i\omega_n) = 1 + \Sigma(\mathbf{k}, -i\omega_n)G(\mathbf{k}, i\omega_n) - \phi(\mathbf{k}, i\omega_n)\bar{F}(\mathbf{k}, i\omega_n), \tag{2.34}$$

and

$$(-i\omega_n - \xi_\mathbf{k})\bar{F}(\mathbf{k}, i\omega_n) = \Sigma(\mathbf{k}, -i\omega_n)\bar{F}(\mathbf{k}, i\omega_n) + \bar{\phi}(\mathbf{k}, i\omega_n)G(\mathbf{k}, i\omega_n). \tag{2.35}$$

After simplifying the above equations we can write

$$G(\mathbf{k}, i\omega_n) = \left[i\omega_n - \xi_\mathbf{k} - \Sigma(\mathbf{k}, i\omega_n) + \frac{\mid \phi(\mathbf{k}, i\omega_n) \mid^2}{-i\omega_n - \xi_\mathbf{k} - \Sigma(\mathbf{k}, -i\omega_n)}\right]^{-1}. \tag{2.36}$$

———

[5]The Fourier transformation of $\delta(\tau_1 - \tau_2)$ function is defined as

$$\delta(\tau_1 - \tau_2) = \frac{1}{\beta} \sum_{i\omega_n} e^{-i\omega_n(\tau_1 - \tau_2)}. \tag{2.30}$$

$$F(\mathbf{k}, i\omega_n) = F(\mathbf{k}, -i\omega_n) = \frac{\bar{\phi}(\mathbf{k}, i\omega_n)G(\mathbf{k}, i\omega_n)}{-i\omega_n - \xi_{\mathbf{k}} - \Sigma(\mathbf{k}, -i\omega_n)}. \tag{2.37}$$

Now we apply Dyson's equation

$$G_n^{-1}(\mathbf{k}, i\omega_n) = G_0^{-1}(\mathbf{k}, i\omega_n) - \Sigma(\mathbf{k}, i\omega_n), \tag{2.38}$$

The result can then be obtained as follows:

$$G(\mathbf{k}, i\omega_n) = \frac{G_n^{-1}(-\mathbf{k}, i\omega_n)}{G_n^{-1}(\mathbf{k}, i\omega_n)G_n^{-1}(-\mathbf{k}, -i\omega_n) + \phi(\mathbf{k}, i\omega_n)\bar{\phi}(\mathbf{k}, i\omega_n)}, \tag{2.39}$$

$$F(\mathbf{k}, i\omega_n) = \frac{\phi(\mathbf{k}, i\omega_n)}{G_n^{-1}(\mathbf{k}, i\omega_n)G_n^{-1}(-\mathbf{k}, -i\omega_n) + \phi(-\mathbf{k}, -i\omega_n)\bar{\phi}(-\mathbf{k}, -i\omega_n)}. \tag{2.40}$$

Here, the self energy is written into even and odd parts as follows:

$$i\omega_n[1 - Z(\mathbf{k}, i\omega_n)] \equiv \frac{1}{2}[\Sigma(\mathbf{k}, i\omega_n) - \Sigma(\mathbf{k}, -i\omega_n)]. \tag{2.41}$$

$$\chi(\mathbf{k}, i\omega_n) \equiv \frac{1}{2}[\Sigma(\mathbf{k}, i\omega_n) + \Sigma(\mathbf{k}, -i\omega_n)], \tag{2.42}$$

where the renormalization function Z and energy shift, χ[6] are even functions in $i\omega_n$. We have summarized the Eliashberg equations for the electron-phonon interaction as follows [18]:

$$\phi(\mathbf{k}, i\omega_n) = \frac{1}{\beta} \sum_{\mathbf{k}',n'} |g_{\mathbf{k}-\mathbf{k}'}|^2 \frac{D(\mathbf{k} - \mathbf{k}', i\omega_n - i\omega_{n'})\phi(\mathbf{k}', i\omega_{n'})}{\omega_{n'}^2 Z^2(\mathbf{k}', i\omega_{n'}) + (\xi_{\mathbf{k}'} + \chi(\mathbf{k}', i\omega_{n'}))^2 + \phi^2(\mathbf{k}', i\omega_{n'})}. \tag{2.43}$$

$$Z(\mathbf{k}, i\omega_n) = 1 + \frac{1}{\beta} \sum_{\mathbf{k}',n'} |g_{\mathbf{k}-\mathbf{k}'}|^2 \frac{D(\mathbf{k} - \mathbf{k}', i\omega_n - i\omega_{n'})(\omega_{n'}/\omega_n)Z(\mathbf{k}', i\omega_{n'})}{\omega_{n'}^2 Z^2(\mathbf{k}', i\omega_{n'}) + (\xi_{\mathbf{k}'} + \chi(\mathbf{k}', i\omega_{n'}))^2 + \phi^2(\mathbf{k}', i\omega_{n'})}. \tag{2.44}$$

$$\chi(\mathbf{k}, i\omega_n) = -\frac{1}{\beta} \sum_{\mathbf{k}',n'} |g_{\mathbf{k}-\mathbf{k}'}|^2 \frac{D(\mathbf{k} - \mathbf{k}', i\omega_n - i\omega_{n'})(\xi_{\mathbf{k}'} + \chi(\mathbf{k}', i\omega_{n'}))}{\omega_{n'}^2 Z^2(\mathbf{k}', i\omega_{n'}) + (\xi_{\mathbf{k}'} + \chi(\mathbf{k}', i\omega_{n'}))^2 + \phi^2(\mathbf{k}', i\omega_{n'})}. \tag{2.45}$$

$$n = 1 - \frac{2}{\beta} \sum_{\mathbf{k}',n'} \frac{(\xi_{\mathbf{k}'} + \chi(\mathbf{k}', i\omega_{n'}))}{\omega_{n'}^2 Z^2(\mathbf{k}', i\omega_{n'}) + (\xi_{\mathbf{k}'} + \chi(\mathbf{k}', i\omega_{n'}))^2 + \phi^2(\mathbf{k}', i\omega_{n'})}. \tag{2.46}$$

Here, n is the electron number equation, which calculates the chemical potential. The gap function is

$$\Delta(\mathbf{k}, i\omega_n) \equiv \phi(\mathbf{k}, i\omega_n)/Z(\mathbf{k}, i\omega_n).$$

The frequency-dependent gap function $\Delta(\mathbf{k}, i\omega_n)$ is the essential effect of retardation in the Eliashberg theory [10]. Assuming $Z = 1$, the gap function can then be written as

$$\Delta(\mathbf{k}, i\omega_n) = \frac{1}{\beta} \sum_{\mathbf{k}',n'} |g_{\mathbf{k}-\mathbf{k}'}|^2 \frac{D(\mathbf{k} - \mathbf{k}', i\omega_n - i\omega_{n'})\Delta(\mathbf{k}', i\omega_{n'})}{\omega_{n'}^2 + (\xi_{\mathbf{k}'} + \chi(\mathbf{k}', i\omega_{n'}))^2 + \Delta^2(\mathbf{k}', i\omega_{n'})}. \tag{2.47}$$

B. Electron self energy on the real axis

In this subsection we study the electron self energy calculation on the real frequency axis [22, 23]. Dyson's equation for the electron Green's function on the imaginary axis can be written as

$$G^{-1}(\mathbf{k}, i\omega_n) = G_0^{-1}(\mathbf{k}, i\omega_n) - \Sigma(\mathbf{k}, i\omega_n), \tag{2.48}$$

―――――

[6]We assume the particle-hole symmetry. Then the even part of the self energy χ, is zero.

where the non-interacting inverse Nambu Green's function[7] is

$$G_0^{-1}(\mathbf{k}, i\omega_n) = i\omega_n \boldsymbol{\tau}_0 - \xi_\mathbf{k} \boldsymbol{\tau}_3. \tag{2.49}$$

The fermionic Matsubara frequency is defined by $\omega_n = \pi k_B T (2n+1)$ and the dispersion relation is $\xi_\mathbf{k}$. The electron self-energy $\Sigma(\mathbf{k}, i\omega_n)$ is given in [17]; to compute it, we follow the method outlined in [22]

$$\Sigma(\mathbf{k}, i\omega_n) = -T\sum_{i\omega_m} \int \frac{d^3\mathbf{q}}{(2\pi)^3} \boldsymbol{\tau}_3 G(\mathbf{q}, i\omega_m)\boldsymbol{\tau}_3 \alpha^2(\mathbf{q},\mathbf{k}) D(\mathbf{k}-\mathbf{q}, i\omega_n - i\omega_m),$$

$$= -T\sum_{i\omega_m \neq i\omega_n} \int \frac{d^3\mathbf{q}}{(2\pi)^3} \boldsymbol{\tau}_3 G(\mathbf{q}, i\omega_m)\boldsymbol{\tau}_3 \alpha^2(\mathbf{q},\mathbf{k}) D(\mathbf{k}-\mathbf{q}, i\omega_n - i\omega_m)$$

$$-T\int \frac{d^3\mathbf{q}}{(2\pi)^3} \boldsymbol{\tau}_3 G(\mathbf{q}, i\omega_n)\boldsymbol{\tau}_3 \alpha^2(\mathbf{q},\mathbf{k}) D(\mathbf{k}-\mathbf{q}, 0). \tag{2.50}$$

The Matsubara frequency summation in the first line of Eq.(2.50) includes all fermionic Matsubara frequencies. Included in this sum is the term $i\omega_n = i\omega_m$, which leads to a phonon propagator evaluated at zero bosonic frequency. When evaluating this sum by contour integration the closed contour excludes the term $i\omega_n = i\omega_m$. Here, α is the average coupling constant of the electron-phonon interaction and $D(\mathbf{k}-\mathbf{q}, i\omega_n - i\omega_m)$ is the phonon propagator. Pauli matrices $\tau_i, i = 1, 2, 3, ...$ define the 2×2 Nambu formalism of the superconducting state.

$$\boldsymbol{\tau}_0 = \begin{bmatrix} 1 & 0 \\ 0 & 1 \end{bmatrix}, \quad \boldsymbol{\tau}_1 = \begin{bmatrix} 0 & 1 \\ 1 & 0 \end{bmatrix}, \quad \boldsymbol{\tau}_2 = \begin{bmatrix} 0 & -i \\ i & 0 \end{bmatrix}, \quad \boldsymbol{\tau}_3 = \begin{bmatrix} 1 & 0 \\ 0 & -1 \end{bmatrix}, \tag{2.51}$$

and

$$\boldsymbol{\tau}_3 \boldsymbol{\tau}_0 \boldsymbol{\tau}_3 = \boldsymbol{\tau}_0, \tag{2.52}$$

$$\boldsymbol{\tau}_3 \boldsymbol{\tau}_1 \boldsymbol{\tau}_3 = -\boldsymbol{\tau}_1. \tag{2.53}$$

The Feynman diagram for the electron self energy is depicted in Fig.(2), where the dashed line is the phonon propagator. The fermionic Matsubara summation formula is [24]
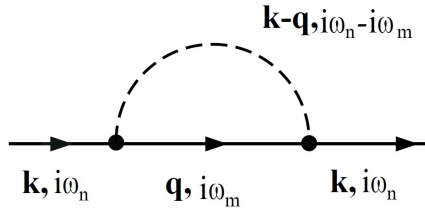
Figure 2. Feynman diagram for the electron self-energy. The dashed line shows the phonon propagator.

$$T\sum_{i\omega_m} f(\mathbf{q}, i\omega_m) = \frac{1}{4\pi i} \oint dz f(\mathbf{q}, z) \tanh\left(\frac{1}{2}\beta z\right). \tag{2.54}$$

The Matsubara frequency summation is performed using the Eliashberg contour integration approach.[8] Contour integration around the poles enables us to convert the discrete Matsubara summation into a

---

[7]The Nambu Green's function method is discussed in Appendix (B).
[8]Contour integration technique is useful in the calculations of the finite temperature Green's function in the frequency domain.

continuous integral which is depicted in Fig.(3) [25, 26]. We obtain

$$
T \sum_{i\omega_m \neq i\omega_n} \boldsymbol{\tau}_3 G(\mathbf{q}, i\omega_m) \boldsymbol{\tau}_3 \alpha^2(\mathbf{q}, \mathbf{k}) D(\mathbf{k} - \mathbf{q}, i\omega_n - i\omega_m)
$$

$$
= \frac{1}{4\pi i} \oint_{C_1+C_2+C_3} dz \tanh\left(\frac{1}{2}\beta z\right) \boldsymbol{\tau}_3 G_{R/A}(\mathbf{q}, z) \boldsymbol{\tau}_3 \alpha^2(\mathbf{q}, \mathbf{k}) D_{R/A}(\mathbf{k} - \mathbf{q}, i\omega_n - z),
$$

$$
= \frac{1}{4\pi i} \int_{-\infty}^{\infty} dz \tanh\left(\frac{1}{2}\beta z\right) \boldsymbol{\tau}_3 [G_R(\mathbf{q}, z) - G_A(\mathbf{q}, z)] \boldsymbol{\tau}_3 \alpha^2(\mathbf{q}, \mathbf{k}) D_R(\mathbf{k} - \mathbf{q}, i\omega_n - z)
$$

$$
+ \frac{1}{4\pi i} \int_{-\infty-i\omega_n}^{\infty+i\omega_n} dz \tanh\left(\frac{1}{2}\beta z\right) \boldsymbol{\tau}_3 G_R(\mathbf{q}, z) \boldsymbol{\tau}_3 \alpha^2(\mathbf{q}, \mathbf{k}) [D_A(\mathbf{k} - \mathbf{q}, i\omega_n - z) - D_R(\mathbf{k} - \mathbf{q}, i\omega_n - z)]
$$

$$
+ T \boldsymbol{\tau}_3 G(\mathbf{q}, i\omega_n) \boldsymbol{\tau}_3 \alpha^2(\mathbf{q}, \mathbf{k}) D(\mathbf{k} - \mathbf{q}, 0). \tag{2.55}
$$

We have assumed $i\omega_n > 0$. The third term in Eq.(2.55) comes from the contribution to the contour
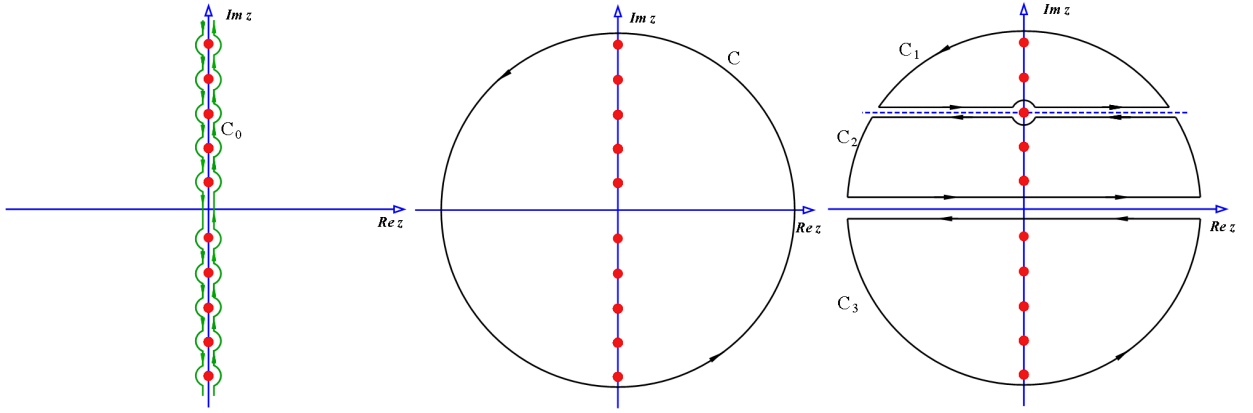
Figure 3. The contour of integration in the complex plane of Matsubara frequencies.

integral arising from the indentation about $z = i\omega_n$. The closed contours C_1, C_2, and C_3 enclose all of the frequencies $z \neq i\omega_n$. To compute the full Matsubara frequency summation the frequency $i\omega_m = i\omega_n$ must be included by hand, as indicated in Eq.(2.50). Remember that the bosonic frequencies are even, and thus zero frequency is permissible. Also, the semi-circle contribution at infinity vanishes. We shift the variable z to $i\omega_n - z'$ in the second integral and use the identity

$$
\tanh\left(\frac{1}{2}\beta(i\omega_n - z')\right) = -\coth\left(\frac{1}{2}\beta z'\right). \tag{2.56}
$$

The Matsubara frequency summation becomes

$$
T \sum_{i\omega_m \neq i\omega_n} \boldsymbol{\tau}_3 G(\mathbf{q}, i\omega_m) \boldsymbol{\tau}_3 \alpha^2(\mathbf{q}, \mathbf{k}) D(\mathbf{k} - \mathbf{q}, i\omega_n - i\omega_m)
$$

$$
= \int_{-\infty}^{\infty} \frac{dz}{2\pi} \tanh\left(\frac{1}{2}\beta z\right) \boldsymbol{\tau}_3 \mathrm{Im} G_R(\mathbf{q}, z) \boldsymbol{\tau}_3 \alpha^2(\mathbf{q}, \mathbf{k}) D_R(\mathbf{k} - \mathbf{q}, i\omega_n - z)
$$

$$
+ \int_{-\infty}^{\infty} \frac{dz'}{2\pi} \coth\left(\frac{1}{2}\beta z'\right) \boldsymbol{\tau}_3 G_R(\mathbf{q}, i\omega_n - z') \boldsymbol{\tau}_3 \alpha^2(\mathbf{q}, \mathbf{k}) \mathrm{Im} D_R(\mathbf{k} - \mathbf{q}, z')
$$

$$
+ T \boldsymbol{\tau}_3 G(\mathbf{q}, i\omega_n) \boldsymbol{\tau}_3 \alpha^2(\mathbf{q}, \mathbf{k}) D(\mathbf{k} - \mathbf{q}, 0). \tag{2.57}
$$

10

Substituting Eq.(2.57) in Eq.(2.50), the electron self energy on the real axis can be written as

$$\Sigma(\mathbf{k}, \omega) = - \int \frac{d^3\mathbf{q}}{(2\pi)^3} \int_{-\infty}^{\infty} \frac{dz}{2\pi} \tanh\left(\frac{1}{2}\beta z\right) \boldsymbol{\tau}_3 \mathrm{Im}G_R(\mathbf{q}, z)\boldsymbol{\tau}_3 \alpha^2(\mathbf{q}, \mathbf{k})D_R(\mathbf{k} - \mathbf{q}, \omega - z)$$

$$- \int \frac{d^3\mathbf{q}}{(2\pi)^3} \int_{-\infty}^{\infty} \frac{dz'}{2\pi} \coth\left(\frac{1}{2}\beta z'\right) \boldsymbol{\tau}_3 G_R(\mathbf{q}, \omega - z')\boldsymbol{\tau}_3 \alpha^2(\mathbf{q}, \mathbf{k})\mathrm{Im}D_R(\mathbf{k} - \mathbf{q}, z'). \quad (2.58)$$

Here ω is a short form for $\omega + i0^+$. Now, we introduce the spectral representation of the electron and phonon Green's function to convert them into the integral form.

$$G_R(\mathbf{p}, \omega) = \int_{-\infty}^{\infty} \frac{dz}{\pi} \frac{\mathrm{Im}G_R(\mathbf{p}, z)}{z - \omega - i\eta}, \quad (2.59)$$

$$D_R(\mathbf{p}, \nu) = \int_{-\infty}^{\infty} \frac{dz}{\pi} \frac{\mathrm{Im}D_R(\mathbf{p}, z)}{z - \nu - i\eta}. \quad (2.60)$$

The electron self energy then becomes

$$\Sigma(\mathbf{k}, \omega) = - \int \frac{d^3\mathbf{q}}{(2\pi)^3} \int_{-\infty}^{\infty} \frac{dz}{2\pi} \tanh\left(\frac{1}{2}\beta z\right) \boldsymbol{\tau}_3 \mathrm{Im}G_R(\mathbf{q}, z)\boldsymbol{\tau}_3 \alpha^2(\mathbf{q}, \mathbf{k}) \int_{-\infty}^{\infty} \frac{dz'}{\pi} \frac{\mathrm{Im}D_R(\mathbf{k} - \mathbf{q}, z')}{z' - (\omega - z) - i\eta}$$

$$- \int \frac{d^3\mathbf{q}}{(2\pi)^3} \int_{-\infty}^{\infty} \frac{dz'}{2\pi} \coth\left(\frac{1}{2}\beta z'\right) \boldsymbol{\tau}_3 \int_{-\infty}^{\infty} \frac{dz}{\pi} \frac{\mathrm{Im}G_R(\mathbf{q}, z)}{z - (\omega - z') - i\eta} \boldsymbol{\tau}_3 \alpha^2(\mathbf{q}, \mathbf{k})\mathrm{Im}D_R(\mathbf{k} - \mathbf{q}, z'). \quad (2.61)$$

The electron spectral function is defined as

$$S(\mathbf{p}, z) = -\frac{1}{\pi}\mathrm{Im}G_R(\mathbf{p}, z), \quad (2.62)$$

and the phonon spectral function is

$$B(\mathbf{p}, z) = -\frac{1}{\pi}\mathrm{Im}D_R(\mathbf{p}, z). \quad (2.63)$$

As a result, we can write

$$\Sigma(\mathbf{k}, \omega) = -\frac{1}{\pi} \int \frac{d^3\mathbf{q}}{(2\pi)^3} \int_{-\infty}^{\infty} dz' \int_{-\infty}^{\infty} dz \boldsymbol{\tau}_3 \frac{\mathrm{Im}G_R(\mathbf{q}, z)}{\omega - z - z' + i\eta}\boldsymbol{\tau}_3$$

$$\times \frac{1}{2}\alpha^2(\mathbf{q}, \mathbf{k})B(\mathbf{k} - \mathbf{q}, z')[\tanh\left(\frac{1}{2}\beta z\right) + \coth\left(\frac{1}{2}\beta z'\right)]. \quad (2.64)$$

Separating $(\omega - z - z' + i\eta)^{-1}$ into its real and imaginary parts using the Sokhotski-Plemelj formula [27], which is

$$\lim_{\varepsilon \to 0} \frac{1}{x - x_0 \pm i\varepsilon} = \mathcal{P}\frac{1}{x - x_0} \mp i\pi\delta(x - x_0), \quad (2.65)$$

where $\varepsilon > 0$ is an infinitesimal quantity and $\mathcal{P}$ is the principle value, we obtain

$$\Sigma(\mathbf{k}, \omega) = -\frac{1}{\pi} \int \frac{d^3\mathbf{q}}{(2\pi)^3} \int_{-\infty}^{\infty} dz' \int_{-\infty}^{\infty} dz \boldsymbol{\tau}_3 \mathrm{Im}G_R(\mathbf{q}, z)\left[\mathcal{P}\frac{1}{\omega - (z + z')} - i\pi\delta(\omega - z - z')\right]\boldsymbol{\tau}_3$$

$$\times \alpha^2(\mathbf{q}, \mathbf{k})B(\mathbf{k} - \mathbf{q}, z')\frac{1}{2}\left[\tanh\left(\frac{1}{2}\beta z\right) + \coth\left(\frac{1}{2}\beta z'\right)\right]. \quad (2.66)$$

We now use the identities for complex numbers, $\text{Re}w = \frac{1}{2}(w + w^*)$ and $\text{Im}w = \frac{1}{2i}(w - w^*)$, where $w \in \mathbb{C}$. Thus, we obtain

$$\Sigma(\mathbf{k}, \omega) = -\frac{1}{4\pi} \int \frac{d^3\mathbf{q}}{(2\pi)^3} \int_{-\infty}^{\infty} dz' \boldsymbol{\tau}_3 \text{Im} \left\{ \int_{-\infty}^{\infty} dz G_R(\mathbf{q}, z) \left[\frac{1}{\omega - (z + z') + i\eta} + \frac{1}{\omega - (z + z') - i\eta} \right] \boldsymbol{\tau}_3 \right.$$

$$\left. \times \alpha^2(\mathbf{q}, \mathbf{k}) B(\mathbf{k} - \mathbf{q}, z') \left[\tanh\left(\frac{1}{2}\beta z\right) + \coth\left(\frac{1}{2}\beta z'\right) \right] \right\}$$

$$+\frac{1}{4\pi} \int \frac{d^3\mathbf{q}}{(2\pi)^3} \int_{-\infty}^{\infty} dz' \boldsymbol{\tau}_3 i\text{Re} \left\{ \int_{-\infty}^{\infty} dz G_R(\mathbf{q}, z) \left[\frac{1}{\omega - (z + z') + i\eta} - \frac{1}{\omega - (z + z') - i\eta} \right] \boldsymbol{\tau}_3 \right.$$

$$\left. \times \alpha^2(\mathbf{q}, \mathbf{k}) B(\mathbf{k} - \mathbf{q}, z') \left[\tanh\left(\frac{1}{2}\beta z\right) + \coth\left(\frac{1}{2}\beta z'\right) \right] \right\}. \tag{2.67}$$

We integrate over z by deforming the contour integration into the upper half of the complex plane. Here, G_R, which is the retarded Green's function, is an analytic function in the upper half plane. Thus, only the poles at $z = \omega - z' + i\eta$ and $z = i(2m + 1)\pi T = i\omega_m$, $m \in \mathbb{N} = \{0, 1, 2, ...\}$ are included. The pole of the tanh function is $z = i(2m + 1)\pi T$ and the residue of the poles is $2T$, whereas the residue of the poles at $z = \omega - z' + i\eta$ is -1. The semi-circle contribution vanishes because $G_R \to 1/z$ as $z \to \infty$. Thus, the electron self energy is

$$\Sigma(\mathbf{k}, \omega) = -\frac{1}{4\pi} \int \frac{d^3\mathbf{q}}{(2\pi)^3} \int_{-\infty}^{\infty} dz' \alpha^2(\mathbf{q}, \mathbf{k}) B(\mathbf{k} - \mathbf{q}, z') \boldsymbol{\tau}_3$$

$$\times \text{Im} \left\{ 2\pi i \times 2T \sum_{m=0}^{\infty} G_R(\mathbf{q}, i\omega_m) \left[\frac{1}{\omega - (i\omega_m + z') + i\eta} + \frac{1}{\omega - (i\omega_m + z') - i\eta} \right] \right.$$

$$\left. - 2\pi i G_R(\mathbf{q}, \omega - z' + i\eta) \left[\tanh\left(\frac{1}{2}\beta(\omega - z')\right) + \coth\left(\frac{1}{2}\beta z'\right) \right] \right\} \boldsymbol{\tau}_3$$

$$+\frac{1}{4\pi} \int \frac{d^3\mathbf{q}}{(2\pi)^3} \int_{-\infty}^{\infty} dz' \alpha^2(\mathbf{q}, \mathbf{k}) B(\mathbf{k} - \mathbf{q}, z') \boldsymbol{\tau}_3$$

$$\times i\text{Re} \left\{ 2\pi i \times 2T \sum_{m=0}^{\infty} G_R(\mathbf{q}, i\omega_m) \left[\frac{1}{\omega - (i\omega_m + z') + i\eta} - \frac{1}{\omega - (i\omega_m + z') - i\eta} \right] \right.$$

$$\left. - 2\pi i G_R(\mathbf{q}, \omega - z' + i\eta) \left[\tanh\left(\frac{1}{2}\beta(\omega - z')\right) + \coth\left(\frac{1}{2}\beta z'\right) \right] \right\} \boldsymbol{\tau}_3. \tag{2.68}$$

Since the Matsubara frequencies are non-zero, we set η to zero. We drop the prime notation on z and write:[9]

$$\Sigma(\mathbf{k}, \omega) = -\int \frac{d^3\mathbf{q}}{(2\pi)^3} \int_{-\infty}^{\infty} dz \alpha^2(\mathbf{q}, \mathbf{k}) B(\mathbf{k} - \mathbf{q}, z) \boldsymbol{\tau}_3 2\text{Im} \left[iT \sum_{m=0}^{\infty} \frac{G_R(\mathbf{q}, i\omega_m)}{\omega - i\omega_m - z} \right] \boldsymbol{\tau}_3$$

$$+\frac{1}{2} \int \frac{d^3\mathbf{q}}{(2\pi)^3} \int_{-\infty}^{\infty} dz \alpha^2(\mathbf{q}, \mathbf{k}) B(\mathbf{k} - \mathbf{q}, z) \boldsymbol{\tau}_3 G_R(\mathbf{q}, \omega - z + i\eta) \boldsymbol{\tau}_3$$

$$\times \left[\tanh\left(\frac{1}{2}\beta(\omega - z)\right) + \coth\left(\frac{1}{2}\beta z\right) \right]. \tag{2.69}$$

---

[9]We apply the identities $\text{Im}(iw) = \text{Re}(w)$, $\text{Re}(-iw) = \text{Im}(w)$, and $2\text{Im}(iw) = 2\text{Re}(w) = w + w^*$.

Therefore, we have

$$\Sigma(\mathbf{k}, \omega) = -\int \frac{d^3\mathbf{q}}{(2\pi)^3} \int_{-\infty}^{\infty} dz \, \alpha^2(\mathbf{q}, \mathbf{k}) B(\mathbf{k} - \mathbf{q}, z) \boldsymbol{\tau}_3 \left[T \sum_{m=0}^{\infty} \frac{G_R(\mathbf{q}, i\omega_m)}{\omega - i\omega_m - z} + T \sum_{m=0}^{\infty} \frac{G_R^*(\mathbf{q}, i\omega_m)}{\omega + i\omega_m - z} \right] \boldsymbol{\tau}_3$$

$$+ \frac{1}{2} \int \frac{d^3\mathbf{q}}{(2\pi)^3} \int_{-\infty}^{\infty} dz \, \alpha^2(\mathbf{q}, \mathbf{k}) B(\mathbf{k} - \mathbf{q}, z) \boldsymbol{\tau}_3 G_R(\mathbf{q}, \omega - z + i\eta) \boldsymbol{\tau}_3$$

$$\times \left[\tanh\left(\frac{1}{2}\beta(\omega - z)\right) + \coth\left(\frac{1}{2}\beta z\right) \right]. \tag{2.70}$$

The conjugate of the Green's function is defined as $G_R^*(\mathbf{q}, i\omega_m) = G_R(\mathbf{q}, -i\omega_m)$. Also, the Fermi-Dirac and Bose-Einstein distribution functions obeys the following relations:

$$1 - 2f(x) = \tanh\left(\frac{1}{2}\beta x\right), \tag{2.71}$$

$$1 + 2N(x) = \coth\left(\frac{1}{2}\beta x\right). \tag{2.72}$$

As a result, the electron self energy becomes

$$\Sigma(\mathbf{k}, \omega) = -\int \frac{d^3\mathbf{q}}{(2\pi)^3} \int_{-\infty}^{\infty} dz \, \alpha^2(\mathbf{q}, \mathbf{k}) B(\mathbf{k} - \mathbf{q}, z) \boldsymbol{\tau}_3 \left[T \sum_{m=0}^{\infty} \frac{G_R(\mathbf{q}, i\omega_m)}{\omega - i\omega_m - z} + T \sum_{m=0}^{\infty} \frac{G_R(\mathbf{q}, -i\omega_m)}{\omega + i\omega_m - z} \right] \boldsymbol{\tau}_3$$

$$+ \int \frac{d^3\mathbf{q}}{(2\pi)^3} \int_{-\infty}^{\infty} dz \, \alpha^2(\mathbf{q}, \mathbf{k}) B(\mathbf{k} - \mathbf{q}, z) \boldsymbol{\tau}_3 G_R(\mathbf{q}, \omega - z + i\eta) \boldsymbol{\tau}_3 \left[f(z - \omega) + N(z) \right]. \tag{2.73}$$

Now, let us consider density of states which is constant near the Fermi surface. Therefore, the integration over momentum $\mathbf{q}$ is approximated as follows

$$\int \frac{d^3\mathbf{q}}{(2\pi)^3} h(\mathbf{q}) = \int_{-\mu}^{\infty} d\xi N(\xi) \int \frac{d\Omega}{4\pi} h(\xi, \Omega) \approx N(0) \int_{-\infty}^{\infty} d\xi h(\xi). \tag{2.74}$$

Here, h depends on the magnitude of $\mathbf{q}$, and $N(0)$ is the density of states at the Fermi surface. In addition, B is peaked about the Fermi surface, so we can write

$$\Sigma(\mathbf{k}, \omega) = -\int_{-\infty}^{\infty} dz \frac{\alpha^2 F(z)}{N(0)} T \sum_{m=0}^{\infty} \int \frac{d^3\mathbf{q}}{(2\pi)^3} \boldsymbol{\tau}_3 \left[\frac{G_R(\mathbf{q}, i\omega_m)}{\omega - i\omega_m - z} + \frac{G_R(\mathbf{q}, -i\omega_m)}{\omega + i\omega_m - z} \right] \boldsymbol{\tau}_3$$

$$+ \int_{-\infty}^{\infty} dz \frac{\alpha^2 F(z)}{N(0)} \int \frac{d^3\mathbf{q}}{(2\pi)^3} \boldsymbol{\tau}_3 G_R(\mathbf{q}, \omega - z + i\eta) \boldsymbol{\tau}_3 \left[f(z - \omega) + N(z) \right], \tag{2.75}$$

where $\alpha^2 F(z)$ is defined as the Eliashberg function. The inverse of the Nambu Green's function is

$$G^{-1}(\mathbf{q}, i\omega_m) = \widetilde{\omega}(i\omega_m) \boldsymbol{\tau}_0 - \xi_{\mathbf{q}} \boldsymbol{\tau}_3 - \phi(i\omega_m) \boldsymbol{\tau}_2. \tag{2.76}$$

Inverting this equation gives

$$G(\mathbf{q}, i\omega_m) = \frac{\widetilde{\omega}(i\omega_m) \boldsymbol{\tau}_0 + \xi_{\mathbf{q}} \boldsymbol{\tau}_3 + \phi(i\omega_m) \boldsymbol{\tau}_2}{\widetilde{\omega}^2 - E^2}, \tag{2.77}$$

13

where $E^2(i\omega_m) = \xi^2 + \phi^2(i\omega_m)$. The momentum integration of the Green's function is

$$
\begin{aligned}
\int \frac{d^3\mathbf{q}}{(2\pi)^3} G_R(\mathbf{q}, \omega - z + i\eta) &= N(0) \int_{-\infty}^{\infty} d\xi \frac{\widetilde{\omega}(\omega - z)\boldsymbol{\tau}_0 + \xi\boldsymbol{\tau}_3 + \phi(\omega - z)\boldsymbol{\tau}_2}{\widetilde{\omega}^2 - \xi^2 - \phi^2(i\omega_m)} \\
&= N(0) \int_{-\infty}^{\infty} d\xi \frac{\widetilde{\omega}(\omega - z)\boldsymbol{\tau}_0 + \phi(\omega - z)\boldsymbol{\tau}_2}{\widetilde{\omega}^2(\omega - z) - \xi^2 - \phi^2(\omega - z)} \\
&= -N(0)[\widetilde{\omega}(\omega - z)\boldsymbol{\tau}_0 + \phi(\omega - z)\boldsymbol{\tau}_2] \int_{-\infty}^{\infty} \frac{d\xi}{(\xi - \xi_0)(\xi + \xi_0)} \\
&= -i\pi N(0)[\widetilde{\omega}(\omega - z)\boldsymbol{\tau}_0 + \phi(\omega - z)\boldsymbol{\tau}_2] \frac{\mathrm{sgn}(\mathrm{Im}(\xi_0))}{\xi_0},
\end{aligned}
\tag{2.78}
$$

where $\xi_0 = \sqrt{\widetilde{\omega}^2(\omega - z) - \phi^2(\omega - z)}$ has positive imaginary part. The momentum integration of the Green's function is

$$
\int \frac{d^3\mathbf{q}}{(2\pi)^3} \boldsymbol{\tau}_3 G_R(\mathbf{q}, \omega - z + i\eta)\boldsymbol{\tau}_3 = -i\pi N(0) \frac{[\widetilde{\omega}(\omega - z)\boldsymbol{\tau}_0 - \phi(\omega - z)\boldsymbol{\tau}_2]}{\sqrt{\widetilde{\omega}^2(\omega - z) - \phi^2(\omega - z)}}.
\tag{2.79}
$$

Then, the electron self energy becomes

$$
\begin{aligned}
\Sigma(\mathbf{k}, \omega) = &-\int_{-\infty}^{\infty} dz \frac{\alpha^2 F(z)}{N(0)} T \sum_{m=0}^{\infty} \int \frac{d^3\mathbf{q}}{(2\pi)^3} \boldsymbol{\tau}_3 \left[\frac{G_R(\mathbf{q}, i\omega_m)}{\omega - i\omega_m - z} + \frac{G_R(\mathbf{q}, -i\omega_m)}{\omega + i\omega_m - z} \right] \boldsymbol{\tau}_3 \\
&+ \int_{-\infty}^{\infty} dz \alpha^2 F(z) i\pi \frac{[\widetilde{\omega}(\omega - z)\boldsymbol{\tau}_0 - \phi(\omega - z)\boldsymbol{\tau}_2]}{\sqrt{\phi^2(\omega - z) - \widetilde{\omega}^2(\omega - z)}} [f(z - \omega) + N(z)].
\end{aligned}
\tag{2.80}
$$

We define the function λ by:

$$
\lambda(\nu) = -\int_{-\infty}^{\infty} dz \frac{\alpha^2 F(z)}{\nu - z + i\eta}.
\tag{2.81}
$$

The function ϕ is an even function and $\widetilde{\omega}$ is an odd function of frequency. Now, we write

$$
\begin{aligned}
\Sigma(\mathbf{k}, \omega) = &-T \sum_{m=0}^{\infty} \int \frac{d^3\mathbf{q}}{(2\pi)^3} [\lambda(\omega - i\omega_m) - \lambda(\omega + i\omega_m)]i\pi \frac{\widetilde{\omega}(i\omega_m)\boldsymbol{\tau}_0}{\sqrt{\widetilde{\omega}^2(i\omega_m) - \phi^2(i\omega_m)}} \\
&+ T \sum_{m=0}^{\infty} \int \frac{d^3\mathbf{q}}{(2\pi)^3} [\lambda(\omega - i\omega_m) + \lambda(\omega + i\omega_m)]i\pi \frac{\phi(i\omega_m)\boldsymbol{\tau}_2}{\sqrt{\widetilde{\omega}^2(i\omega_m) - \phi^2(i\omega_m)}} \\
&- \int_{-\infty}^{\infty} dz \alpha^2 F(z) i\pi \frac{[\widetilde{\omega}(\omega - z)\boldsymbol{\tau}_0 - \phi(\omega - z)\boldsymbol{\tau}_2]}{\sqrt{\widetilde{\omega}^2(\omega - z) - \phi^2(\omega - z)}} [f(z - \omega) + N(z)].
\end{aligned}
\tag{2.82}
$$

The Green's function is defined as

$$
G^{-1}(\mathbf{k}, \omega) = \widetilde{\omega}(\omega)\boldsymbol{\tau}_0 - \xi_\mathbf{k}\boldsymbol{\tau}_3 - \phi(\omega)\boldsymbol{\tau}_2 = G_0^{-1}(\mathbf{k}, \omega) - \Sigma(\mathbf{k}, \omega) = \omega\boldsymbol{\tau}_0 - \xi_\mathbf{k}\boldsymbol{\tau}_3 - \Sigma(\mathbf{k}, \omega).
\tag{2.83}
$$

Comparing the coefficients of $\boldsymbol{\tau}_0$ and $\boldsymbol{\tau}_2$ determines the self-consistent equations for $\widetilde{\omega}$ and ϕ.

$$
\begin{aligned}
\widetilde{\omega}(\omega) = \omega &+ T \sum_{m=0}^{\infty} [\lambda(\omega - i\omega_m) - \lambda(\omega + i\omega_m)]i\pi \frac{\widetilde{\omega}(i\omega_m)}{\sqrt{\widetilde{\omega}^2(i\omega_m) - \phi^2(i\omega_m)}} \\
&+ \int_{-\infty}^{\infty} dz \alpha^2 F(z) i\pi \frac{\widetilde{\omega}(\omega - z)}{\sqrt{\widetilde{\omega}^2(\omega - z) - \phi^2(\omega - z)}} [f(z - \omega) + N(z)],
\end{aligned}
\tag{2.84}
$$

14

and

$$\phi(\omega) = i\pi T \sum_{m=0}^{\infty} [\lambda(\omega - i\omega_m) + \lambda(\omega + i\omega_m)] \frac{\phi(i\omega_m)}{\sqrt{\widetilde{\omega}^2(i\omega_m) - \phi^2(i\omega_m)}}$$
$$+ \int_{-\infty}^{\infty} dz \alpha^2 F(z) i\pi \frac{\phi(\omega - z)}{\sqrt{\widetilde{\omega}^2(\omega - z) - \phi^2(\omega - z)}} [f(z - \omega) + N(z)]. \tag{2.85}$$

We define the functions $Z(\omega)$ and $\phi(\omega)$ by

$$Z(\omega)\Delta(\omega) = \phi(\omega), \tag{2.86}$$
$$\widetilde{\omega}(\omega) = \omega Z(\omega). \tag{2.87}$$

Therefore,

$$Z(\omega) = 1 + \frac{\pi T}{\omega} \sum_{m=0}^{\infty} [\lambda(\omega - i\omega_m) - \lambda(\omega + i\omega_m)] \frac{i\omega_m}{\sqrt{\omega_m^2 + \Delta^2(i\omega_m)}}$$
$$+ \frac{i\pi}{\omega} \int_{-\infty}^{\infty} dz \alpha^2 F(z) \frac{\omega - z}{\sqrt{(\omega - z)^2 - \Delta^2(\omega - z)}} [f(z - \omega) + N(z)]. \tag{2.88}$$

$$Z(\omega)\Delta(\omega) = \pi T \sum_{m=0}^{\infty} [\lambda(\omega - i\omega_m) + \lambda(\omega + i\omega_m)] \frac{\Delta(i\omega_m)}{\sqrt{\omega_m^2 + \Delta^2(i\omega_m)}}$$
$$+ i\pi \int_{-\infty}^{\infty} dz \alpha^2 F(z) \frac{\Delta(\omega - z)}{\sqrt{(\omega - z)^2 - \Delta^2(\omega - z)}} [f(z - \omega) + N(z)]. \tag{2.89}$$

The model for $F(z)$ is

$$\alpha^2 F(z) = \sum_{z_0} [\delta(z - z_0) - \delta(z + z_0)] A(z_0), \tag{2.90}$$

where the resonant frequency z_0 is the Einstein frequency ω_E. The bosonic propagator can be computed as

$$\lambda(\nu) = -\int_{-\infty}^{\infty} dz \frac{\alpha^2 F(z)}{\nu - z + i\eta},$$
$$= -A(\omega_E) \int_{-\infty}^{\infty} dz \frac{\delta(z - \omega_E) - \delta(z + \omega_E)}{\nu - z + i\eta} = \frac{2\omega_E A(\omega_E)}{\omega_E^2 - \nu^2}. \tag{2.91}$$

Replacing $z = \omega + i0^+$ and the functional form of $\alpha^2 F(z)$ into Eq.(2.88) and Eq.(2.89) gives

$$Z(z)\Delta(z) = \pi T \sum_{m=-\infty}^{\infty} \lambda(z - i\omega_m) \frac{\Delta(i\omega_m)}{\sqrt{\omega_m^2 + \Delta^2(i\omega_m)}}$$
$$+ i\pi A(\omega_E) \left\{ \frac{\Delta(z - \omega_E)[f(\omega_E - z) + N(\omega_E)]}{\sqrt{(z - \omega_E)^2 - \Delta^2(z - \omega_E)}} + \frac{\Delta(z + \omega_E)[f(\omega_E + z) + N(\omega_E)]}{\sqrt{(z + \omega_E)^2 - \Delta^2(z + \omega_E)}} \right\} \tag{2.92}$$

$$Z(z) = 1 + \frac{i\pi T}{z} \sum_{m=-\infty}^{\infty} \lambda(z - i\omega_m) \frac{\omega_m}{\sqrt{\omega_m^2 + \Delta^2(i\omega_m)}}$$
$$+ \frac{i\pi A(\omega_E)}{z} \left\{ \frac{(z - \omega_E)[f(\omega_E - z) + N(\omega_E)]}{\sqrt{(z - \omega_E)^2 - \Delta^2(z - \omega_E)}} + \frac{(z + \omega_E)[f(\omega_E + z) + N(\omega_E)]}{\sqrt{(z + \omega_E)^2 - \Delta^2(z + \omega_E)}} \right\}. \tag{2.93}$$

Equation (2.92) and Eq.(2.93) are the Eliashberg equations on the real frequency axis and are valid for any temperature [17].

C. Electron self energy on the imaginary axis

By substituting $z = i\omega_n$ in the Eliashberg equations on the real axis, we obtain the imaginary Eliashberg equations by analytic continuation.

$$Z(i\omega_n)\Delta(i\omega_n) = \pi T \sum_{m=-\infty}^{\infty} \lambda(i\omega_n - i\omega_m)\frac{\Delta(i\omega_m)}{\sqrt{\omega_m^2 + \Delta^2(i\omega_m)}}$$
$$+i\pi A(\omega_E)\frac{\Delta(i\omega_n - \omega_E)[f(\omega_E - i\omega_n) + N(\omega_E)]}{\sqrt{(i\omega_n - \omega_E)^2 - \Delta^2(i\omega_n - \omega_E)}}$$
$$+i\pi A(\omega_E)\frac{\Delta(i\omega_n + \omega_E)[f(\omega_E + i\omega_n) + N(\omega_E)]}{\sqrt{(i\omega_n + \omega_E)^2 - \Delta^2(i\omega_n + \omega_E)}}, \tag{2.94}$$

and

$$Z(i\omega_n) = 1 + \frac{\pi T}{\omega_n} \sum_{m=-\infty}^{\infty} \lambda(i\omega_n - i\omega_m)\frac{\omega_m}{\sqrt{\omega_m^2 + \Delta^2(i\omega_m)}}$$
$$+\frac{\pi A(\omega_E)}{\omega_n}\frac{(i\omega_n - \omega_E)[f(\omega_E - i\omega_n) + N(\omega_E)]}{\sqrt{(i\omega_n - \omega_E)^2 - \Delta^2(i\omega_n - \omega_E)}}$$
$$+\frac{\pi A(\omega_E)}{\omega_n}\frac{(i\omega_n + \omega_E)[f(\omega_E + i\omega_n) + N(\omega_E)]}{\sqrt{(i\omega_n + \omega_E)^2 - \Delta^2(i\omega_n + \omega_E)}}, \tag{2.95}$$

Since

$$f(\omega_E - i\omega_n) + N(\omega_E) = \frac{1}{[\exp(\beta\omega_E) - 1]} + \frac{1}{[\exp(\beta\omega_E - i(2m+1)\pi) + 1)]} = 0, \tag{2.96}$$

and

$$f(\omega_E + i\omega_n) + N(\omega_E) = 0, \tag{2.97}$$

the second terms of Eq.(2.94) and Eq.(2.95) do not contribute. The imaginary frequency axis Eliashberg equations are thus

$$Z(i\omega_n)\Delta(i\omega_n) = \pi T \sum_{m=-\infty}^{\infty} \lambda(i\omega_n - i\omega_m)\frac{\Delta(i\omega_m)}{\sqrt{\omega_m^2 + \Delta^2(i\omega_m)}}, \tag{2.98}$$

$$Z(i\omega_n) = 1 + \frac{\pi T}{\omega_n} \sum_{m=-\infty}^{\infty} \lambda(i\omega_n - i\omega_m)\frac{\omega_m}{\sqrt{\omega_m^2 + \Delta^2(i\omega_m)}}, \tag{2.99}$$

The electron self energy on the imaginary axis can also be explicitly calculated using imaginary frequency from the outset in a similar manner to the previous section as follows:

$$\Sigma(\mathbf{k}, i\omega_n) = -\frac{1}{\pi} \int \frac{d^3\mathbf{q}}{(2\pi)^3} \int_{-\infty}^{\infty} dz' \int_{-\infty}^{\infty} dz\boldsymbol{\tau}_3 \frac{\text{Im}G_R(\mathbf{q}, z)}{i\omega_n - (z + z')}\boldsymbol{\tau}_3\alpha^2(\mathbf{q}, \mathbf{k})B(\mathbf{k} - \mathbf{q}, z')$$
$$\times\frac{1}{2}\left[\tanh\left(\frac{1}{2}\beta z\right) + \coth\left(\frac{1}{2}\beta z'\right)\right]. \tag{2.100}$$

16

Writing this equation in terms of real and imaginary parts gives

$$\Sigma(\mathbf{k}, i\omega_n) = \int \frac{d^3\mathbf{q}}{(2\pi)^3} \int_{-\infty}^{\infty} dz' \boldsymbol{\tau}_3 \mathrm{Im} \left\{ \int_{-\infty}^{\infty} \frac{dz}{4\pi} G_R(\mathbf{q}, z) \left[\frac{1}{z + z' - i\omega_n} + \frac{1}{z + z' + i\omega_n} \right] \right\} \boldsymbol{\tau}_3$$

$$\times \alpha^2(\mathbf{q}, \mathbf{k}) B(\mathbf{k} - \mathbf{q}, z') \left[\tanh\left(\frac{1}{2}\beta z\right) + \coth\left(\frac{1}{2}\beta z'\right) \right],$$

$$- \int \frac{d^3\mathbf{q}}{(2\pi)^3} \int_{-\infty}^{\infty} dz' \boldsymbol{\tau}_3 i\mathrm{Re} \left\{ \int_{-\infty}^{\infty} \frac{dz}{4\pi} G_R(\mathbf{q}, z) \left[\frac{1}{z + z' - i\omega_n} - \frac{1}{z + z' + i\omega_n} \right] \right\} \boldsymbol{\tau}_3$$

$$\times \alpha^2(\mathbf{q}, \mathbf{k}) B(\mathbf{k} - \mathbf{q}, z') \left[\tanh\left(\frac{1}{2}\beta z\right) + \coth\left(\frac{1}{2}\beta z'\right) \right]. \tag{2.101}$$

Again, we compute the integration over z as a contour integral in the upper half plane. The retarded Green's function is an analytic function in the upper half plane, therefore only the pole at $z = i\omega_n - z'$ and the poles of the tanh function at $z = i(2m+1)\pi T = i\omega_m$, $m \in \{0, 1, 2, ...\}$ are included. The residue of the pole at $z = i(2m+1)\pi T = i\omega_m$ is $2T$ whereas the residue of the poles at $z = i\omega_n - z'$ is -1. Moreover, the semi-circle contribution to the contour integral vanishes because $G_R \to 1/z$ as $z \to \infty$. Since $\tanh(\frac{1}{2}(i\omega_n - z')) = -\coth(\frac{1}{2}\beta z')$, the poles at $z = i\omega_n - z'$ give zero contribution to the self energy. Assuming the phonon spectral function is peaked about the Fermi surface, the electron self energy is

$$\Sigma(\mathbf{k}, i\omega_n) = \int \frac{d^3\mathbf{q}}{(2\pi)^3} \int_{-\infty}^{\infty} dz \boldsymbol{\tau}_3 \mathrm{Im} \left\{ iT \sum_{m=0}^{\infty} G_R(\mathbf{q}, i\omega_m) \left[\frac{1}{z + i\omega_m - i\omega_n} + \frac{1}{z + i\omega_m + i\omega_n} \right] \right\} \boldsymbol{\tau}_3 \frac{\alpha^2 F(z)}{N(0)}$$

$$- \int \frac{d^3\mathbf{q}}{(2\pi)^3} \int_{-\infty}^{\infty} dz \boldsymbol{\tau}_3 i\mathrm{Re} \left\{ iT \sum_{m=0}^{\infty} G_R(\mathbf{q}, i\omega_m) \left[\frac{1}{z + i\omega_m - i\omega_n} - \frac{1}{z + i\omega_m + i\omega_n} \right] \right\} \boldsymbol{\tau}_3 \frac{\alpha^2 F(z)}{N(0)}. \tag{2.102}$$

Now, the integration over z gives

$$\Sigma(\mathbf{k}, i\omega_n) = \frac{1}{N(0)} \int \frac{d^3\mathbf{q}}{(2\pi)^3} \boldsymbol{\tau}_3 \mathrm{Im} \left\{ iT \sum_{m=0}^{\infty} G_R(\mathbf{q}, i\omega_m)[\lambda(i\omega_n - i\omega_m) + \lambda(i\omega_n + i\omega_m)] \right\} \boldsymbol{\tau}_3$$

$$- \frac{1}{N(0)} \int \frac{d^3\mathbf{q}}{(2\pi)^3} \boldsymbol{\tau}_3 i\mathrm{Re} \left\{ iT \sum_{m=0}^{\infty} G_R(\mathbf{q}, i\omega_m)[\lambda(i\omega_n - i\omega_m) - \lambda(i\omega_n + i\omega_m)] \right\} \boldsymbol{\tau}_3$$

$$= \frac{1}{2N(0)} \int \frac{d^3\mathbf{q}}{(2\pi)^3} \boldsymbol{\tau}_3 T \sum_{m=0}^{\infty} [G_R(\mathbf{q}, i\omega_m) + G_R(\mathbf{q}, -i\omega_m)][\lambda(i\omega_n - i\omega_m) + \lambda(i\omega_n + i\omega_m)]\boldsymbol{\tau}_3$$

$$+ \frac{1}{2N(0)} \int \frac{d^3\mathbf{q}}{(2\pi)^3} \boldsymbol{\tau}_3 T \sum_{m=0}^{\infty} [G_R(\mathbf{q}, i\omega_m) - G_R(\mathbf{q}, -i\omega_m)][\lambda(i\omega_n - i\omega_m) - \lambda(i\omega_n + i\omega_m)]\boldsymbol{\tau}_3. \tag{2.103}$$

Here, we have used the fact that λ is a purely-real function, which can be proved using the property that $F(-z) = -F(z)$ as follows

$$\lambda(-i\nu_n) = -\int_{-\infty}^{\infty} dz \frac{\alpha^2 F(z)}{-i\nu_n - z} = \int_{-\infty}^{\infty} dz \frac{\alpha^2 F(z)}{i\nu_n + z} = -\int_{-\infty}^{\infty} dz \frac{\alpha^2 F(z)}{i\nu_n - z} = \lambda(i\nu_n). \tag{2.104}$$

17

The momentum integration of the Green's function is performed

$$\Sigma(\mathbf{k}, i\omega_n) = \frac{-i\pi T}{2} \sum_{m=0}^{\infty} \left[\frac{\widetilde{\omega}(i\omega_m)\boldsymbol{\tau}_0 - \phi(i\omega_m)\boldsymbol{\tau}_2}{\sqrt{\widetilde{\omega}^2(i\omega_m) - \phi^2(i\omega_m)}} - \frac{\widetilde{\omega}(i\omega_m)\boldsymbol{\tau}_0 + \phi(i\omega_m)\boldsymbol{\tau}_2}{\sqrt{\widetilde{\omega}^2(i\omega_m) - \phi^2(i\omega_m)}} \right] [\lambda(i\omega_n - i\omega_m) + \lambda(i\omega_n + i\omega_m)]$$

$$-\frac{i\pi T}{2} \sum_{m=0}^{\infty} \left[\frac{\widetilde{\omega}(i\omega_m)\boldsymbol{\tau}_0 - \phi(i\omega_m)\boldsymbol{\tau}_2}{\sqrt{\widetilde{\omega}^2(i\omega_m) - \phi^2(i\omega_m)}} + \frac{\widetilde{\omega}(i\omega_m)\boldsymbol{\tau}_0 + \phi(i\omega_m)\boldsymbol{\tau}_2}{\sqrt{\widetilde{\omega}^2(i\omega_m) - \phi^2(i\omega_m)}} \right] [\lambda(i\omega_n - i\omega_m) - \lambda(i\omega_n + i\omega_m)]. \quad (2.105)$$

Simplifying this equation further gives

$$\Sigma(\mathbf{k}, i\omega_n) = i\pi T \sum_{m=0}^{\infty} \frac{\phi(i\omega_m)\boldsymbol{\tau}_2}{\sqrt{\widetilde{\omega}^2(i\omega_m) - \phi^2(i\omega_m)}} [\lambda(i\omega_n - i\omega_m) + \lambda(i\omega_n + i\omega_m)]$$

$$- i\pi T \sum_{m=0}^{\infty} \frac{\widetilde{\omega}(i\omega_m)\boldsymbol{\tau}_0}{\sqrt{\widetilde{\omega}^2(i\omega_m) - \phi^2(i\omega_m)}} [\lambda(i\omega_n - i\omega_m) - \lambda(i\omega_n + i\omega_m)]$$

$$= - i\pi T \sum_{m=-\infty}^{\infty} \lambda(i\omega_n - i\omega_m) \left[\frac{\widetilde{\omega}(i\omega_m)\boldsymbol{\tau}_0}{\sqrt{\widetilde{\omega}^2(i\omega_m) - \phi^2(i\omega_m)}} - \frac{\phi(i\omega_m)\boldsymbol{\tau}_2}{\sqrt{\widetilde{\omega}^2(i\omega_m) - \phi^2(i\omega_m)}} \right]. \quad (2.106)$$

Using the definition of the Green's function and comparing the coefficient of the Pauli matrices determines the self-consistent equations for $\widetilde{\omega}$ and ϕ on the imaginary axis.

$$\widetilde{\omega}(i\omega_n) = i\omega_n + i\pi T \sum_{m=-\infty}^{\infty} \lambda(i\omega_n - i\omega_m) \frac{\widetilde{\omega}(i\omega_m)}{\sqrt{\widetilde{\omega}^2(i\omega_m) - \phi^2(i\omega_m)}}, \quad (2.107)$$

$$\phi(i\omega_n) = i\pi T \sum_{m=-\infty}^{\infty} \lambda(i\omega_n - i\omega_m) \frac{\phi(i\omega_m)}{\sqrt{\widetilde{\omega}^2(i\omega_m) - \phi^2(i\omega_m)}}. \quad (2.108)$$

Here, we define the functions $Z(\omega)$ and $\Delta(\omega)$ using $\widetilde{\omega} = \omega Z(\omega)$ and $Z(\omega)\Delta(\omega) = \phi(\omega)$. To the lowest order in λ, $Z \approx 1$ and inserting this approximation into Eq.(2.107) and Eq.(2.108) then produces the same result as Eq.(2.98) and Eq.(2.99) [21].

$$Z(i\omega_n)\Delta(i\omega_n) = \pi T \sum_{m=-\infty}^{\infty} \lambda(i\omega_n - i\omega_m) \frac{\Delta(i\omega_n)}{\sqrt{\omega_m^2 + \Delta^2(i\omega_m)}}, \quad (2.109)$$

$$Z(i\omega_n) = 1 + \frac{\pi}{\omega_n} T \sum_{m=-\infty}^{\infty} \lambda(i\omega_n - i\omega_m) \frac{\omega_m}{\sqrt{\omega_m^2 + \Delta^2(i\omega_m)}}. \quad (2.110)$$

III.   ELIASHBERG THEORY IN THE WEAK-COUPLING LIMIT

A.   Imaginary-axis calculations

1.   Renormalization factor

At the transition temperature $T = T_c$ the gap function vanishes. The energy gap and renormalization functions at the transition temperature are defined as follows [21]:

$$Z(i\omega_n)\Delta(i\omega_n) = \pi T_c \sum_{m=-\infty}^{\infty} \lambda(i\omega_n - i\omega_m) \frac{\Delta(i\omega_m)}{|\omega_m|}, \quad (3.1)$$

$$Z(i\omega_n) = 1 + \frac{\pi T_c}{\omega_n} \sum_{m=-\infty}^{\infty} \lambda(i\omega_n - i\omega_m)\text{sgn}(\omega_m). \quad (3.2)$$

These two equations are the standard linearized Eliashberg equations. Here, $\omega_m = (2m+1)\pi k_B T$ and $\nu_m = 2m\pi k_B T$ are the fermionic and bosonic Matsubara frequencies respectively. One can rewrite $Z(i\omega_n)$ appearing in Eq.(3.1) in a closed form:

$$Z(i\omega_n) = 1 + \frac{\pi T_c}{\omega_n}\left[\sum_{m=0}^{\infty}\lambda(i\omega_n - i\omega_m) - \sum_{m=-\infty}^{-1}\lambda(i\omega_n - i\omega_m)\right]$$

$$= 1 + \frac{\pi T_c}{\omega_n}\sum_{m=0}^{\infty}[\lambda(i\omega_n - i\omega_m) - \lambda(i\omega_n + i\omega_m)]. \tag{3.3}$$

The first sum in the above equation can be calculated as

$$\sum_{m=0}^{\infty}\lambda(i\omega_n - i\omega_m) = \sum_{m=0}^{2n}\lambda(i\omega_n - i\omega_m) + \sum_{m=2n+1}^{\infty}\lambda(i\omega_n - i\omega_m),$$

$$= \sum_{m=0}^{2n}\lambda(i\omega_n - i\omega_m) + \sum_{k=0}^{\infty}\lambda(-i\omega_n - i\omega_k). \tag{3.4}$$

Since $\lambda(i\omega_n)$ is an even function of ω_n, one can write

$$\sum_{m=0}^{\infty}\lambda(i\omega_n - i\omega_m) = \sum_{m=0}^{2n}\lambda(i\omega_n - i\omega_m) + \sum_{m=0}^{\infty}\lambda(i\omega_n + i\omega_m). \tag{3.5}$$

Thus, the function $Z(i\omega_n)$ becomes

$$Z(i\omega_n) = 1 + \frac{\pi T_c}{\omega_n}\sum_{m=0}^{2n}\lambda(i\omega_n - i\omega_m),$$

$$= 1 + \frac{\pi T_c}{\omega_n}\sum_{m=0}^{n-1}\lambda(i\omega_n - i\omega_m) + \frac{\pi T_c}{\omega_n}\lambda(0) + \frac{\pi T_c}{\omega_n}\sum_{m=n+1}^{2n}\lambda(i\omega_n - i\omega_m),$$

$$= 1 + \frac{\pi T_c}{\omega_n}\sum_{k=0}^{n-1}\lambda(i\nu_{k+1}) + \frac{\pi T_c}{\omega_n}\lambda + \frac{\pi T_c}{\omega_n}\sum_{k=0}^{n-1}\lambda(i\nu_{k+1}),$$

$$= 1 + \frac{\pi T_c}{\omega_n}\left[\lambda + 2\sum_{m=0}^{n-1}\lambda(i\nu_{m+1})\right]. \tag{3.6}$$

The dimensionless electron-phonon coupling constant λ on the imaginary axis is

$$\lambda(i\nu_n) = \frac{\lambda\omega_E^2}{\omega_E^2 + \nu_n^2}. \tag{3.7}$$

The phonon spectral function is

$$\alpha^2 F(\nu) = \frac{\lambda\omega_E}{2}\delta(\nu - \omega_E), \tag{3.8}$$

which represents a single Einstein harmonic oscillator with weighting factor A at frequency ω_E. Here,

$$A(\omega_E) = \frac{\lambda\omega_E}{2}. \tag{3.9}$$

The linearized gap equation is

$$Z(i\omega_n)\Delta(i\omega_n) = \pi T_c \sum_{m=-\infty}^{\infty} \frac{\lambda\omega_E^2}{\omega_E^2 + (\omega_n - \omega_m)^2} \frac{\Delta(i\omega_m)}{|\omega_m|} = \lambda\pi\bar{T}_c \sum_{m=-\infty}^{\infty} \frac{1}{1 + (\bar{\omega}_n - \bar{\omega}_m)^2} \frac{\Delta(i\omega_m)}{|\bar{\omega}_m|}, \quad (3.10)$$

where $\bar{Q} \equiv Q/\omega_E$ and $\bar{\omega}_E \equiv \omega_E/(2\pi T)$. Utilizing the form of $\lambda(i\nu_n)$, the renormalization function $Z(i\omega_n)$ is evaluated as follows:

$$\begin{aligned}
Z(i\omega_n) &= 1 + \frac{\pi T_c}{\omega_n}\left[\lambda + 2\sum_{m=0}^{n-1}\lambda(i\nu_{m+1})\right], \\
&= 1 + \frac{\pi T_c}{\omega_n}\left\{\lambda + 2\sum_{m=0}^{n-1}\frac{\lambda\omega_E^2}{\omega_E^2 + [2\pi T_c(m+1)]^2}\right\}, \\
&= 1 + \frac{\lambda}{2\bar{\omega}_E\bar{\omega}_n}\left\{1 - i\bar{\omega}_E\sum_{m=0}^{n-1}\left[\frac{1}{m+1-i\bar{\omega}_E} - \frac{1}{m+1+i\bar{\omega}_E}\right]\right\}.
\end{aligned} \quad (3.11)$$

Using the properties of digamma functions[10], we obtain

$$\begin{aligned}
Z(i\omega_n) =& 1 + \frac{\lambda}{2\bar{\omega}_E\bar{\omega}_n}\bigg\{1 - i\bar{\omega}_E\Big[\psi(n+1-i\bar{\omega}_E) - \psi(1-i\bar{\omega}_E), \\
&- \psi(n+1+i\bar{\omega}_E) + \psi(1+i\bar{\omega}_E)\Big]\bigg\}, \\
=& 1 + \frac{\lambda}{2\bar{\omega}_E\bar{\omega}_n}\bigg\{1 - i\bar{\omega}_E[\psi(n+1-i\bar{\omega}_E) - \psi(n+1+i\bar{\omega}_E) - i/\bar{\omega}_E + i\pi\coth(\pi\bar{\omega}_E)]\bigg\}, \\
=& 1 - \frac{i\lambda}{2\bar{\omega}_n}\big[\psi(n+1-i\bar{\omega}_E) - \psi(n+1+i\bar{\omega}_E) + i\pi\coth(\pi\bar{\omega}_E)]\big], \\
=& 1 - \frac{i\lambda}{2\bar{\omega}_n}[\psi((\bar{\omega}_n-i)\bar{\omega}_E + 1/2) - \psi((\bar{\omega}_n+i)\bar{\omega}_E + 1/2) + i\pi\coth(\pi\bar{\omega}_E)].
\end{aligned} \quad (3.12)$$

Applying the asymptotic expansion of the digamma function, namely, $\psi(z + 1/2) \to \log(z) + \mathcal{O}(z^{-2})$, as $z \to \infty$, it follows that, as $T_c/\omega_E \to 0$, $Z(i\omega_n)$ becomes

$$\begin{aligned}
Z(i\omega_n) =& 1 - \frac{i\lambda}{2\bar{\omega}_n}[\log((1 + i\bar{\omega}_n) - \log(1 - i\bar{\omega}_n) - i\pi + i\pi\coth(\pi\bar{\omega}_E)], \\
=& 1 + \frac{\lambda}{\bar{\omega}_n}\{\arctan(\bar{\omega}_n) + \pi[\coth(\pi\bar{\omega}_E) - 1]\}.
\end{aligned} \quad (3.13)$$

Thus, we have

$$Z(i\omega_n) \approx 1 + \frac{\lambda}{\bar{\omega}_n}\arctan(\bar{\omega}_n). \quad (3.14)$$

In this subsection, the frequency-dependant gap equation on the imaginary axis at the critical temperature is obtained including the renormalization factor. The strength of the interaction will be lowered by including the renormalization function.

---

[10]The properties of gamma and digamma functions are give in Appendix (C).

2. Gap function without renormalization factor

We use Eq.(3.10) and set $Z(i\omega_n) = 1$. The dimensionless gap equation can be written as [21]

$$
\Delta(i\omega_n) = \lambda\pi\bar{T}_c \sum_{m=-\infty}^{\infty} \frac{1}{1+(\bar{\omega}_n-\bar{\omega}_m)^2} \frac{\Delta(i\omega_m)}{|\bar{\omega}_m|}
$$

$$
= \frac{\lambda\pi\bar{T}_c}{1+\bar{\omega}_n^2} \sum_{m=-\infty}^{\infty} \left[1+\frac{2\bar{\omega}_n\bar{\omega}_m-\bar{\omega}_m^2}{1+(\bar{\omega}_n-\bar{\omega}_m)^2}\right] \frac{\Delta(i\omega_m)}{|\bar{\omega}_m|}. \tag{3.15}
$$

As a perturbative solution for Δ in powers of λ, we consider the ansatz

$$
\Delta(i\omega_m) = \frac{1+\lambda f_1(\bar{\omega}_m)}{1+\bar{\omega}_m^2}. \tag{3.16}
$$

If the term proportional to f_1 is neglected, then it follows that

$$
1 = \lambda\pi\bar{T}_c \sum_{m=-\infty}^{\infty} \left[1+\frac{2\bar{\omega}_n\bar{\omega}_m-\bar{\omega}_m^2}{1+(\bar{\omega}_n-\bar{\omega}_m)^2}\right] \frac{1}{|\bar{\omega}_m|} \frac{1}{1+\bar{\omega}_m^2}
$$

$$
= \lambda I_0 + \lambda\pi\bar{T}_c \sum_{m=-\infty}^{\infty} \left[\frac{2\bar{\omega}_n\mathrm{sgn}(\bar{\omega}_m)-|\bar{\omega}_m|}{1+(\bar{\omega}_n-\bar{\omega}_m)^2}\right] \frac{1}{1+\bar{\omega}_m^2}. \tag{3.17}
$$

This equation is an approximation, since the second term depends on ω_n whereas the left-hand side is independent of ω_n. We multiply both sides of this equation by $\pi\bar{T}_c/[|\bar{\omega}_n|(1+\bar{\omega}_n^2)]$ and sum over n, which gives

$$
I_0 = \lambda I_0^2 + \lambda(\pi\bar{T}_c)^2 \sum_{m,n=-\infty}^{\infty} \left[\frac{2\bar{\omega}_n\mathrm{sgn}(\bar{\omega}_m)-|\bar{\omega}_m|}{1+(\bar{\omega}_n-\bar{\omega}_m)^2}\right] \frac{1}{1+\bar{\omega}_m^2} \frac{1}{1+\bar{\omega}_n^2} \frac{1}{|\bar{\omega}_n|},
$$

$$
= \lambda I_0^2 - \lambda(\pi\bar{T}_c)^2 \sum_{m,n=-\infty}^{\infty} \left\{\frac{1}{1+\bar{\omega}_m^2}+\left[\frac{1}{1+(\bar{\omega}_n-\bar{\omega}_m)^2}-\frac{1}{1+\bar{\omega}_m^2}\right]\right\} \frac{|\bar{\omega}_m|-2\bar{\omega}_n\mathrm{sgn}(\bar{\omega}_m)}{(1+\bar{\omega}_m^2)(1+\bar{\omega}_n^2)|\bar{\omega}_n|},
$$

$$
\approx \lambda I_0^2 - \lambda(\pi\bar{T}_c)^2 \sum_{m,n=-\infty}^{\infty} \frac{|\bar{\omega}_m|}{(1+\bar{\omega}_m^2)^2(1+\bar{\omega}_n^2)|\bar{\omega}_n|},
$$

$$
= \lambda I_0^2 - (\pi\bar{T}_c) \sum_{m=-\infty}^{\infty} \frac{|\bar{\omega}_m|}{(1+\bar{\omega}_m^2)^2}. \tag{3.18}
$$

The sum of this series can be computed analytically:

$$
\sum_{m=-\infty}^{\infty} \frac{|\bar{\omega}_m|}{(1+\bar{\omega}_m^2)^2} = \frac{1}{2i} \sum_{m=0}^{\infty} \left[\frac{1}{(1-i\bar{\omega}_m)^2}-\frac{1}{(1+i\bar{\omega}_m)^2}\right],
$$

$$
= \frac{1}{2i} \sum_{m=0}^{\infty} \left[\frac{1}{(i\pi\bar{T}_c(2m+1)-1)^2}-\frac{1}{(i\pi\bar{T}_c(2m+1)+1)^2}\right],
$$

$$
= \frac{\bar{\omega}_E^2}{2i} \sum_{m=0}^{\infty} \left[\frac{1}{(m+1/2-i\bar{\omega}_E)^2}-\frac{1}{(m+1/2+i\bar{\omega}_E)^2}\right]. \tag{3.19}
$$

Now we use the identity

$$
\sum_{m=0}^{\infty} \frac{1}{(m+a)^2} = \psi'(a), \tag{3.20}
$$

21

to obtain

$$\sum_{m=-\infty}^{\infty} \frac{|\bar{\omega}_m|}{(1+\bar{\omega}_m^2)^2} = \frac{\bar{\omega}_E^2}{2i}[\psi'(1/2-i\bar{\omega}_E) - \psi'(1/2+i\bar{\omega}_E)],$$

$$= \bar{\omega}_E^2 \text{Im}[\psi'(1/2-i\bar{\omega}_E)]. \tag{3.21}$$

Thus, in the limit that $T_c/\omega_E \to 0$, we obtain

$$\pi\bar{T}_c \sum_{m=-\infty}^{\infty} \frac{|\bar{\omega}_m|}{(1+\bar{\omega}_m^2)^2} = \pi\bar{T}_c\bar{\omega}_E = \frac{1}{2}. \tag{3.22}$$

Therefore the gap equation is approximately

$$I_0 = \lambda I_0^2 - 1/2. \tag{3.23}$$

Solving this equation to $\mathcal{O}(\lambda)$ gives

$$I_0 = \frac{1}{\lambda} + \frac{1}{2} + \mathcal{O}(\lambda). \tag{3.24}$$

The expression for I_0 can be obtained as follows:

$$\begin{aligned}
I_0 &= \pi\bar{T}_c \sum_{m=-\infty}^{\infty} \frac{1}{|\bar{\omega}_m|} \frac{1}{1+\bar{\omega}_m^2}, \\
&= \pi\bar{T}_c \sum_{m=0}^{\infty} \frac{1}{\bar{\omega}_m}\left(\frac{1}{1-i\bar{\omega}_m} + \frac{1}{1+i\bar{\omega}_m}\right), \\
&= \frac{i\bar{\omega}_E}{2} \sum_{m=0}^{\infty} \frac{1}{m+1/2}\left(\frac{1}{m+1/2+i\bar{\omega}_E} - \frac{1}{m+1/2-i\bar{\omega}_E}\right), \\
&= \frac{1}{2} \sum_{m=0}^{\infty} \left[\frac{1}{m+1/2} - \frac{1}{m+1/2+i\bar{\omega}_E} + \frac{1}{m+1/2} - \frac{1}{m+1/2-i\bar{\omega}_E}\right].
\end{aligned} \tag{3.25}$$

Now we evaluate the above summations

$$\begin{aligned}
I_0 &= \frac{1}{2}\left[\psi\left(\frac{1}{2}+i\bar{\omega}_E\right) + \psi\left(\frac{1}{2}-i\bar{\omega}_E\right) - 2\psi\left(\frac{1}{2}\right)\right], \\
&= \frac{1}{2}\left[\psi\left(\frac{1}{2}+i\bar{\omega}_E\right) + \psi\left(1-\left(\frac{1}{2}+i\bar{\omega}_E\right)\right) - 2\psi\left(\frac{1}{2}\right)\right], \\
&= \frac{1}{2}\left[2\psi\left(\frac{1}{2}+i\bar{\omega}_E\right) + \pi\cot\left(\pi\left(\frac{1}{2}+i\bar{\omega}_E\right)\right) - 2\psi\left(\frac{1}{2}\right)\right], \\
&= \psi\left(\frac{1}{2}+i\bar{\omega}_E\right) - \frac{i\pi}{2}\tanh(\pi\bar{\omega}_E) - \psi\left(\frac{1}{2}\right).
\end{aligned} \tag{3.26}$$

Note that $\psi(1/2) = -\gamma - 2\log(2) \approx -1.96$ where $\gamma \approx 0.5772$ is the Euler-Mascheroni constant. Using the asymptotic expansion of $\psi(z)$, namely, $\psi(z+1/2) \to \log(z) + \frac{1}{24z^2} + \mathcal{O}(z^{-4})$, as $z \to \infty$, it follows that, as $T_c/\omega_E \to 0$, I_0 becomes [28, 29]

$$I_0 \to \log(i\bar{\omega}_E) - \frac{1}{24\bar{\omega}_E^2} - \frac{i\pi}{2} - \psi(1/2) = \log\left(\frac{\exp[-\psi(1/2)]}{2\pi}\frac{\omega_E}{T_c}\right) - \frac{\pi^2}{6}\left(\frac{T_c}{\omega_E}\right)^2. \tag{3.27}$$

22

The approximate form of the first term is found using the result $\exp[-\psi(1/2)]/(2\pi) \approx 1.13$. Solving Eq. (3.24) for T_c gives

$$T_c = \frac{\exp[-\psi(1/2)]/(2\pi)}{\sqrt{\exp(1)}}\omega_E \exp\left(-\frac{1}{\lambda}\right) \approx \frac{1.13}{\sqrt{e}}\omega_E \exp\left(-\frac{1}{\lambda}\right), \tag{3.28}$$

whereas the BCS result is

$$T_c = 1.13\omega_E \exp\left(-\frac{1}{\lambda}\right). \tag{3.29}$$

An additional pre-factor of $1/\sqrt{e}$ exists in Eq.(3.28) in comparison to the BCS result. In order to improve the gap function in the weak-coupling limit, we calculate $f_1(\omega_m)$ to the zeroth order in λ. Using Eq.(3.15) and isolating $f_1(\omega_n)$ we obtain

$$f_1(\omega_n) = c - g_1(\bar{\omega}_n) - \lambda g_2(\bar{\omega}_n), \tag{3.30}$$

where both $g_1(\bar{\omega}_n)$ and $g_2(\bar{\omega}_n)$ are functions of $\bar{\omega}_n$ and non-singular as the coupling becomes weaker. We keep those terms in $f_1(\omega_n)$ which are of the order of unity. Also, the value of c is $1/2$, which is obtained from the eigenvalue relation of Eq.(3.24). Since $g_2(\bar{\omega}_n)$ is pre-multiplied by λ, it can be ignored [21]. The expression for $g_1(\bar{\omega}_n)$ can be defined as

$$g_1(\bar{\omega}_n) = \pi T_c \sum_{m=-\infty}^{\infty} \frac{1}{1+\bar{\omega}_m^2}\left\{\frac{|\bar{\omega}_m| - 2\bar{\omega}_n \mathrm{sgn}(\bar{\omega}_m)}{1+(\bar{\omega}_n-\bar{\omega}_m)^2}\right\}. \tag{3.31}$$

We can split up the sum into two terms

$$g_1(\bar{\omega}_n) = I(\bar{\omega}_n) - J(\bar{\omega}_n). \tag{3.32}$$

The first term is

$$I(\bar{\omega}_n) = \sum_{m=-\infty}^{\infty} \frac{|\bar{\omega}_m|}{(1+\bar{\omega}_m^2)} \frac{1}{\left[1+(\bar{\omega}_n-\bar{\omega}_m)^2\right]}, \tag{3.33}$$

where $\bar{\omega}_m \equiv \omega_m/\omega_E$ and $\bar{\omega}_E \equiv \omega_E/(2\pi T)$ with $\omega_m = (2m+1)\pi k_B T$. The sum can be written as

$$I(\bar{\omega}_n) = \sum_{m=0}^{\infty} \frac{\bar{\omega}_m}{(1+\bar{\omega}_m^2)} \frac{1}{\left[1+(\bar{\omega}_n-\bar{\omega}_m)^2\right]} - \sum_{m=-\infty}^{-1} \frac{\bar{\omega}_m}{(1+\bar{\omega}_m^2)} \frac{1}{\left[1+(\bar{\omega}_n-\bar{\omega}_m)^2\right]}. \tag{3.34}$$

We redefine the second term using $m = -k-1$, then $\bar{\omega}_m = -(2k+1)\pi T/\omega_E = -\bar{\omega}_k$. The sum becomes

$$I(\bar{\omega}_n) = \sum_{m=0}^{\infty} \frac{\bar{\omega}_m}{(1+\bar{\omega}_m^2)} \frac{1}{\left[1+(\bar{\omega}_n-\bar{\omega}_m)^2\right]} + \sum_{k=0}^{\infty} \frac{\bar{\omega}_k}{(1+\bar{\omega}_k^2)} \frac{1}{\left[1+(\bar{\omega}_n+\bar{\omega}_k)^2\right]} = h(\bar{\omega}_n) + h(-\bar{\omega}_n). \tag{3.35}$$

Using partial fractions, this becomes

$$h(\bar{\omega}_n) = \frac{1}{4}\sum_{m=0}^{\infty}\left\{\frac{1}{2-i\bar{\omega}_n}\left[\frac{1}{i+\bar{\omega}_m}+\frac{1}{i+\bar{\omega}_n-\bar{\omega}_m}\right]-\frac{1}{-i\bar{\omega}_n}\left[\frac{1}{i-\bar{\omega}_m}-\frac{1}{i+\bar{\omega}_n-\bar{\omega}_m}\right]\right\},$$

$$+\frac{1}{4}\sum_{m=0}^{\infty}\left\{\frac{1}{i\bar{\omega}_n}\left[\frac{1}{i+\bar{\omega}_m}-\frac{1}{i+\bar{\omega}_m-\bar{\omega}_n}\right]-\frac{1}{2+i\bar{\omega}_n}\left[\frac{1}{i-\bar{\omega}_m}+\frac{1}{i+\bar{\omega}_m-\bar{\omega}_n}\right]\right\}. \tag{3.36}$$

23

Therefore,

$$h(\bar{\omega}_n) = \frac{\omega_E}{8\pi T} \sum_{m=0}^{\infty} \left\{ \frac{1}{2 - i\bar{\omega}_n} \left[\frac{1}{m + i\bar{\omega}_E + 1/2} - \frac{1}{m - n - i\bar{\omega}_E} \right] + \frac{1}{i\bar{\omega}_n} \left[\frac{1}{m - n - i\bar{\omega}_E} - \frac{1}{m + 1/2 - i\bar{\omega}_E} \right] \right\},$$

$$+ \frac{\omega_E}{8\pi T} \sum_{m=0}^{\infty} \left\{ \frac{1}{i\bar{\omega}_n} \left[\frac{1}{m + i\bar{\omega}_E + 1/2} - \frac{1}{m - n + i\bar{\omega}_E} \right] - \frac{1}{2 + i\bar{\omega}_n} \left[\frac{1}{m - n + i\bar{\omega}_E} - \frac{1}{m + 1/2 - i\bar{\omega}_E} \right] \right\}. \tag{3.37}$$

Here, we have applied the digamma functions to compute the summation. The digamma functions are an analytical function of a complex variable.

$$h(\bar{\omega}_n) = \frac{\omega_E}{8\pi T} \left\{ \frac{\psi(-n - i\bar{\omega}_E) - \psi(1/2 + i\bar{\omega}_E)}{2 - i\bar{\omega}_n} + \frac{\psi(1/2 - i\bar{\omega}_E) - \psi(-n - i\bar{\omega}_E)}{i\bar{\omega}_n} \right\},$$

$$+ \frac{\omega_E}{8\pi T} \left\{ \frac{\psi(-n + i\bar{\omega}_E) - \psi(1/2 + i\bar{\omega}_E)}{i\bar{\omega}_n} - \frac{\psi(1/2 - i\bar{\omega}_E) - \psi(-n + i\bar{\omega}_E)}{2 + i\bar{\omega}_n} \right\}. \tag{3.38}$$

This can be written in terms of $\bar{\omega}_n$ as follows

$$h(\bar{\omega}_n) = \frac{\omega_E}{8\pi T} \left\{ \frac{\psi(-(\bar{\omega}_n + i)\bar{\omega}_E + 1/2) - \psi(1/2 + i\bar{\omega}_E)}{2 - i\bar{\omega}_n} + \frac{\psi(-(\bar{\omega}_n - i)\bar{\omega}_E + 1/2) - \psi(1/2 - i\bar{\omega}_E)}{2 + i\bar{\omega}_n} \right\},$$

$$+ \frac{\omega_E}{8\pi T} \left\{ \frac{\psi(-(\bar{\omega}_n - i)\bar{\omega}_E + 1/2) - \psi(-(\bar{\omega}_n + i)\bar{\omega}_E + 1/2)}{i\bar{\omega}_n} + \frac{\psi(1/2 - i\bar{\omega}_E) - \psi(1/2 + i\bar{\omega}_E)}{i\bar{\omega}_n} \right\}. \tag{3.39}$$

In the limit $\bar{\omega}_E \gg 1$ and with the use of the asymptotic formula one can write $\psi(z + 1/2) \to \log(z) + \mathcal{O}(z^{-2})$. Thus, we have

$$h(\bar{\omega}_n) = \frac{\omega_E}{8\pi T} \left\{ \frac{\log(1 - i\bar{\omega}_n) - i\pi}{2 - i\bar{\omega}_n} + \frac{\log(1 + i\bar{\omega}_n) + i\pi}{2 + i\bar{\omega}_n} + \frac{\log(1 + i\bar{\omega}_n) - \log(1 - i\bar{\omega}_n)}{i\bar{\omega}_n} \right\}. \tag{3.40}$$

Simplifying this then produces

$$h(\bar{\omega}_n) = \frac{\omega_E}{8\pi T} \left\{ \frac{\frac{1}{2}\log(1 + \bar{\omega}_n^2) - i\arctan(\bar{\omega}_n) - i\pi}{2 - i\bar{\omega}_n} + \frac{\frac{1}{2}\log(1 + \bar{\omega}_n^2) + i\arctan(\bar{\omega}_n) + i\pi}{2 + i\bar{\omega}_n} + 2i\frac{\arctan(\bar{\omega}_n)}{i\bar{\omega}_n} \right\}. \tag{3.41}$$

The asymptotic behaviour of the original sum is

$$I(\bar{\omega}_n) = \frac{\omega_E}{8\pi T} \left\{ \frac{\frac{1}{2}\log(1 + \bar{\omega}_n^2) - i\arctan(\bar{\omega}_n) - i\pi}{2 - i\bar{\omega}_n} + \frac{\frac{1}{2}\log(1 + \bar{\omega}_n^2) + i\arctan(\bar{\omega}_n) + i\pi}{2 + i\bar{\omega}_n} + 2i\frac{\arctan(\bar{\omega}_n)}{i\bar{\omega}_n} \right\},$$

$$+ \frac{\omega_E}{8\pi T} \left\{ \frac{\frac{1}{2}\log(1 + \bar{\omega}_n^2) + i\arctan(\bar{\omega}_n) - i\pi}{2 + i\bar{\omega}_n} + \frac{\frac{1}{2}\log(1 + \bar{\omega}_n^2) - i\arctan(\bar{\omega}_n) + i\pi}{2 - i\bar{\omega}_n} + 2i\frac{\arctan(\bar{\omega}_n)}{i\bar{\omega}_n} \right\}$$

$$= \frac{\omega_E}{2\pi T} \left\{ \frac{1}{4 + \bar{\omega}_n^2} [\log(1 + \bar{\omega}_n^2) + \bar{\omega}_n \arctan(\bar{\omega}_n)] + \frac{\arctan(\bar{\omega}_n)}{\bar{\omega}_n} \right\}. \tag{3.42}$$

Consider the series

$$J(\bar{\omega}_n) = \sum_{m=-\infty}^{\infty} \frac{\text{sgn}(\bar{\omega}_m)}{(1 + \bar{\omega}_m^2)} \frac{2\bar{\omega}_n}{[1 + (\bar{\omega}_n - \bar{\omega}_m)^2]}. \tag{3.43}$$

24

Splitting the sum into two terms:

$$J(\bar{\omega}_n) = 2\bar{\omega}_n \sum_{m=0}^{\infty} \frac{1}{(1+\bar{\omega}_m^2)} \frac{1}{[1+(\bar{\omega}_n - \bar{\omega}_m)^2]} - 2\bar{\omega}_n \sum_{m=-\infty}^{-1} \frac{1}{(1+\bar{\omega}_m^2)} \frac{1}{[1+(\bar{\omega}_n - \bar{\omega}_m)^2]}. \tag{3.44}$$

Redefining the last term using $m = -k - 1$, then $\bar{\omega}_m = (2m+1)\pi T/\omega_E = -(2k+1)\pi T/\omega_E = -\bar{\omega}_k$. The sum becomes

$$J(\bar{\omega}_n) = 2\bar{\omega}_n \sum_{m=0}^{\infty} \frac{1}{(1+\bar{\omega}_m^2)} \frac{1}{[1+(\bar{\omega}_n - \bar{\omega}_m)^2]} - 2\bar{\omega}_n \sum_{k=0}^{\infty} \frac{1}{(1+\bar{\omega}_k^2)} \frac{1}{[1+(\bar{\omega}_n + \bar{\omega}_k)^2]} = g(\bar{\omega}_n) + g(-\bar{\omega}_n). \tag{3.45}$$

Thus we have

$$g(\bar{\omega}_n) = 2\bar{\omega}_n \sum_{m=0}^{\infty} \frac{1}{(1+\bar{\omega}_m^2)} \frac{1}{[1+(\bar{\omega}_n - \bar{\omega}_m)^2]}. \tag{3.46}$$

Therefore,

$$g(\bar{\omega}_n) = \frac{i\bar{\omega}_n}{2} \sum_{m=0}^{\infty} \left\{ \frac{1}{2 - i\bar{\omega}_n} \left[\frac{1}{i+\bar{\omega}_m} + \frac{1}{i+(\bar{\omega}_n - \bar{\omega}_m)} \right] + \frac{1}{-i\bar{\omega}_n} \left[\frac{1}{i-\bar{\omega}_m} - \frac{1}{i+(\bar{\omega}_n - \bar{\omega}_m)} \right] \right\}$$
$$+ \frac{i\bar{\omega}_n}{2} \sum_{m=0}^{\infty} \left\{ \frac{1}{i\bar{\omega}_n} \left[\frac{1}{i+\bar{\omega}_m} - \frac{1}{i-\bar{\omega}_n + \bar{\omega}_m} \right] + \frac{1}{2 + i\bar{\omega}_n} \left[\frac{1}{i-\bar{\omega}_m} + \frac{1}{i-\bar{\omega}_n + \bar{\omega}_m} \right] \right\}. \tag{3.47}$$

The series thus becomes

$$g(\bar{\omega}_n) = \frac{i\bar{\omega}_n \omega_E}{4\pi T} \sum_{m=0}^{\infty} \left\{ \frac{1}{2 - i\bar{\omega}_n} \left[\frac{1}{m + i\bar{\omega}_E + 1/2} - \frac{1}{m - n - i\bar{\omega}_E} \right] + \frac{1}{-i\bar{\omega}_n} \left[\frac{1}{m - n - i\bar{\omega}_E} - \frac{1}{m + 1/2 - i\bar{\omega}_E} \right] \right\}$$
$$+ \frac{i\bar{\omega}_n \omega_E}{4\pi T} \sum_{m=0}^{\infty} \left\{ \frac{1}{i\bar{\omega}_n} \left[\frac{1}{m + i\bar{\omega}_E + 1/2} - \frac{1}{m - n + i\bar{\omega}_E} \right] + \frac{1}{2 + i\bar{\omega}_n} \left[\frac{1}{m - n + i\bar{\omega}_E} - \frac{1}{m + 1/2 - i\bar{\omega}_E} \right] \right\}. \tag{3.48}$$

Applying the digamma summation formula

$$g(\bar{\omega}_n) = \frac{i\bar{\omega}_n \omega_E}{4\pi T} \left\{ \frac{\psi(-n - i\bar{\omega}_E) - \psi(1/2 + i\bar{\omega}_E)}{2 - i\bar{\omega}_n} - \frac{\psi(1/2 - i\bar{\omega}_E) - \psi(-n - i\bar{\omega}_E)}{i\bar{\omega}_n} \right\}$$
$$+ \frac{i\bar{\omega}_n \omega_E}{4\pi T} \left\{ \frac{\psi(-n + i\bar{\omega}_E) - \psi(1/2 + i\bar{\omega}_E)}{i\bar{\omega}_n} + \frac{\psi(1/2 - i\bar{\omega}_E) - \psi(-n + i\bar{\omega}_E)}{2 + i\bar{\omega}_n} \right\}. \tag{3.49}$$

Writing the series in terms of $\bar{\omega}_n$ gives

$$g(\bar{\omega}_n) = \frac{i\bar{\omega}_n \omega_E}{4\pi T} \left\{ \frac{\psi(-(\bar{\omega}_n + i)\bar{\omega}_E + 1/2) - \psi(1/2 + i\bar{\omega}_E)}{2 - i\bar{\omega}_n} - \frac{\psi(-(\bar{\omega}_n - i)\bar{\omega}_E + 1/2) - \psi(1/2 - i\bar{\omega}_E)}{2 + i\bar{\omega}_n} \right\}$$
$$+ \frac{i\bar{\omega}_n \omega_E}{4\pi T} \left\{ \frac{\psi(-(\bar{\omega}_n - i)\bar{\omega}_E + 1/2) + \psi(-(\bar{\omega}_n + i)\bar{\omega}_E + 1/2)}{i\bar{\omega}_n} - \frac{\psi(1/2 - i\bar{\omega}_E) + \psi(1/2 + i\bar{\omega}_E)}{i\bar{\omega}_n} \right\}. \tag{3.50}$$

Applying the asymptotic expansion of the digamma function, namely, $\psi(z + 1/2) \to \log(z) + \mathcal{O}(z^{-2})$, as

25

$z \to \infty$, it follows that, as $T_c/\omega_E \to 0$, $g(i\omega_n)$ becomes

$$g(\bar{\omega}_n) = \frac{i\bar{\omega}_n \omega_E}{4\pi T} \left\{ \frac{\log(1 - i\bar{\omega}_n) - i\pi}{2 - i\omega_n} - \frac{\log(1 + i\bar{\omega}_n) + i\pi}{2 + i\bar{\omega}_n} + \frac{\log(1 + i\bar{\omega}_n) + \log(1 - i\bar{\omega}_n)}{i\bar{\omega}_n} \right\}$$

$$= \frac{i\bar{\omega}_n \omega_E}{4\pi T} \left\{ \frac{\frac{1}{2}\log(1 + \bar{\omega}_n^2) - i\arctan(\bar{\omega}_n) - i\pi}{2 - i\bar{\omega}_n} - \frac{\frac{1}{2}\log(1 + \bar{\omega}_n^2) + i\arctan(\bar{\omega}_n) + i\pi}{2 + i\bar{\omega}_n} \right\}$$

$$+ \frac{i\bar{\omega}_n \omega_E}{4\pi T} \left\{ \frac{\frac{1}{2}\log(1 + \bar{\omega}_n^2) + \frac{1}{2}\log(1 + \bar{\omega}_n^2)}{i\bar{\omega}_n} \right\},$$

$$= \frac{i\bar{\omega}_n \omega_E}{4\pi T} \left\{ \frac{1}{4 + \bar{\omega}_n^2} [-4i\arctan(\bar{\omega}_n) + i\bar{\omega}_n \log(1 + \bar{\omega}_n^2) - 2i\pi] \right\} + \frac{\omega_E}{4\pi T} \log(1 + \bar{\omega}_n^2). \tag{3.51}$$

The original sum has the asymptotic behavior

$$J(\bar{\omega}_n) = \frac{i\bar{\omega}_n \omega_E}{2\pi T} \left\{ \frac{1}{4 + \bar{\omega}_n^2} [-4i\arctan(\bar{\omega}_n) + i\bar{\omega}_n \log(1 + \bar{\omega}_n^2)] \right\} + \frac{\omega_E}{2\pi T} \log(1 + \bar{\omega}_n^2). \tag{3.52}$$

The subtraction of the two sums gives

$$I(\bar{\omega}_n) - J(\bar{\omega}_n) = \frac{\omega_E}{2\pi T} \left\{ \frac{1}{4 + \bar{\omega}_n^2} [\log(1 + \bar{\omega}_n^2) + \bar{\omega}_n \arctan(\bar{\omega}_n)] + \frac{\arctan(\bar{\omega}_n)}{\bar{\omega}_n} \right\}$$

$$- \frac{i\bar{\omega}_n \omega_E}{2\pi T} \left\{ \frac{1}{4 + \bar{\omega}_n^2} [-4i\arctan(\bar{\omega}_n) + i\bar{\omega}_n \log(1 + \bar{\omega}_n^2)] \right\} - \frac{\omega_E}{2\pi T} \log(1 + \bar{\omega}_n^2),$$

$$= \frac{\omega_E}{2\pi T} \frac{2}{4 + \bar{\omega}_n^2} \left\{ \frac{2 - \bar{\omega}_n^2}{\bar{\omega}_n} \arctan(\bar{\omega}_n) - \frac{3}{2} \log(1 + \bar{\omega}_n^2) \right\}. \tag{3.53}$$

Therefore, the function $g_1(\bar{\omega}_n) = \pi \bar{T}_c [I(\bar{\omega}_n) - J(\bar{\omega}_n)]$ can be written as

$$g_1(\bar{\omega}_n) = \frac{1}{4 + \bar{\omega}_n^2} \left\{ \frac{2 - \bar{\omega}_n^2}{\bar{\omega}_n} \arctan(\bar{\omega}_n) - \frac{3}{2} \log(1 + \bar{\omega}_n^2) \right\}. \tag{3.54}$$

A more explicit expression for the gap function is

$$\Delta(\omega_n) = \frac{1}{1 + \bar{\omega}_n^2} \left(1 + \lambda \left(\frac{1}{2} - g_1(\omega_n) \right) \right). \tag{3.55}$$

If we set $\lambda = 0$ we obtain

$$\Delta_0(\omega_n) = \frac{1}{1 + \bar{\omega}_n^2}. \tag{3.56}$$

In Fig.(4a) we plot the approximate gap function on the imaginary axis without the renormalization function.

3. Gap function with renormalization factor

Including $Z(i\omega_n)$ in the calculations the ansatz is written as follows:

$$\Delta(\omega_n) = \frac{1}{1 + \bar{\omega}_n^2} \left(1 + \lambda \left[f_Z(\omega_n) - \frac{1}{|\omega_n|} \tan^{-1} |\omega_n| \right] \right), \tag{3.57}$$

where $f_Z(\omega_n) = 3/2 - g_1(\omega_n)$. Figure (4b) shows the gap function versus imaginary frequency for small values of λ including the renormalization function.

26
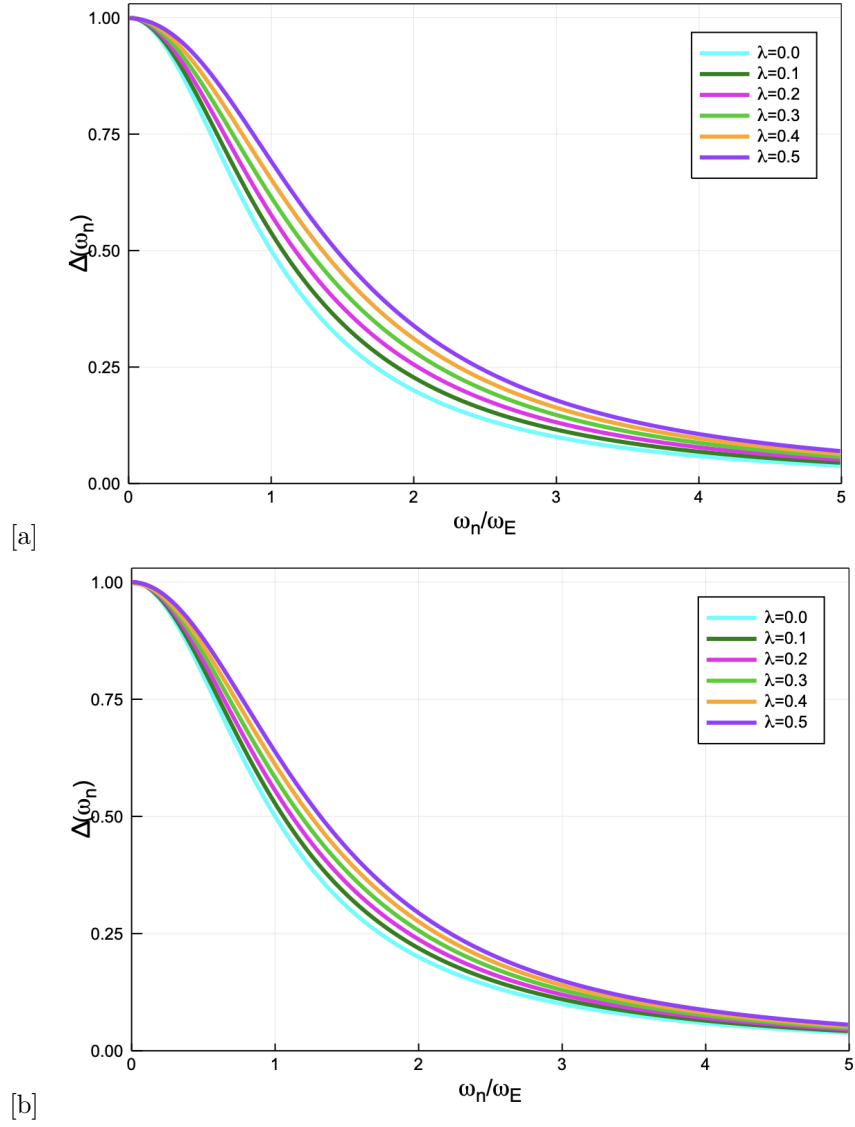
Figure 4. [a] A plot of $\Delta(\bar{\omega}_n)$ in units of ω_E versus ω_n/ω_E for various λ values without the renormalization factor, [b] with the renormalization factor at the critical temperature.

4. $T \to 0$ limit

In the zero temperature limit, the asymptotic result for $g_1(\omega_n)$ can be derived using the following prescription [22]:

$$\bar{T}\sum_{i\omega_n} \to \int_{-\infty}^{\infty} \frac{dz}{2\pi}. \tag{3.58}$$

Since $\omega_E \gg T_c$, thus $\bar{T} = T_c/\omega_E \to 0$. The Matsubara frequency summation will be converted into an integral. Now, we define $g_1(\bar{\omega}_n)$ as $\bar{T} \to 0$ as follows:

$$g_1(\bar{\omega}_n) = \pi\bar{T}_c \int_{-\infty}^{\infty} \frac{dz}{2\pi} \frac{1}{(1+z^2)} \left\{ \frac{|z| - 2\bar{\omega}_n\text{sgn}(z)}{1 + (z - \bar{\omega}_n)^2} \right\}. \tag{3.59}$$

27

We separate the integration into two terms

$$\bar{T}I(\bar{\omega}_n) \to \int_{-\infty}^{\infty} \frac{dz}{2\pi} \frac{|z|}{(1+z^2)} \frac{1}{[1+(\bar{\omega}_n - z)^2]},$$
$$= \int_0^{\infty} \frac{dz}{2\pi} \frac{z}{(1+z^2)} \frac{1}{[1+(\bar{\omega}_n - z)^2]} + \int_0^{\infty} \frac{dz}{2\pi} \frac{z}{(1+z^2)} \frac{1}{[1+(\bar{\omega}_n + z)^2]}. \tag{3.60}$$

We compute these integrals as follows [11]:

$$\int_0^{\infty} \frac{dz}{2\pi} \frac{z}{(1+z^2)} \frac{1}{[1+(\bar{\omega}_n - z)^2]} = \frac{1}{4i} \int_0^{\infty} \frac{dz}{2\pi} \left(\frac{1}{1-iz} - \frac{1}{1+iz} \right) \left(\frac{1}{1-i(z-\bar{\omega}_n)} + \frac{1}{1+i(z-\bar{\omega}_n)} \right),$$
$$= \frac{1}{4i} \int_0^{\infty} \frac{dz}{2\pi} \left(\frac{1}{1-iz} \frac{1}{1-i(z-\bar{\omega}_n)} - \frac{1}{1+iz} \frac{1}{1+i(z-\bar{\omega}_n)} \right)$$
$$+ \frac{1}{4i} \int_0^{\infty} \frac{dz}{2\pi} \left(\frac{1}{1-iz} \frac{1}{1+i(z-\bar{\omega}_n)} - \frac{1}{1+iz} \frac{1}{1-i(z-\bar{\omega}_n)} \right),$$
$$= -\frac{1}{4i} \int_0^{\infty} \frac{dz}{2\pi} \left[\frac{1}{z+i} \frac{1}{z-(\bar{\omega}_n - i)} - \frac{1}{z-i} \frac{1}{z-(\bar{\omega}_n + i)} \right]$$
$$+ \frac{1}{4i} \int_0^{\infty} \frac{dz}{2\pi} \left[\frac{1}{z+i} \frac{1}{z-(\bar{\omega}_n + i)} - \frac{1}{z-i} \frac{1}{z-(\bar{\omega}_n - i)} \right]. \tag{3.62}$$

The original integral is now

$$\int_0^{\infty} dz \frac{z}{(1+z^2)} \frac{1}{[1+(\bar{\omega}_n - z)^2]}$$
$$= \frac{1}{4i} \left[\frac{1}{\bar{\omega}_n} \log\left(\frac{\bar{\omega}_n - i}{-i} \right) - \frac{1}{\bar{\omega}_n} \log\left(\frac{\bar{\omega}_n + i}{i} \right) \right]$$
$$+ \frac{1}{4i} \left[\frac{1}{-2i - \bar{\omega}_n} \log\left(\frac{\bar{\omega}_n + i}{-i} \right) - \frac{1}{2i - \bar{\omega}_n} \log\left(\frac{\bar{\omega}_n - i}{i} \right) \right]$$
$$= \frac{1}{4i} \frac{1}{\bar{\omega}_n} [\log(1 + i\bar{\omega}_n) - \log(1 - i\bar{\omega}_n)] - \frac{1}{4i} \left[\frac{\log(-1 + i\bar{\omega}_n)}{2i + \bar{\omega}_n} + \frac{\log(-1 - i\bar{\omega}_n)}{2i - \bar{\omega}_n} \right]$$
$$= \frac{1}{4i} \frac{1}{\bar{\omega}_n} 2i \arctan(\bar{\omega}_n)$$
$$- \frac{1}{4i} \left[\frac{\frac{1}{2}\log(1 + \bar{\omega}_n^2) - i\pi - i\arctan(\bar{\omega}_n)}{2i + \bar{\omega}_n} + \frac{\frac{1}{2}\log(1 + \bar{\omega}_n^2) + i\pi + i\arctan(\bar{\omega}_n)}{2i - \bar{\omega}_n} \right]. \tag{3.63}$$

Simplifying this further we obtain

$$\int_0^{\infty} \frac{dz}{2\pi} \frac{z}{(1+z^2)} \frac{1}{[1+(\bar{\omega}_n - z)^2]} = \frac{1}{4\pi} \left\{ \frac{1}{4 + \bar{\omega}_n^2} [\log(1 + \bar{\omega}_n^2) + \pi\bar{\omega}_n + \bar{\omega}_n \arctan(\bar{\omega}_n)] + \frac{\arctan(\bar{\omega}_n)}{\bar{\omega}_n} \right\}. \tag{3.64}$$

Therefore, the asymptotic limit of the series $\bar{T}I(\bar{\omega}_n)$ is written as

$$\bar{T}I(\bar{\omega}_n) \to \frac{1}{2\pi} \left\{ \frac{1}{4 + \bar{\omega}_n^2} [\log(1 + \bar{\omega}_n^2) + \bar{\omega}_n \arctan(\bar{\omega}_n)] + \frac{\arctan(\bar{\omega}_n)}{\bar{\omega}_n} \right\}. \tag{3.65}$$

─────────

[11] This is because

$$\int_0^{\infty} dz \left(\frac{1}{z-a} \frac{1}{z-b} \right) = \frac{1}{a-b} \int_0^{\infty} dz \left(\frac{1}{z-a} - \frac{1}{z-b} \right),$$
$$= \frac{1}{a-b} \lim_{L \to \infty} [\log(z-a) - \log(z-b)]|_0^L = \frac{1}{a-b} \log\left(\frac{b}{a} \right). \tag{3.61}$$

The second series has the asymptotic limit which is

$$
\begin{aligned}
J(\bar{\omega}_n) &\to 2\bar{\omega}_n \int_{-\infty}^{\infty} \frac{dz}{2\pi} \frac{\mathrm{sgn}(z)}{(1+z^2)} \frac{1}{[1+(\bar{\omega}_n - z)^2]} \\
&= 2\bar{\omega}_n \int_0^{\infty} \frac{dz}{2\pi} \frac{1}{(1+z^2)} \frac{1}{[1+(\bar{\omega}_n - z)^2]} - 2\bar{\omega}_n \int_0^{\infty} \frac{dz}{2\pi} \frac{1}{(1+z^2)} \frac{1}{[1+(\bar{\omega}_n + z)^2]}.
\end{aligned}
\tag{3.66}
$$

We follow the same approach to obtain

$$
\begin{aligned}
\int_0^{\infty} \frac{dz}{2\pi} \frac{1}{(1+z^2)} \frac{1}{[1+(\bar{\omega}_n - z)^2]} &= -\frac{1}{4} \int_0^{\infty} \frac{dz}{2\pi} \left[\frac{1}{z+i} \frac{1}{z-(\bar{\omega}_n - i)} + \frac{1}{z-i} \frac{1}{z-(\bar{\omega}_n + i)} \right] \\
&+ \frac{1}{4} \int_0^{\infty} \frac{dz}{2\pi} \left[\frac{1}{z+i} \frac{1}{z-(\bar{\omega}_n + i)} + \frac{1}{z-i} \frac{1}{z-(\bar{\omega}_n - i)} \right].
\end{aligned}
\tag{3.67}
$$

Utilizing the integration techniques, we write

$$
\begin{aligned}
&\int_0^{\infty} dz \frac{1}{(1+z^2)} \frac{1}{[1+(\bar{\omega}_n - z)^2]} \\
&= \frac{1}{4} \left[\frac{1}{\bar{\omega}_n} \log\left(\frac{\bar{\omega}_n - i}{-i}\right) + \frac{1}{\bar{\omega}_n} \log\left(\frac{\bar{\omega}_n + i}{i}\right) \right] \\
&\quad - \frac{1}{4} \left[\frac{1}{-2i-\bar{\omega}_n} \log\left(\frac{\bar{\omega}_n + i}{-i}\right) + \frac{1}{2i-\bar{\omega}_n} \log\left(\frac{\bar{\omega}_n - i}{i}\right) \right] \\
&= \frac{1}{4} \frac{1}{\bar{\omega}_n} [\log(1+i\bar{\omega}_n) + \log(1-i\bar{\omega}_n)] + \frac{1}{4} \left[\frac{\log(-1+i\bar{\omega}_n)}{2i+\bar{\omega}_n} - \frac{\log(-1-i\bar{\omega}_n)}{2i-\bar{\omega}_n} \right] \\
&= \frac{1}{4\bar{\omega}_n} \log(1+\bar{\omega}_n^2) \\
&\quad - \frac{1}{4} \left[\frac{\frac{1}{2}\log(1+\bar{\omega}_n^2) - i\pi - i\arctan(\bar{\omega}_n)}{2i+\bar{\omega}_n} - \frac{\frac{1}{2}\log(1+\bar{\omega}_n^2) + i\pi + i\arctan(\bar{\omega}_n)}{2i-\bar{\omega}_n} \right].
\end{aligned}
\tag{3.68}
$$

Simplifying the above equation we obtain

$$
\begin{aligned}
&\int_0^{\infty} \frac{dz}{2\pi} \frac{1}{(1+z^2)} \frac{1}{[1+(\bar{\omega}_n - z)^2]} \\
&= \frac{1}{8\pi} \left\{ \frac{1}{4+\bar{\omega}_n^2} [-\bar{\omega}_n \log(1+\bar{\omega}_n^2) + 4\pi + 4\arctan(\bar{\omega}_n)] + \frac{1}{\bar{\omega}_n} \log(1+\bar{\omega}_n^2) \right\}.
\end{aligned}
\tag{3.69}
$$

The asymptotic limit of $\bar{T}J(\bar{\omega}_n)$ is

$$
\bar{T}J(\bar{\omega}_n) \to \frac{2}{\pi} \left\{ \frac{1}{4+\bar{\omega}_n^2} [\log(1+\bar{\omega}_n^2) + \bar{\omega}_n \arctan(\bar{\omega}_n)] \right\}.
\tag{3.70}
$$

Finally, the function $g_1(\bar{\omega}_n)$ is

$$
\begin{aligned}
g_1(\bar{\omega}_n) &= \frac{1}{2} \left\{ \frac{1}{4+\bar{\omega}_n^2} [\log(1+\bar{\omega}_n^2) + \bar{\omega}_n \arctan(\bar{\omega}_n)] + \frac{\arctan(\bar{\omega}_n)}{\bar{\omega}_n} \right\} \\
&\quad - 2 \left\{ \frac{1}{4+\bar{\omega}_n^2} [\log(1+\bar{\omega}_n^2) + \bar{\omega}_n \arctan(\bar{\omega}_n)] \right\} \\
&= \frac{1}{4+\bar{\omega}_n^2} \left[\frac{2-\bar{\omega}_n^2}{\bar{\omega}_n} \arctan(\bar{\omega}_n) - \frac{3}{2} \log(1+\bar{\omega}_n^2) \right].
\end{aligned}
\tag{3.71}
$$

29

In addition, one can also calculate the zero temperature limit of $Z(i\bar\omega_n)$ in the same manner.

$$
\begin{aligned}
Z(i\bar\omega_n) =& 1 + \frac{\pi}{\bar\omega_n} T_c \sum_{m=-\infty}^{\infty} \lambda(i\bar\omega_n - i\bar\omega_m)\mathrm{sgn}(\bar\omega_m) \\
=& 1 + \frac{\pi}{\bar\omega_n} T_c \sum_{m=-\infty}^{\infty} \frac{\lambda\bar\omega_E}{\bar\omega_E^2 - (i\bar\omega_n - i\bar\omega_m)^2}\mathrm{sgn}(\bar\omega_m) \\
=& 1 + \frac{\pi\lambda\bar\omega_E}{\bar\omega_n} \int_{-\infty}^{\infty} \frac{dz}{2\pi} \frac{\mathrm{sgn}(z)}{\bar\omega_E^2 + (\bar\omega_n - z)^2} \\
=& 1 + \frac{\lambda}{\bar\omega_n} \arctan(\bar\omega_n),
\end{aligned}
\tag{3.72}
$$

which reproduces the result of Eq.(3.14).

<div align="center">5. Final result for $g_1(i\omega_n)$ in terms of digamma functions</div>

We now present a simplified expression for $g_1(i\omega_n)$ on the imaginary axis. This will be beneficial when we consider the real axis. We simplify $I(\bar\omega_n)$ as follows

$$
\begin{aligned}
I(\bar\omega_n) =& \frac{\bar\omega_E}{4} \left\{ \frac{\psi(-(\bar\omega_n+i)\bar\omega_E + 1/2) - \psi(1/2 + i\bar\omega_E) + \psi((\bar\omega_n+i)+1/2) - \psi(1/2 - i\bar\omega_E)}{2 - i\bar\omega_n} \right\} \\
&+ \frac{\bar\omega_E}{4} \left\{ \frac{\psi((\bar\omega_n-i)\bar\omega_E + 1/2) - \psi(1/2 + i\bar\omega_E) + \psi((-\bar\omega_n+i)+1/2) - \psi(1/2 - i\bar\omega_E)}{2 + i\bar\omega_n} \right\} \\
&+ \frac{\bar\omega_E}{4i\bar\omega_n} \left\{ \psi(-(\bar\omega_n-i)\bar\omega_E + 1/2) - \psi((\bar\omega_n+i)\bar\omega_E + 1/2) + \psi((\bar\omega_n-i)\bar\omega_E + 1/2) \right. \\
&\left. - \psi(-(\bar\omega_n+i)\bar\omega_E + 1/2) \right\}.
\end{aligned}
\tag{3.73}
$$

In addition, the result for $J(\bar\omega_n)$ gives

$$
\begin{aligned}
J(\bar\omega_n) =& \frac{i\bar\omega_n\bar\omega_E}{2} \left\{ \frac{\psi(-(\bar\omega_n+i)\bar\omega_E + 1/2) - \psi(1/2 + i\bar\omega_E)}{2 - i\bar\omega_n} - \frac{\psi(-(\bar\omega_n-i)\bar\omega_E + 1/2) - \psi(1/2 - i\bar\omega_E)}{2 + i\bar\omega_n} \right. \\
&+ \frac{i\bar\omega_n\bar\omega_E}{2} \left\{ \frac{\psi(-(\bar\omega_n-i)\bar\omega_E + 1/2) + \psi(1/2 - (\bar\omega_n+i)\bar\omega_E)}{i\bar\omega_n} - \frac{\psi((-i\bar\omega_E + 1/2) + \psi(1/2 + i\bar\omega_E)}{i\bar\omega_n} \right\} \\
&- \frac{i\bar\omega_n\bar\omega_E}{2} \left\{ \frac{\psi((\bar\omega_n-i)\bar\omega_E + 1/2) - \psi(1/2 + i\bar\omega_E)}{2 + i\bar\omega_n} - \frac{\psi((\bar\omega_n+i)\bar\omega_E + 1/2) - \psi(1/2 - i\bar\omega_E)}{2 - i\bar\omega_n} \right\} \\
&+ \frac{i\bar\omega_n\bar\omega_E}{2} \left\{ \frac{\psi((\bar\omega_n+i)\bar\omega_E + 1/2) + \psi(1/2 + (\bar\omega_n-i)\bar\omega_E)}{i\bar\omega_n} - \frac{\psi((-\bar\omega_E + 1/2) + \psi(1/2 + i\bar\omega_E)}{i\bar\omega_n} \right\}.
\end{aligned}
\tag{3.74}
$$

Since $g_1(\bar{\omega}_n) = \pi T(I(\bar{\omega}_n) - J(\bar{\omega}_n))$, one can write

$$
\begin{aligned}
\frac{g_1(\bar{\omega}_n)}{\pi \bar{T}_c} =& \frac{\bar{\omega}_E}{4}\Big\{\psi(-(\bar{\omega}_n + i)\bar{\omega}_E + 1/2) + \psi((\bar{\omega}_n + i)\bar{\omega}_E + 1/2) - \psi(1/2 - i\bar{\omega}_E) - \psi(1/2 + i\bar{\omega}_E)\Big\} \\
& \times \left[2 - \frac{3}{2 - i\bar{\omega}_n}\right] + \frac{\bar{\omega}_E}{4}\Big\{\psi((\bar{\omega}_n - i)\bar{\omega}_E + 1/2) + \psi((-\bar{\omega}_n + i)\bar{\omega}_E + 1/2) - \psi(1/2 + i\bar{\omega}_E) \\
& - \psi(1/2 - i\bar{\omega}_E)\Big\}\left[2 - \frac{3}{2 + i\bar{\omega}_n}\right] + \frac{\bar{\omega}_E}{4i\omega_n}\Big\{\psi(-(\bar{\omega}_n - i)\bar{\omega}_E + 1/2) - \psi((\bar{\omega}_n + i)\bar{\omega}_E + 1/2) \\
& + \psi((\bar{\omega}_n - i)\bar{\omega}_E + 1/2) - \psi(-(\bar{\omega}_n + i)\bar{\omega}_E + 1/2)\Big\} + \bar{\omega}_E\Big\{\psi(1/2 - i\bar{\omega}_E) + \psi(1/2 + i\bar{\omega}_E)\Big\} \\
& - \frac{\bar{\omega}_E}{2}\Big\{\psi((\bar{\omega}_n + i)\bar{\omega}_E + 1/2) + \psi((\bar{\omega}_n - i)\bar{\omega}_E + 1/2) + \psi(-(\bar{\omega}_n - i)\bar{\omega}_E + 1/2) \\
& + \psi(-(\bar{\omega}_n + i)\bar{\omega}_E + 1/2)\Big\}.
\end{aligned}
\tag{3.75}
$$

Thus,

$$
\begin{aligned}
\frac{g_1(\bar{\omega}_n)}{\pi \bar{T}_c} =& \frac{\bar{\omega}_E}{4}\left(-\frac{3}{2 - i\bar{\omega}_n}\right)\left[\psi(-(\bar{\omega}_n + i)\bar{\omega}_E + 1/2) + \psi((\bar{\omega}_n + i)\bar{\omega}_E + 1/2) - \psi(1/2 - i\bar{\omega}_E) - \psi(1/2 + i\bar{\omega}_E)\right] \\
& + \frac{\bar{\omega}_E}{4}\left(-\frac{3}{2 + i\bar{\omega}_n}\right)\left[\psi((\bar{\omega}_n - i)\bar{\omega}_E + 1/2) - \psi((-\bar{\omega}_n + i)\bar{\omega}_E + 1/2) - \psi(1/2 - i\bar{\omega}_E) - \psi(1/2 + i\bar{\omega}_E)\right] \\
& + \frac{\bar{\omega}_E}{4i\bar{\omega}_n}\Big[\psi(-(\bar{\omega}_n - i)\bar{\omega}_E + 1/2) - \psi((\bar{\omega}_n + i)\bar{\omega}_E + 1/2) + \psi((\bar{\omega}_n - i)\bar{\omega}_E + 1/2) \\
& - \psi(-(\bar{\omega}_n + i)\bar{\omega}_E + 1/2)\Big].
\end{aligned}
\tag{3.76}
$$

B.   Real-axis calculations

The analytical continuation to the real frequency axis is easy to compute. The correct analytical continuation is obtained by doing the Matsubara summation first and then analytically continue ($i\omega_n \to \omega + i\delta$) to the real axis, otherwise the result will be incorrect [7].

1.   Renormalization factor

The real axis Eliashberg equation for $Z(z)$ is given by:

$$
\begin{aligned}
Z(z) =& 1 + \frac{i\pi T}{z}\sum_{m=-\infty}^{\infty}\lambda(z - i\omega_m)\frac{\omega_m}{\sqrt{\omega_m^2 + \Delta^2(i\omega_m)}} \\
& + \frac{i\pi A(\omega_E)}{z}\left\{\frac{(z - \omega_E)[f(\omega_E - z) + N(\omega_E)]}{\sqrt{(z - \omega_E)^2 - \Delta^2(z - \omega_E)}} + \frac{(z + \omega_E)[f(\omega_E + z) + N(\omega_E)]}{\sqrt{(z + \omega_E)^2 - \Delta^2(z + \omega_E)}}\right\}.
\end{aligned}
\tag{3.77}
$$

First we compute the first term involving the summation in the weak-coupling limit to obtain $Z(\omega)$ in terms of digamma expressions as follows

$$Z(\omega) \approx 1 + \frac{\lambda}{2\bar{\omega}}\text{Re}\left[\psi\left(\frac{1}{2} - i\left(\frac{\omega_E + \omega}{2\pi T}\right)\right) - \psi\left(\frac{1}{2} + i\left(\frac{\omega_E - \omega}{2\pi T}\right)\right)\right]. \tag{3.78}$$

Applying the asymptotic expansion of the digamma function, namely, $\psi(z + 1/2) \to \log(z) + \mathcal{O}(z^{-2})$, as $z \to \infty$, it follows that, as $T_c/\omega_E \to 0$, the renormalization function on the real axis becomes

$$Z(\omega) \approx 1 + \frac{\lambda}{2\bar{\omega}}\log\left|\frac{1 + \bar{\omega}}{1 - \bar{\omega}}\right|. \tag{3.79}$$

2. Gap function without renormalization factor

The real axis Eliashberg equation is given by:

$$\begin{aligned} Z(z)\Delta(z) = & \pi T \sum_{m=-\infty}^{\infty} \lambda(z - i\omega_m)\frac{\Delta(i\omega_m)}{\sqrt{\omega_m^2 + \Delta^2(i\omega_m)}} \\ & + i\pi A(\omega_E)\frac{\Delta(z - \omega_E)[N(\omega_E) + f(\omega_E - z)]}{\sqrt{(z - \omega_E)^2 - \Delta^2(z - \omega_E)}} \\ & + i\pi A(\omega_E)\frac{\Delta(z + \omega_E)[N(\omega_E) + f(\omega_E + z)]}{\sqrt{(z + \omega_E)^2 - \Delta^2(z + \omega_E)}}. \end{aligned} \tag{3.80}$$

Here, we consider $Z(z) = 1$. We now proceed to compute the first term involving the summation in the weak-coupling limit. Thus, the analytical approximation for the gap function at the critical temperature can be written as follows

$$\Delta(\bar{\omega}) = \frac{1}{1 - \bar{\omega}^2}\left[1 + \lambda\left(\frac{1}{2} - g_1(\bar{\omega})\right)\right]. \tag{3.81}$$

Now, if we consider the gap below critical temperature we multiply by Δ_0 (which is the gap edge) as follows:

$$\Delta(\bar{\omega}) = \frac{\Delta_0}{1 - \bar{\omega}^2}\left[1 + \lambda\left(\frac{1}{2} - g_1(\bar{\omega})\right)\right], \tag{3.82}$$

where the asymptotic limit of $g_1(\bar{\omega})$ function is given as

$$g_1(\bar{\omega}) = \frac{1}{4 - \bar{\omega}^2}\left\{\frac{2 + \bar{\omega}^2}{2\bar{\omega}}\log\left|\frac{1 + \bar{\omega}}{1 - \bar{\omega}}\right| - \frac{3}{2}\log\left|1 - \bar{\omega}^2\right|\right\}. \tag{3.83}$$

The asymptotic expansion of $g_1(\omega)$ on the real frequency axis is obtained in Sec. III B 5. In this subsection, we showed the analytical apprroximation form of the gap function on the real frequency axis without including the renormalization factor.

3. Gap function with renormalization factor

The gap function with re-normalization factor included is given as

$$Z(\bar{\omega})\Delta(\bar{\omega}) = \frac{1}{1 - \bar{\omega}^2}\left\{1 + \lambda\left(\frac{3}{2} - g_1(\bar{\omega})\right)\right\}. \tag{3.84}$$

Also, the gap function below the critical temperature including the renormalization factor is

$$Z(\bar{\omega})\Delta(\bar{\omega}) = \frac{\Delta_0}{1 - \bar{\omega}^2}\left\{1 + \lambda\left(\frac{3}{2} - g_1(\bar{\omega})\right)\right\}. \tag{3.85}$$

For large $\bar{\omega}$, the asymptotic behavior of the gap function on the real and imaginary frequency axes are not equal. This dichotomy is due to the fact that $g_1(i\omega_n)$ on the Matsubara frequency axis is the real part of a function of $i\omega_n$. Thus, when one takes the real part of an analytically continued function, different behaviour can be obtained on the imaginary axis versus the real frequency axis.

4. $T \to 0$ limit

To derive the asymptotic solution of $g_1(\bar{\omega})$, one can take the $T \to 0$ limit for the first term in the summation. Here, we analytically continue $g_1(\bar{\omega}_n)$ on the real axis. Using the prescription

$$\bar{T}\sum_{i\omega_n} \to \int_{-\infty}^{\infty} \frac{dz}{2\pi}. \tag{3.86}$$

We define $g_1(\bar{\omega})$ as follows

$$g_1(\bar{\omega}) = \pi\bar{T}_c\int_{-\infty}^{\infty} \frac{dz}{2\pi(1+z^2)}\left\{\frac{|z| + 2i\bar{\omega}\mathrm{sgn}(z)}{1 + (-i\bar{\omega} - z)^2}\right\}. \tag{3.87}$$

The first term in the integral can be written as follows:

$$\bar{T}I(\bar{\omega}) \to \int_{-\infty}^{\infty} \frac{dz}{2\pi} \frac{|z|}{(1+z^2)} \frac{1}{[1 + (-i\bar{\omega} - z)^2]},$$
$$= \int_0^{\infty} \frac{dz}{2\pi} \frac{z}{(1+z^2)} \frac{1}{[1 + (-i\bar{\omega} - z)^2]} + \int_0^{\infty} \frac{dz}{2\pi} \frac{z}{(1+z^2)} \frac{1}{[1 + (-i\bar{\omega} + z)^2]}. \tag{3.88}$$

Thus

$$\int_0^{\infty} \frac{dz}{2\pi} \frac{|z|}{(1+z^2)} \frac{1}{[1 + (-i\bar{\omega} - z)^2]} = -\frac{1}{4i}\int_0^{\infty} \frac{dz}{2\pi}\left[\frac{1}{z+i}\frac{1}{i+i\bar{\omega}+z} + \frac{1}{z+i}\frac{1}{i-(i\bar{\omega}+z)}\right]$$
$$+ \frac{1}{4i}\int_0^{\infty} \frac{dz}{2\pi}\left[\frac{1}{-z+i}\frac{1}{i+i\bar{\omega}+z} + \frac{1}{i-z}\frac{1}{i-(i\bar{\omega}+z)}\right]. \tag{3.89}$$

The original integral is now

$$\int_0^{\infty} \frac{dz}{2\pi} \frac{|z|}{(1+z^2)} \frac{1}{[1 + (-i\bar{\omega} - z)^2]}$$
$$= -\frac{1}{8i\pi}\left[\frac{1}{(-i+i+i\bar{\omega})}\log\left(\frac{-i-i\bar{\omega}}{-i}\right) - \frac{1}{(-i-i+i\bar{\omega})}\log\left(\frac{-i\bar{\omega}+i}{-i}\right)\right]$$
$$- \frac{1}{8i\pi}\left[\frac{1}{(i+i+i\bar{\omega})}\log\left(\frac{-i-i\bar{\omega}}{i}\right) - \frac{1}{(i-i+i\bar{\omega})}\log\left(\frac{-i\bar{\omega}+i}{i}\right)\right]$$
$$= \frac{1}{8\pi}\left[\frac{1}{\bar{\omega}}\log(1+\bar{\omega}) - \frac{1}{\bar{\omega}}\log(1-\bar{\omega}) + \frac{1}{\bar{\omega}+2}\log(-1-\bar{\omega}) - \frac{1}{\bar{\omega}-2}\log(\bar{\omega}-1)\right]. \tag{3.90}$$

Suppose $0 \leq \bar{\omega} < 1$, we can write

$$\int_{-\infty}^{\infty} \frac{dz}{2\pi} \frac{|z|}{(1+z^2)} \frac{1}{[1+(-i\bar{\omega}-z)^2]}$$
$$= \frac{1}{2\pi} \left[\frac{1}{\bar{\omega}} \operatorname{arctanh}(\bar{\omega}) + \frac{\log(1-\bar{\omega}^2) - \bar{\omega}\operatorname{arctanh}(\bar{\omega})}{4-\bar{\omega}^2} \right]. \tag{3.91}$$

Similarly, if $\bar{\omega} > 1$

$$\int_{-\infty}^{\infty} \frac{dz}{2\pi} \frac{|z|}{(1+z^2)} \frac{1}{[1+(-i\bar{\omega}-z)^2]}$$
$$= \frac{1}{2\pi} \left\{ \frac{1}{2\bar{\omega}} \log\left(\frac{\bar{\omega}+1}{\bar{\omega}-1}\right) + \frac{1}{4-\bar{\omega}^2} \left[\log(\bar{\omega}^2-1) - \frac{\bar{\omega}}{2} \log\left(\frac{\bar{\omega}+1}{\bar{\omega}-1}\right) \right] \right\}. \tag{3.92}$$

The second series has the asymptotic limit given by

$$\bar{T}J(\bar{\omega}) \to (-2i\bar{\omega}) \int_{-\infty}^{\infty} \frac{dz}{2\pi} \frac{\operatorname{sgn}(z)}{(1+z^2)} \frac{1}{1+(-i\bar{\omega}-z)^2}$$
$$= (-2i\bar{\omega}) \int_{0}^{\infty} \frac{dz}{2\pi} \frac{\operatorname{sgn}(z)}{(1+z^2)} \frac{1}{1+(-i\bar{\omega}-z)^2} + (-2i\bar{\omega}) \int_{0}^{\infty} \frac{dz}{2\pi} \frac{\operatorname{sgn}(z)}{(1+z^2)} \frac{1}{1+(-i\bar{\omega}+z)^2}. \tag{3.93}$$

The integral can be computed as follows:

$$(-2i\bar{\omega}) \int_{0}^{\infty} \frac{dz}{2\pi} \frac{\operatorname{sgn}(z)}{(1+z^2)} \frac{1}{1+(-i\bar{\omega}-z)^2} = \frac{(i\bar{\omega})}{4\pi} \int_{0}^{\infty} dz \left[\frac{1}{z+i} \frac{1}{i+i\bar{\omega}+z} - \frac{1}{i+z} \frac{1}{z-i+(i\bar{\omega})} \right]$$
$$- \frac{(i\bar{\omega})}{4\pi} \int_{0}^{\infty} dz \left[\frac{1}{z-i} \frac{1}{z+i\bar{\omega}+i} - \frac{1}{z-i} \frac{1}{z+i\bar{\omega}-i} \right]. \tag{3.94}$$

The original integral now becomes

$$(-2i\bar{\omega}) \int_{0}^{\infty} \frac{dz}{2\pi} \frac{\operatorname{sgn}(z)}{(1+z^2)} \frac{1}{1+(-i\bar{\omega}-z)^2}$$
$$= \frac{i\bar{\omega}}{4\pi} \left[\frac{1}{-i+i+i\bar{\omega}} \log\left(\frac{-i-i\bar{a}}{-i}\right) - \frac{1}{-i+i\bar{\omega}-i} \log\left(\frac{-i\bar{\omega}+i}{-i}\right) \right]$$
$$- \frac{i\bar{\omega}}{4\pi} \left[\frac{1}{i+i+i\bar{\omega}} \log\left(\frac{-i-i\bar{\omega}}{i}\right) - \frac{1}{i+i\bar{\omega}-i} \log\left(\frac{-i\bar{\omega}+i}{i}\right) \right]$$
$$= \frac{\bar{\omega}}{4\pi} \left[\frac{1}{\bar{\omega}} \log(1+\bar{\omega}) - \frac{1}{\bar{\omega}-2} \log(\bar{\omega}-1) \right]$$
$$+ \frac{\bar{\omega}}{4\pi} \left[\frac{1}{\bar{\omega}} \log(1-\bar{\omega}) - \frac{1}{\bar{\omega}+2} \log(-\bar{\omega}-1) \right]. \tag{3.95}$$

Suppose $0 \leq \bar{\omega} < 1$, the integral can be written as

$$(-2i\bar{\omega}) \int_{-\infty}^{\infty} \frac{dz}{2\pi} \frac{\operatorname{sgn}(z)}{(1+z^2)} \frac{1}{1+(-i\bar{\omega}-z)^2}$$
$$= \frac{1}{2\pi} \log(1-\bar{\omega}^2) + \frac{\bar{\omega}}{2\pi} \left(\frac{1}{4-\bar{\omega}^2} \left[-4\operatorname{arctanh}(\bar{\omega}) + \bar{\omega}\log\left(1-\bar{\omega}^2\right) \right] \right). \tag{3.96}$$

34

For $\bar{\omega} > 1$,

$$(-2i\bar{\omega}) \int_{-\infty}^{\infty} \frac{dz}{2\pi} \frac{\text{sgn(z)}}{(1+z^2)} \frac{1}{1+(-i\bar{\omega}-z)^2}$$

$$= \frac{1}{2\pi} \log(\bar{\omega}^2 - 1) + \frac{\bar{\omega}}{2\pi} \left(\frac{1}{4-\bar{\omega}^2} \left[-2\log\left(\frac{\bar{\omega}+1}{\bar{\omega}-1}\right) + \bar{\omega}\log(\bar{\omega}^2-1) \right] \right). \tag{3.97}$$

5. Final result for $g_1(\bar{\omega})$ in terms of digamma functions

In this subsection the final result for $g_1(i\omega_n)$ is given and if we convert this to the real axis thus we obtain

$$g_1(\bar{\omega}) = \left(-\frac{3}{2-\bar{\omega}}\right) \frac{1}{8} [\psi(-(-i\bar{\omega}+i)\bar{\omega}_E + 1/2) + \psi((-i\bar{\omega}+i)\bar{\omega}_E + 1/2) - \psi(1/2 - i\bar{\omega}_E) - \psi(1/2 + i\bar{\omega}_E)]$$

$$+ \frac{1}{8\bar{\omega}} \left[\psi(-(-i\bar{\omega}-i)\bar{\omega}_E + 1/2) - \psi((-i\bar{\omega}+i)\bar{\omega}_E + 1/2) + \psi((-i\bar{\omega}-i)\bar{\omega}_E + 1/2) \right.$$

$$\left. - \psi(-(-i\bar{\omega}+i)\bar{\omega}_E + 1/2) \right] + \frac{1}{8} \left(-\frac{3}{2+\bar{\omega}}\right) [\psi((-i\bar{\omega}-i)\bar{\omega}_E + 1/2)$$

$$- \psi(1/2 + i\bar{\omega}_E) + \psi((i\bar{\omega}+i)\bar{\omega}_E + 1/2) - \psi(1/2 - \bar{\omega}_E)))]. \tag{3.98}$$

Simplifying this result then gives

$$g_1(\bar{\omega}) = \frac{1}{4\bar{\omega}} \text{Re}\left[\psi\left(i(\bar{\omega}+1)\bar{\omega}_E + \frac{1}{2} \right) - \psi\left(i(1-\bar{\omega})\bar{\omega}_E + \frac{1}{2} \right) \right]$$

$$+ \frac{3}{4} \left(\frac{1}{2-\bar{\omega}}\right) \text{Re}\left[\psi\left(\frac{1}{2} + i\bar{\omega}_E \right) - \psi\left(\frac{1}{2} - i(\bar{\omega}-1)\bar{\omega}_E \right) \right]$$

$$+ \frac{3}{4} \left(\frac{1}{2+\bar{\omega}}\right) \text{Re}\left[\psi\left(\frac{1}{2} + i\bar{\omega}_E \right) - \psi\left(\frac{1}{2} + i(\bar{\omega}+1)\bar{\omega}_E \right) \right]. \tag{3.99}$$

This can be written as

$$g_1(\bar{\omega}) = \frac{\omega_E}{4\omega} \text{Re}\left[\psi\left(\frac{1}{2} + i\frac{(\omega_E+\omega)}{2\pi T} \right) - \psi\left(\frac{1}{2} + i\frac{(\omega_E-\omega)}{2\pi T} \right) \right]$$

$$+ \frac{3}{4} \left(\frac{\omega_E}{2\omega_E-\omega}\right) \text{Re}\left[\psi\left(\frac{1}{2} + i\frac{\omega_E}{2\pi T} \right) - \psi\left(\frac{1}{2} + i\frac{(\omega_E-\omega)}{2\pi T} \right) \right]$$

$$+ \frac{3}{4} \left(\frac{\omega_E}{2\omega_E+\omega}\right) \text{Re}\left[\psi\left(\frac{1}{2} + i\frac{\omega_E}{2\pi T} \right) - \psi\left(\frac{1}{2} + i\frac{(\omega+\omega_E)}{2\pi T} \right) \right]. \tag{3.100}$$

Utilizing the asymptotic expansion of the digamma function, namely, $\psi(z+1/2) \to \log(z) + \mathcal{O}(z^{-2})$, as $z \to \infty$, it follows that, as $T_c/\omega_E \to 0$, the asymptotic limit of $g_1(\bar{\omega})$ function is given as

$$g_1(\bar{\omega}) = \frac{1}{4-\bar{\omega}^2} \left\{ \frac{2+\bar{\omega}^2}{2\bar{\omega}} \log\left|\frac{1+\bar{\omega}}{1-\bar{\omega}}\right| - \frac{3}{2} \log\left|1-\bar{\omega}^2\right| \right\}. \tag{3.101}$$

Note that, this expression is invalid at $\bar{\omega} = 1$. In the next subsection, we will compute this limits exactly for $(\omega_E - \omega)/T \gg 1$ and $\omega_E/T \gg 1$.

In this subsection we compute $g_1(\bar{\omega} = 1)$ using the digamma solutions. In Fig.(5) we plot the graph of $g_1(\omega)$ versus $\bar{\omega}$ using the analytical digamma solutions and the asymptotic result for $\lambda = 0.1$. Note that, there is no singularity at $\bar{\omega} = 2$:

$$g_1(\bar{\omega} \to 2) = \frac{3}{4}\left[1 - \frac{1}{12}\log(3)\right]. \tag{3.102}$$

At the origin the limiting behaviour when $\bar{\omega} \to 0^+$ is given by

$$g_1(\bar{\omega} \to 0^+) = \frac{1}{4}\left\{\frac{2}{\bar{\omega}}\text{arctanh}(\bar{\omega}) - \frac{3}{2}\log(1)\right\} = \frac{1}{2}. \tag{3.103}$$

Now let us find the exact value at $\bar{\omega} = 1$ from the exact expression on real axis. The value of the function
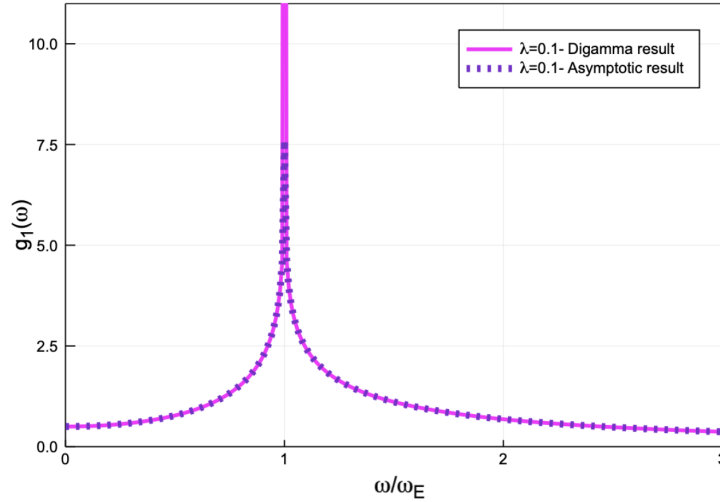
Figure 5. A plot of the asymptotic result and the analytical digamma solution of the gap function in units of ω_E versus frequency for $\lambda = 0.1$ (without renormalization factor) at the critical temperature.

$g_1(\bar{\omega} = 1)$ is obtained as follows

$$\begin{aligned}g_1(\bar{\omega} = 1) &= \log(2)\frac{1}{3} - \left\{\psi(1/2) + \frac{1}{3}[\log(2) - 3\log(\bar{\omega}_E)]\right\}, \\ &= \log(\bar{\omega}_E) - \psi(1/2).\end{aligned} \tag{3.104}$$

For $\lambda = 0.1$, the value of $g_1(\bar{\omega} = 1)$ is 10.475 which is finite (but large) compared to T_c/ω_E. Here, we plot $g_1(\bar{\omega})$ using the asymptotic solution and analytical digamma versus frequency. In Fig.(6) we plot the gap function on the real axis in the vicinity of $\bar{\omega} = 1$, to verify that the asymptotic behaviour is indeed $\log(\bar{\omega}_E) - \psi(1/2)$, and there seems to be good agreement between the red dotted curve which is the gap function on the real axis using the digamma expression and the orange curve which is the gap function obtained from the evaluation of the digamma result at $\bar{\omega} = 1$. On the real axis, $i\bar{\omega}_n = 1 + i\delta$, the renormalization factor is

$$Z(1 + i\delta) = 1 + \frac{\lambda}{2}[\psi(-2i\bar{\omega}_E + 1/2) - \psi(1/2)]. \tag{3.105}$$
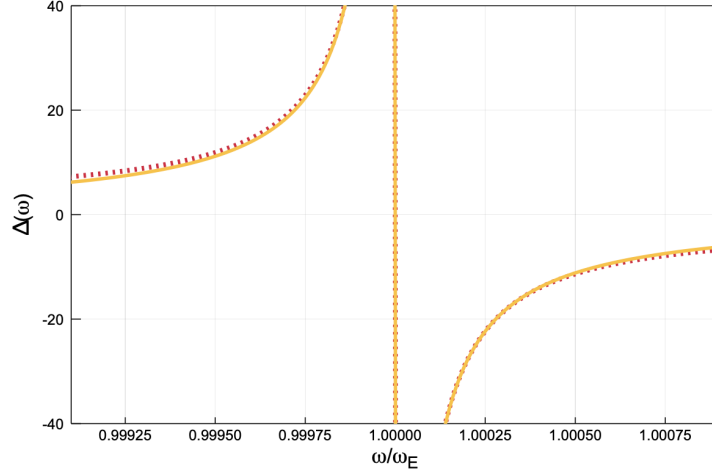
Figure 6. A plot of the gap function in units of ω_E on the real axis in the vicinity of $\omega/\omega_E = 1$. The red dotted curve is the gap function which is calculated using the digamma expression and the orange curve is the gap function which is obtained applying $g_1(\bar{\omega}) = \log(\bar{\omega}_E) - \psi(1/2)$.

In the limit of large $\bar{\omega}_E$ this reduces to

$$Z(\bar{\omega} = 1) = 1 + \frac{\lambda}{2}[\log(2\bar{\omega}_E) - \psi(1/2)]. \tag{3.106}$$

C.   Gap edge

The gap equation on the real axis is

$$
\begin{aligned}
Z(z)\Delta(z) =& \pi T \sum_{m=-\infty}^{\infty} \lambda(z - i\omega_m)\frac{\Delta(i\omega_m)}{\sqrt{\omega_m^2 + \Delta^2(i\omega_m)}} \\
&+ i\pi A(\omega_E)\frac{\Delta(z - \omega_E)[N(\omega_E) + f(\omega_E - z)]}{\sqrt{(z - \omega_E)^2 - \Delta^2(z - \omega_E)}} \\
&+ i\pi A(\omega_E)\frac{\Delta(z + \omega_E)[N(\omega_E) + f(\omega_E + z)]}{\sqrt{(z + \omega_E)^2 - \Delta^2(z + \omega_E)}}.
\end{aligned}
\tag{3.107}
$$

To consider the $\bar{T} \to 0$ limit we use the relation

$$\bar{T}\sum_{i\omega_m} \to \int_{-\infty}^{\infty} \frac{d\omega}{2\pi}. \tag{3.108}$$

The next step is to normalize the gap function and frequencies by ω_E to obtain

$$Z(z)\bar{\Delta}(z) = \frac{1}{2}\int_{-\infty}^{\infty} d\bar{\omega}\lambda(\bar{z} - i\bar{\omega})\frac{\bar{\Delta}(i\bar{\omega})}{\sqrt{\bar{\omega}^2 + \bar{\Delta}^2(i\bar{\omega})}}. \tag{3.109}$$

Note that we have neglected the contributions of $[N(\omega_E) + f(\omega - \omega_E)]$ and $[N(\omega_E) + f(\omega + \omega_E)]$ in calculating the gap edge because in the weak-coupling limit $(\omega_E/T_c \gg 1)$, where $e^{-\omega_E/T_c} \ll 1$, and $T_c = (1.13/\sqrt{e})\omega_E e^{-1/\lambda}$. Therefore, the contribution of these terms are very small. The gap edge is very small in the weak-coupling limit, so it is not of the order of ω_E. Here, $\bar{Q} \equiv Q/\omega_E$ and $\bar{\omega}_E = \omega_E/(2\pi T)$.

37

Also, $\bar{z}$ denotes z/ω_E. To a good approximation $Z = 1$. The bosonic propagator λ is

$$\lambda(z) = \frac{\lambda}{1 - \bar{z}^2}. \tag{3.110}$$

The gap function on the real axis is thus

$$\bar{\Delta}(\bar{z}) = \frac{1}{2} \int_{-\infty}^{\infty} d\bar{\omega} \frac{\lambda}{1 - (\bar{z} - i\bar{\omega})^2} \frac{\bar{\Delta}(i\bar{\omega})}{\sqrt{\bar{\omega}^2 + \bar{\Delta}^2(i\bar{\omega})}}. \tag{3.111}$$

The gap edge is defined by $\Delta(z = \Delta_0) = \Delta_0$, using the above result it satisfies

$$\bar{\Delta}_0 = \frac{\lambda}{2} \int_{-\infty}^{\infty} \frac{d\bar{\omega}}{1 - (\bar{\Delta}_0 - i\bar{\omega})^2} \frac{\bar{\Delta}(i\bar{\omega})}{\sqrt{\bar{\omega}^2 + \bar{\Delta}^2(i\bar{\omega})}}. \tag{3.112}$$

From numerical analysis, in the weak-coupling limit $\bar{\Delta}_0$ is small compared to unity, thus we can drop it in the integrand to obtain

$$\bar{\Delta}_0 = \frac{\lambda}{2} \int_{-\infty}^{\infty} \frac{d\bar{\omega}}{1 + \bar{\omega}^2} \frac{\bar{\Delta}(i\bar{\omega})}{\sqrt{\bar{\omega}^2 + \bar{\Delta}^2(i\bar{\omega})}}. \tag{3.113}$$

The gap function is approximated by

$$\bar{\Delta}(i\omega_m) \approx \frac{\bar{\Delta}_0}{1 + \bar{\omega}_m^2} \Rightarrow \bar{\Delta}(i\bar{\omega}) = \frac{\bar{\Delta}_0}{1 + \bar{\omega}^2}. \tag{3.114}$$

Thus, the gap edge obeys the following equation

$$1 = \frac{\lambda}{2} \int_{-\infty}^{\infty} \frac{d\bar{\omega}}{1 + \bar{\omega}^2} \frac{\frac{1}{1+\bar{\omega}^2}}{\sqrt{\bar{\omega}^2 + \left(\frac{\bar{\Delta}_0}{1+\bar{\omega}^2}\right)^2}}. \tag{3.115}$$

We drop the $1/(1+\bar{\omega}^2)$ in the term $\Delta_0/(1+\bar{\omega}^2)$. When $\bar{\omega} \gg 1$, Δ_0 does not provide a large contribution, and when $\bar{\omega} \ll 1$, $1 + \bar{\omega}^2 \approx 1$, therefore,

$$1 = \frac{\lambda}{2} \int_{-\infty}^{\infty} \frac{d\bar{\omega}}{(1 + \bar{\omega}^2)^2} \frac{1}{\sqrt{\bar{\omega}^2 + \bar{\Delta}_0^2}}, \tag{3.116}$$

The solution to this integral equation gives $\bar{\Delta}_0(\lambda)$. Now, we turn our attention to this integral [30].

$$I = \int_{-\infty}^{\infty} \frac{dx}{\sqrt{x^2 + y^2}} \frac{1}{(1 + x^2)^2}$$
$$= \frac{1}{(y^2 - 1)} \left[\frac{(y^2 - 2) \arctan(\sqrt{y^2 - 1})}{\sqrt{y^2 - 1}} + 1 \right]. \tag{3.117}$$

Therefore, the gap edge obeys

$$1 = \frac{\lambda}{2} \int_{-\infty}^{\infty} \frac{d\bar{\omega}}{(1 + \bar{\omega}^2)^2} \frac{1}{\sqrt{\bar{\omega}^2 + \bar{\Delta}_0^2}} = \frac{\lambda}{2} \frac{1}{(\bar{\Delta}_0^2 - 1)} \left[\frac{(\bar{\Delta}_0^2 - 2) \arctan(\sqrt{\bar{\Delta}_0^2 - 1})}{\sqrt{\bar{\Delta}_0^2 - 1}} + 1 \right]. \tag{3.118}$$

38

Since the gap edge is smaller than unity, the above result can be written in the form

$$1 = \frac{\lambda}{2} \frac{1}{(\bar{\Delta}_0^2 - 1)} \left[\frac{(\bar{\Delta}_0^2 - 2)\text{arctanh}(\sqrt{1 - \bar{\Delta}_0^2})}{\sqrt{1 - \bar{\Delta}_0^2}} + 1 \right]. \tag{3.119}$$

Recall the definition of arctanh:

$$\text{arctanh}(x) = \frac{1}{2} \log \left(\frac{1+x}{1-x} \right), -1 < x < 1. \tag{3.120}$$

Using this definition in the gap-edge equation then gives

$$1 = \frac{\lambda}{2} \frac{1}{(\bar{\Delta}_0^2 - 1)} \left[\frac{(\bar{\Delta}_0^2 - 2)}{2\sqrt{1 - \bar{\Delta}_0^2}} \log \left(\frac{1 + \sqrt{1 - \bar{\Delta}_0^2}}{1 - \sqrt{1 - \bar{\Delta}_0^2}} \right) + 1 \right]. \tag{3.121}$$

Expanding this for small Δ_0, we then obtain

$$1 = \frac{\lambda}{2} \left[\log \left(\frac{4}{\bar{\Delta}_0^2} \right) - 1 \right] = \lambda \left[\log \left(\frac{2}{\bar{\Delta}_0} \right) - \frac{1}{2} \right]. \tag{3.122}$$

Solving this for Δ_0, we then obtain

$$\bar{\Delta}_0 = 2 \exp \left(-\frac{1}{\lambda} - \frac{1}{2} \right) = \frac{1}{\sqrt{\exp(1)}} \left[2 \exp \left(-\frac{1}{\lambda} \right) \right]. \tag{3.123}$$

It is of interest to note that the BCS result is what is contained in the square brackets. Thus, we find that the weak-coupling Eliashberg result has a square root of $\exp(1)$ difference from its BCS counterpart. Recall that the weak-coupling limit of T_c is given by

$$\bar{T}_c = \frac{1}{\sqrt{\exp(1)}} \left[\frac{\exp[-\psi(1/2)]}{(2\pi)} \exp \left(\frac{-1}{\lambda} \right) \right]. \tag{3.124}$$

Thus, the ratio of the gap edge to the critical temperature is

$$\frac{\bar{\Delta}_0}{\bar{T}_c} = \frac{2}{\sqrt{\exp(1)}} \exp \left(-\frac{1}{\lambda} \right) \left\{ \frac{\exp[-\psi(1/2)]}{(2\pi)\sqrt{\exp(1)}} \exp \left(-\frac{1}{\lambda} \right) \right\}^{-1} = 4\pi \exp[\psi(1/2)] = \pi \exp(-\gamma_E) = 1.76. \tag{3.125}$$

which is the BCS value.

IV. NUMERICAL SOLUTIONS OF THE ELIASHBERG EQUATIONS

A. Imaginary-axis calculations

1. At the critical temperature

In this section we implement an iteration algorithm to numerically solve for the critical temperature T_c and gap function $\Delta(i\omega_n)$. Using an initial guess for these parameters, the Eliashberg equations are solved self-consistently to obtain an updated approximate solution. We continue this process until the transition temperature and energy gap function converge. Regardless of the initial guess, the iteration procedure converges very well. In the previous chapter it was shown that the critical temperature can be obtained from the linearized form of the self-consistency gap function using the Eliashberg equations shown below:

$$
\begin{aligned}
Z(i\omega_n)\Delta(i\omega_n) &= \pi T_c \sum_{m=-\infty}^{\infty} \frac{\lambda \omega_E^2}{\omega_E^2 + (\omega_n - \omega_m)^2} \frac{\Delta(i\omega_m)}{|\omega_m|} \\
&= \lambda \pi \bar{T}_c \sum_{m=-\infty}^{\infty} \frac{1}{1 + (\bar{\omega}_n - \bar{\omega}_m)^2} \frac{\Delta(i\omega_m)}{|\bar{\omega}_m|},
\end{aligned}
\tag{4.1}
$$

where

$$
Z(i\omega_n) = 1 + \frac{\pi T_c}{\omega_n} \sum_{m=-\infty}^{\infty} \lambda(i\omega_n - i\omega_m)\mathrm{sgn}(\omega_m).
\tag{4.2}
$$

The results for the critical temperature of the weak-coupling limit are included in table (1). In Sec. III,

Electron-phonon coupling constant (λ)	T_c/ω_E with $Z(\omega_n) = 1$	T_c/ω_E with $Z(\omega_n)$
$\lambda = 0.1$	0.000032	0.000012
$\lambda = 0.2$	0.004900	0.001821
$\lambda = 0.3$	0.026744	0.009923
$\lambda = 0.4$	0.063305	0.023415
$\lambda = 0.5$	0.107552	0.039428
$\lambda = 0.6$	0.157241	0.055992

Table I. The numerical values for T_c/ω_E for various λ values

it was shown that the analytical approximation for the gap function on the imaginary frequency axis is obtained using

$$
Z(i\omega_n)\Delta(i\omega_n) = \frac{1}{1 + \bar{\omega}_n^2}\left(1 + \lambda\left(\frac{3}{2} - g_1(i\omega_n) - \frac{1}{|\bar{\omega}_n|}\tan^{-1}(|\bar{\omega}_n|)\right)\right),
\tag{4.3}
$$

where

$$
g_1(i\omega_n) = \frac{1}{4 + \bar{\omega}_n^2}\left(\frac{2 - \bar{\omega}_n^2}{\bar{\omega}_n}\arctan(\bar{\omega}_n) - \frac{3}{2}\log(1 + \bar{\omega}_n^2)\right).
\tag{4.4}
$$

If we set $Z(i\omega_n) = 1$, then the gap function can be written as

$$
\Delta(i\omega_n) = \frac{1}{1 + \bar{\omega}_n^2}\left(1 + \lambda\left(\frac{1}{2} - g_1(i\omega_n)\right)\right).
\tag{4.5}
$$

In Fig.(7a) and Fig.(7b) [21], we plot $\Delta(i\omega_n)$ versus ω_n/ω_E for small values of λ comparing the numerical results with the analytical approximation solutions with and without including the $Z(i\omega_n)$ function at the critical temperature [16]. In the numerical calculations, we choose a cut off for the summation. Furthermore, the number of Matsubara frequencies is inversely proportional to the critical temperature. We have used more than 100,000 positive Matsubara frequencies to obtain convergence in the weak-coupling limit because the number of Matsubara points will increase exponentially as λ decreases.

[a]

[b]
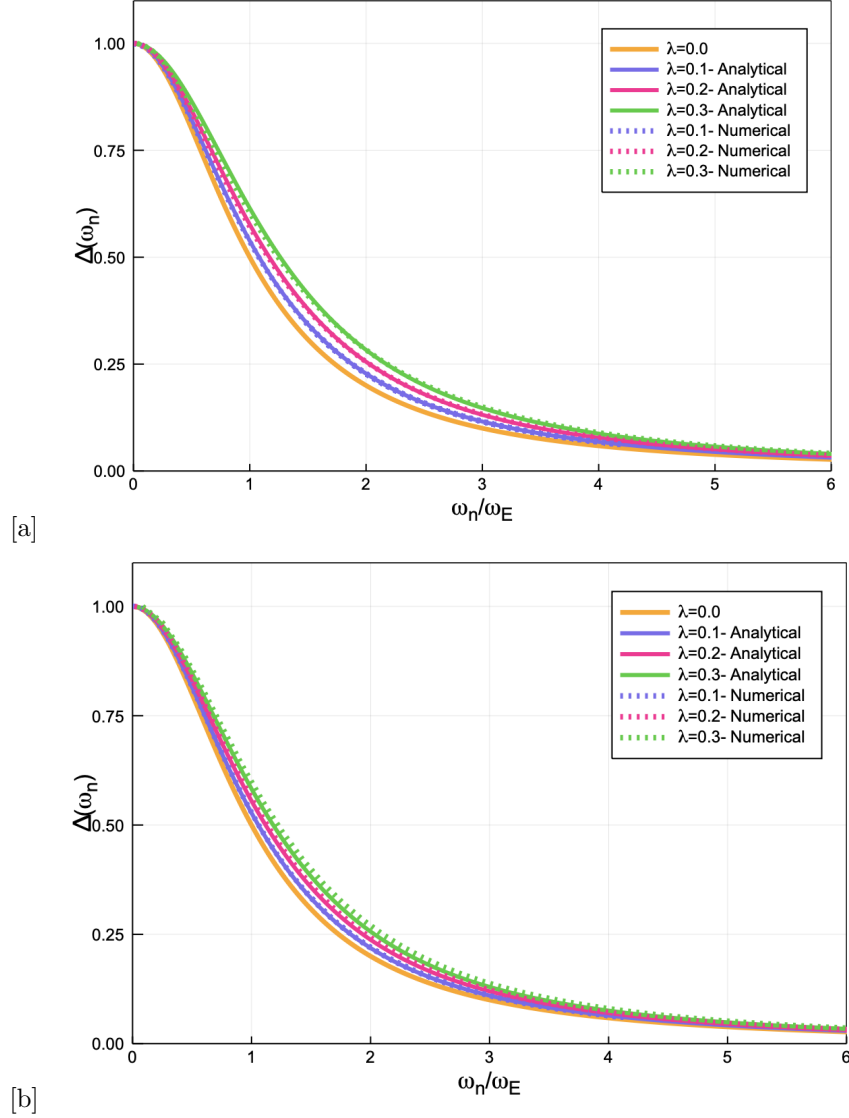
Figure 7. [a] A plot of $\Delta(\omega_n)$ versus ω_n/ω_E for $\lambda = 0.1$, $\lambda = 0.2$, and $\lambda = 0.3$ on the imaginary axis with renormalization factor, [b] without renormalization factor. All the numerical gap functions are normalized by their low frequency value $\Delta(i\omega_{n=1})$. The temperature is set to the critical temperature.

In Fig.(8a) and (8b) [21] we have shown the discrepancies between the the numerical gap function $\Delta_{\text{Numerical}}(\omega_n)$ and the universal result $\tilde{\Delta}_0(\omega_n) = 1/(1 + \omega_n^2)$ in units of ω_E at the critical temperature. The remaining discrepancy comes from second order in electron-phonon coupling constant (λ). We define $\delta\Delta_{\text{Numerical}}(\omega_n)$ as follows [21]:

$$\delta\Delta_{\text{Numerical}}(\omega_n) = \Delta_{\text{Numerical}}(\omega_n) - \tilde{\Delta}_0(\omega_n), \tag{4.6}$$

41

In addition, $\delta\Delta_{\text{Analytical}}(\omega_n)$ is

$$\delta\Delta_{\text{Analytical}}(\omega_n) = \Delta_{\text{Analytical}}(\omega_n) - \tilde{\Delta}_0(\omega_n). \qquad (4.7)$$

The inclusion of $Z(i\omega_n)$ leads to better agreement between the numerical and analytical results [21]. We plot $[\ln(\omega_E/T_c)]^{-1}$ versus λ for the case where the renormalization factor $Z(\omega_n)$ is not included in
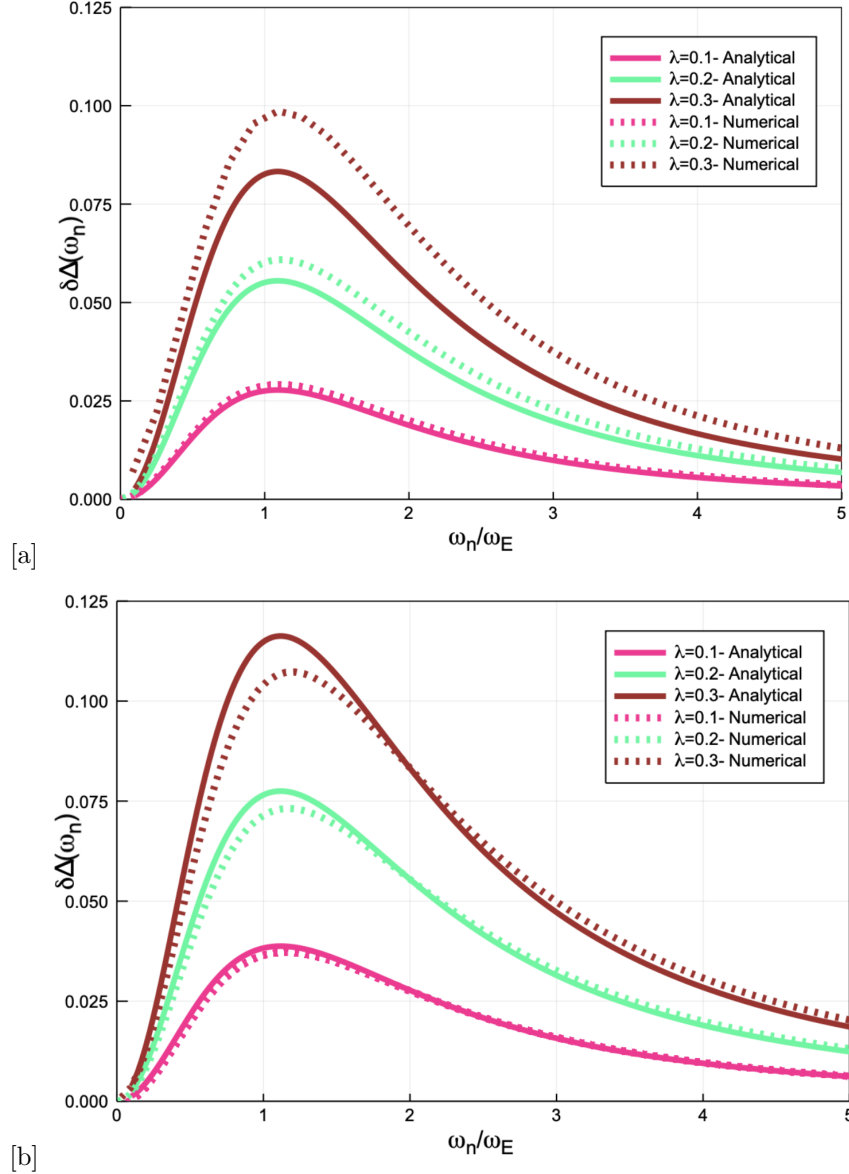
Figure 8. [a] A plot of $\delta\Delta(\omega_n)$ in units of ω_E versus ω_n/ω_E (without renormalization factor), [b] A plot of $\delta\Delta(\omega_n)$ in units of ω_E versus ω_n/ω_E with renormalization factor at the critical temperature.

our calculations, in Fig.(9a), and where the renormalization factor is included, in Fig.(9b), where the green line shows the numerical solution, the blue line represents the BCS approximation, and the red line determines the improved analytical result.

Comparing Fig.(9a) and Fig.(9b) [21], we notice that at larger values of λ the inclusion of the renor-

malization factor decreases $[\ln(\omega_E/T_c)]^{-1}$, which means that $\ln(\omega_E/T_c)$ is larger and T_c is smaller. In the weak-coupling limit, $\omega_E/T_c \gg 1$, the $\ln \omega_E/T_c$ is small. Also, the plot of $\ln(T_c/\omega_E)$ versus λ has a negative y-axis scale. One way to remedy this is to plot $[\ln(\omega_E/T_c)]^{-1}$ which has a positive y-axis scale.

[a]

[b]
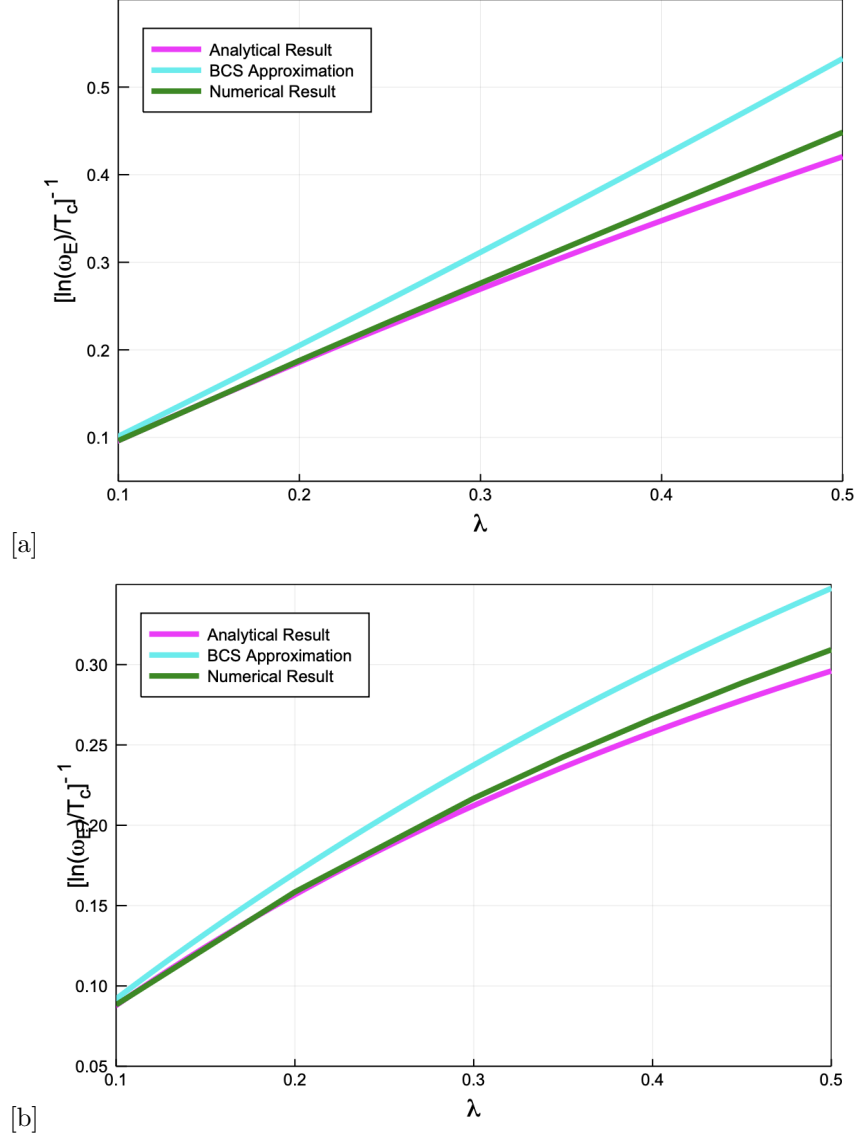
Figure 9. [a] A plot of $[\ln(\omega_E/T_c)]^{-1}$ versus λ without renormalization factor, [b] with renormalization factor at the critical temperature.

2. Below the critical temperature

The Eliashberg equations below critical temperature are defined as

$$Z(i\omega_n)\Delta(i\omega_n) = \pi T \sum_{m=-\infty}^{\infty} \lambda(i\omega_n - i\omega_m) \frac{\Delta(i\omega_m)}{\sqrt{\omega_m^2 + \Delta^2(i\omega_m)}}, \tag{4.8}$$

43

where $Z(i\omega_n)$ is

$$Z(i\omega_n) = Z_N(i\omega_n) + \frac{\pi T}{\omega_m} \sum_m \lambda(i\omega_n - i\omega_m) \left(\frac{\omega_m}{\sqrt{\omega_m^2 + \Delta^2(i\omega_m)}} - \mathrm{sgn}(i\omega_m) \right). \tag{4.9}$$

Also, $Z_N(i\omega_n)$ can be written as

$$Z_N(i\omega_n) = 1 + \frac{\pi T}{\omega_n} \left(\lambda + 2 \sum_{m=0}^{n-1} \lambda(i\nu_{m+1}) \right). \tag{4.10}$$

In Fig.(10a) and (10b) the numerical calculation of the gap function on the imaginary axis below T_c are shown for $\lambda = 0.2$ and $\lambda = 0.3$ [31]. The highest curve is related to the lowest temperature both for $\lambda = 0.2$ and $\lambda = 0.3$. As the temperature is increased, the gap function is decreased.

These plots show that as the frequency increases, the gap will decrease slowly. Furthermore, in the low-temperature limit, the gap has the maximum size, however, as the temperature approaches the critical temperature the gap will be lowered. Now, one can plot $\Delta(\omega_n)/\Delta(\omega_{n=1})$ versus ω_n in Fig.(11) for various temperatures to show that below the critical temperature all the curves for a given coupling constant fall onto one curve, which is indicative of the fact that the normalized gap function for every coupling strength is temperature independent on the imaginary frequency axis. Here, $\Delta(\omega_{n=1})$ means the low-frequency gap function. Using the Eliashberg gap function on the imaginary axis, one can plot the graph of $\Delta(\omega_n)$ versus ω_n/ω_E to obtain the low-frequency superconducting gap $\Delta(\omega_{n=1})$ including the renormalization factor which is shown in Fig.(12a). In Fig.(12b) $\Delta(\omega_1)$ is plotted as a function of temperature for $\lambda = 0.5$ using non-linear Eliashberg equations and including renormalization function. In Fig.(12c) we plot the ratio of zero frequency gap function to zero frequency gap function at $T = 0$ versus temperature using Eliashberg theory and BCS theory. This plot shows that the full temperature dependent gap equation using Eliashberg equation is BCS-like.

B.   Real-axis calculations

The gap function and renormalization function on the real frequency axis are

$$\begin{aligned}
Z(z)\Delta(z) =& \pi T \sum_{m=-\infty}^{\infty} \lambda(z - i\omega_m) \frac{\Delta(i\omega_m)}{\sqrt{\omega_m^2 + \Delta^2(i\omega_m)}} \\
& + i\pi A \left[[N(\omega_E) + f(\omega_E - z)] \frac{\Delta(z - \omega_E)}{\sqrt{(z - \omega_E)^2 - \Delta^2(z - \omega_E)^2}} \right] \\
& + i\pi A \left[[N(\omega_E) + f(\omega_E + z)] \frac{\Delta(z + \omega_E)}{\sqrt{(z + \omega_E)^2 - \Delta^2(z + \omega_E)^2}} \right]. \tag{4.11}
\end{aligned}$$

$$\begin{aligned}
Z(z) =& 1 + \frac{i\pi T}{z} \sum_{m=-\infty}^{\infty} \lambda(z - i\omega_m) \frac{\omega_m}{\sqrt{\omega_m^2 + \Delta^2(i\omega_m)}} \\
& + \frac{i\pi A}{z} \left[[N(\omega_E) + f(\omega_E - z)] \frac{(z - \omega_E)}{\sqrt{(z - \omega_E)^2 - \Delta^2(z - \omega_E)^2}} \right] \\
& + \frac{i\pi A}{z} \left[[N(\omega_E) + f(\omega_E + z)] \frac{(z + \omega_E)}{\sqrt{(z + \omega_E)^2 - \Delta^2(z + \omega_E)^2}} \right]. \tag{4.12}
\end{aligned}$$

where $z \equiv \omega + i\delta$ and δ is an infinitesimal positive value which tells us that analytical continuation is done above the real frequency axis. We used $\delta = 10^{-4}$ in the numerical calculations which are done in this thesis. Equations (4.11) and (4.12) are solved numerically for various temperatures. In order to calculate the gap equation on the real axis using these two equations one needs to do the Matsubara summation first and then self-consistently solve on the real axis. This method was first developed by

[a]

[b]
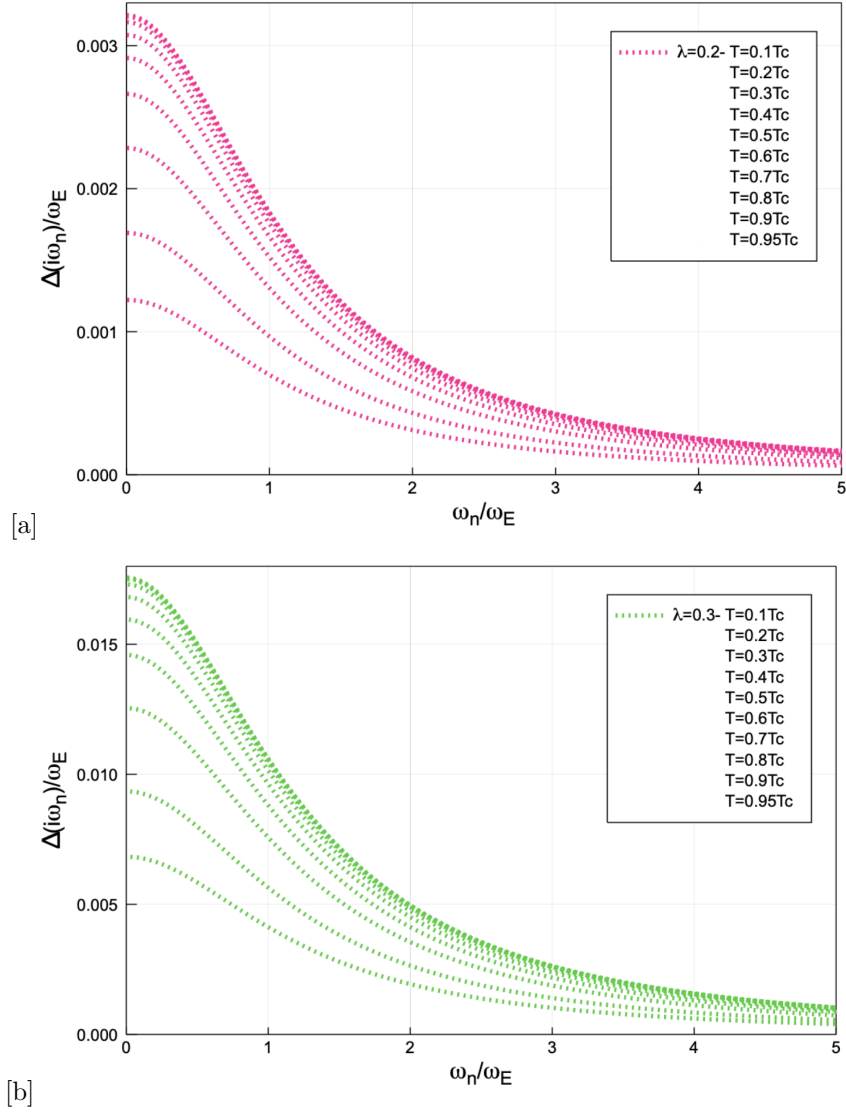
Figure 10. [a] The plot of $\Delta(\omega_n)$ in units of ω_E versus ω_n/ω_E for $\lambda = 0.2$ below T_c on the imaginary axis. [b] The plot of $\Delta(\omega_n)$ in units of ω_E versus ω_n for $\lambda = 0.3$ below T_c on the imaginary axis. The scale of the gap function changes with critical temperature for various electron-phonon coupling strengths. As the temperature decreases from T_c the magnitude of the order parameter increases monotonically at all frequencies.

Marsiglio, Schossmann, and Carbotte [17].

1. Zero-temperature limit

The Eliashberg equations can be solved in the low reduced temperature limit. It was shown that the low-temperature gap equation within BCS theory is obtained from

$$\Delta(T) \approx \Delta_0 - (2\pi\Delta_0 T)^{1/2} e^{-\Delta_0/T}, \tag{4.13}$$

where $\Delta_0 = \Delta(T = 0)$, $T \equiv tT_c$ and t is called the reduced temperature. For the case of $T \ll \Delta_0$, the second term is exponentially small, and we obtain the zero-temperature solution. Now if we set $t = 0.1$,
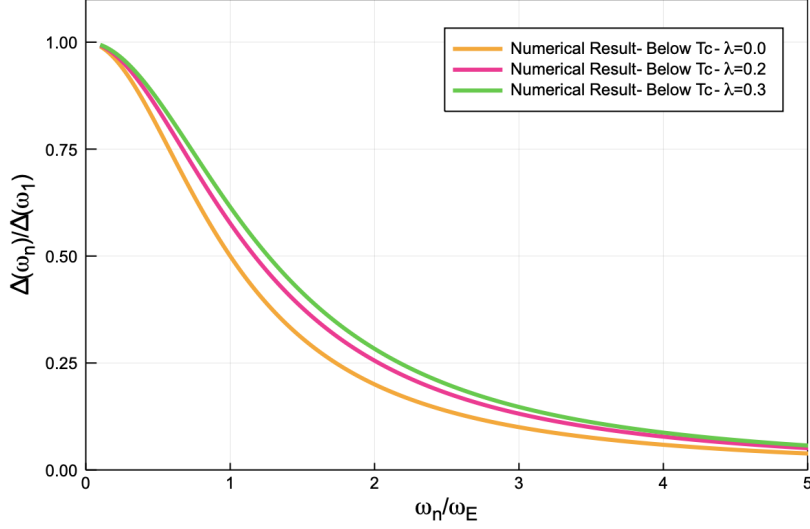
Figure 11. The plot of $\Delta(\omega_n)/\Delta(\omega_{n=1})$ versus ω_n/ω_E for $\lambda = 0.2$ and $\lambda = 0.3$ below T_c on the imaginary frequency axis. All of the ten curves related to the normalized gap function at $T = 0.1T_c, 0.2T_c, 0.3T_c, 0.4T_c, 0.5T_c, 0.6T_c, 0.7T_c, 0.8T_c, 0.9T_c$ and $0.95T_c$ will overlap.

the second term is much smaller than one, which indicates that even at slightly higher temperatures, the zero-temperature solution is a very good approximation [32]. From numerical calculations, sometimes the zero-temperature result occurs at lower values of temperature depending on weighting factor A and Einstein frequency ω_E [33].

For $T = 0$ the Bose-Einstein function $N(\omega_E)$ is zero and the Fermi-Dirac function is a unit step function $f(x) = \Theta(-x)$. Note that as $T \to 0$ the second term in Eq.(4.11), which is $I = N(\omega_E) + f(\omega_E - z)$, can be replaced by $N(\omega_E) = 1/(e^{\beta\omega_E} - 1) = -\Theta(-\omega_E)$ and $f(\omega_E - z) = 1/(e^{\beta(\omega_E - z)} + 1) = \Theta(z - \omega_E)$. Thus, we have

$$I = -\Theta(-\omega_E) + \Theta(z - \omega_E). \tag{4.14}$$

For $0 < z < \omega_E$, $I = 0$ and for $0 < \omega_E < z$, $I = 1$. The third term in Eq.(4.11), which is $J = N(\omega_E) + f(\omega_E + z)$, can be replaced by $N(\omega_E) = 1/(e^{\beta\omega_E} - 1) = -\Theta(-\omega_E)$ and $f(\omega_E + z) = 1/(e^{\beta(\omega_E + z)} + 1) = \Theta(z + \omega_E)$. Thus, we have

$$J = -\Theta(-\omega_E) + \Theta(z + \omega_E). \tag{4.15}$$

For both cases $0 < z < \omega_E$ and $0 < \omega_E < z$, we obtain $J = 0$. Now let us call the first term of Eq.(4.11) by $\Delta_{\mathbf{inhomogenous}}(z)$ as follows

$$\Delta_{\mathbf{inhomogeneous}}(z) = \pi T \sum_{m=-\infty}^{\infty} \lambda(z - i\omega_m) \frac{\Delta(i\omega_m)}{\sqrt{\omega_m^2 + \Delta^2(i\omega_m)}}, \tag{4.16}$$

and the other two terms in Eq.(4.11) are called the homogeneous terms. In the $T \to 0$ limit, for $0 < z < \omega_E$, one can write

$$\Delta(z) = \Delta_{\mathbf{inhomogeneous}}(z), \tag{4.17}$$

46
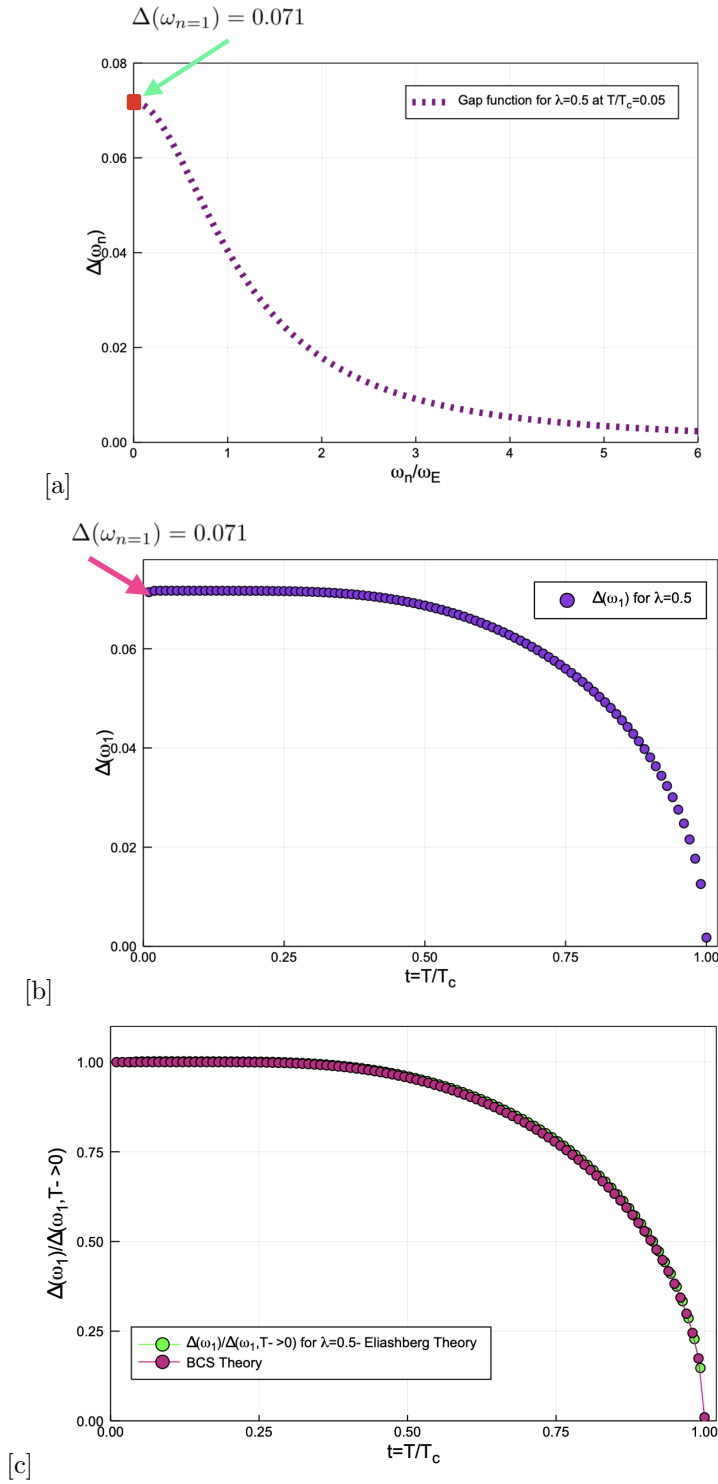
Figure 12. [a] A plot of $\Delta(\omega_n)$ in units of ω_E versus ω_n/ω_E for $\lambda = 0.5$ on the imaginary axis at $T/T_c = 0.05$ (with renormalization factor). [b] A plot of the non-linear temperature dependent gap equation $\Delta(\omega_1)$ in units of ω_E versus $t = T/T_c$. [c] A plot of $\Delta(i\omega_1, T)/\Delta(i\omega_1, T \to 0)$ versus temperature applying the BCS and Eliashberg theories.

47

and for $\omega_E < z < 2\omega_E$ we have

$$\Delta(z) = \Delta_{\textbf{inhomogeneous}}(z) + i\pi A\left[[N(\omega_E) + f(\omega_E - z)]\frac{\Delta_{\textbf{inhomogeneous}}(z - \omega_E)}{\sqrt{(z - \omega_E)^2 - \Delta_{\textbf{inhomogeneous}}^2(z - \omega_E)}}\right]. \quad (4.18)$$

This procedure is followed for higher frequencies to obtain the structures. The zero-temperature limit of $\lambda = 1$ with $\omega_E = 1$ meV at $t = T/T_c = 0.01$ is considered here in Fig.(13)[33]. We plot the real and imaginary parts of $\Delta(\omega)$ [12], $Z(\omega)$, $n(\omega) \equiv N(\omega)/N(0)$ (which is the density of states normalized to the normal state) and $A(K_F, \omega)$ at the Fermi level (which is the spectral function) versus $\bar{\omega}$. The density of states is obtained from the tunneling experiment and the spectral function is considered in photoemission experiment. The unit of energy in all the figures are meV. On the real frequency axis, there exist sharp structures at multiple frequencies. The sharpness of the peaks are the result of using the Einstein frequency in the calculations. The heights of the peaks are the same order of magnitude at (λ=1). The density of states $n(\omega) \equiv N(\omega)/N(0)$ is defined as

$$\frac{N(\omega)}{N(0)} = \text{Re}\left[\frac{\omega}{\sqrt{\omega^2 - \Delta^2(\omega)}}\right], \quad (4.19)$$

and the spectral function $A(K_F, \omega)$ at the Fermi level is

$$A(K_F, \omega) = \frac{-1}{\pi}\text{Im}\left[\frac{\omega}{Z(\omega)[\omega^2 - \Delta^2(\omega)]}\right]. \quad (4.20)$$

The real part of the energy gap $\text{Re}\Delta(\omega)$ represents the strength of effective electron-electron interaction and the imaginary part of the gap $\text{Im}\Delta(\omega)$ determines the damping effect. In Fig.(13a) we observe the structure at $\omega = \Delta_0 + n\omega_E$ as a result of multi-boson emission. Here, $n = 0, 1, 2, 3, ...$ and Δ_0 is the gap-edge which is defined as follows:

$$\Delta_0 = \text{Re}\Delta(\omega = \Delta_0). \quad (4.21)$$

In the zero-temperature limit, the gap function is purely real and constant up to a certain frequency because there are no thermal fluctuations at $T = 0$ which means that all the electrons form Cooper pairs. The low frequency behavior of the real and imaginary part of the gap function and renormalization function in the zero-temperature limit is defined as follows [16]:

$$\begin{aligned}
\text{Re}\Delta(\omega) &= c, \\
\text{Im}\Delta(\omega) &= 0, \\
\text{Re}Z(\omega) &= d, \\
\text{Im}Z(\omega) &= 0.
\end{aligned} \quad (4.22)$$

It is shown in Fig.(13c) that there exists a gap in the density of states. The density of states rises very sharply as the frequency is greater than a definite value. The peak in the density of states determines the location of the gap edge. Sharp peaks in Fig.(13c) of spectral function represents the quasi-particles which are long-lived and followed by a gap. The appearance of resonances at higher frequencies show that the gap is a non-linear function. In Fig.(14) we plot the gap function, renormalization function, density of states and spectral function versus $\bar{\omega}$ for $\lambda = 0.3$. Here, we observe the structures at multiple boson frequencies. For the case of $\lambda = 0.3$, the peak at $\bar{\omega} = 1$ is the highest and smaller peaks are observed at multiples of ω_E as a result of higher order electron-phonon coupling constant. Comparing the gap function for $\lambda = 0.3$ and $\lambda = 1$ it is obvious that the height of the peaks are shorter as the coupling becomes weaker, which means that less energy is required for breaking the Cooper pairs in the weak

---

[12]By $\Delta(\omega)$, we mean $\Delta(\omega + i\delta)$. Here, δ is an infinitesimal value which is 10^{-4} in thesis thesis
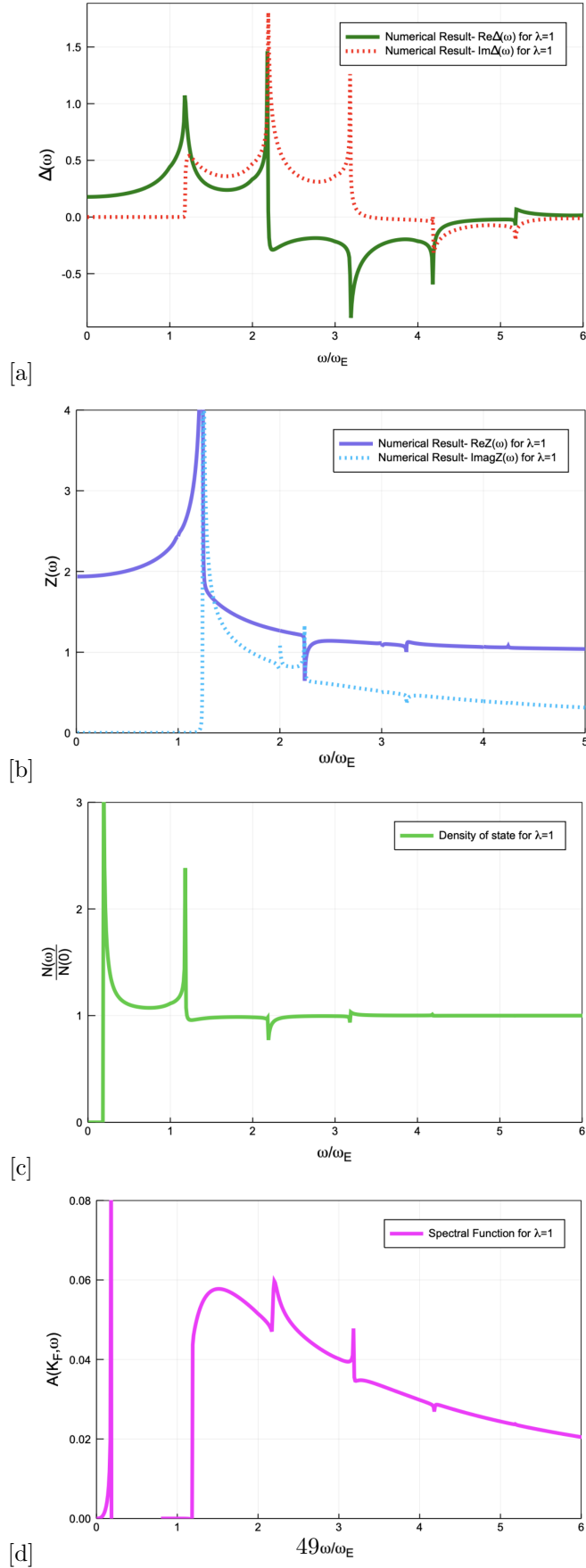
Figure 13. [a] A plot of $\Delta(\omega)$ in units of ω_E versus ω/ω_E. [b] A plot of $Z(\omega)$ versus ω/ω_E. [c] $N(\omega)/N(0)$ versus ω/ω_E. [d] $A(K_F,\omega)$ versus ω/ω_E at $t = T/T_c = 0.01$ for $\lambda = 1$ and $\omega_E = 1.0$ meV.

electron-phonon coupling limit at zero temperature. Here, we plot the real part of $\Delta(\omega)$ versus ω/ω_E at the low temperature limit for three weak-coupling strengths at $T = 0.2T_c$ in Fig.(15a). Furthermore, the imaginary part of the $\Delta(\omega)$ versus ω/ω_E at $T = 0.2T_c$ is plotted in Fig.(15b) [31]. When, $T = 0.2T_c$, the energy scale of the gap function is lowered with decreasing the electron-phonon coupling constant. The frequency-dependent gap function of Eliashberg theory is a complex function

$$\Delta(\omega, T) \equiv \Delta_1(\omega, T) + i\Delta_2(\omega, T), \tag{4.23}$$

which depends on the frequency and temperature, whereas the BCS gap function is a real and frequency independent quantity. We have computed the gap edge (Δ_0) by finding the intersection of two curves ω and the $\Delta(\omega, T)$ on the real axis, starting with $t = 0.1T_c$ which is shown in Fig.(16a). We plot the temperature-dependent gap equation for $\lambda = 0.3$ and $\lambda = 1$ in Fig.(16b) [34]. The gap-edge is single-valued in the weak-coupling superconductors for $\lambda < 0.8$ [35]. The plot of $\Delta_0(T)/\Delta_0(0)$ versus T/T_c shows that both BCS and Eliashberg theories are from the same universality class which are the classic mean field behavior of the order parameter. It identifies the class of phase transition that they belong to [36].

We plot $1/[\ln(\omega_E/\Delta_0)]$ versus λ in the weak coupling limit without including the renormalization factor in Fig.(17a) and with including the renormalization factor in Fig.(17b) [31]. In order to find the numerical gap edge in these two figures we have found the intersection of the real part of energy gap function at $T/T_c = 0.1$. The BCS gap edge is

$$\Delta_0 = 2\omega_E \exp(-1/\lambda), \tag{4.24}$$

and the Eliashberg gap edge without including the renormalization factor is

$$\Delta_0 = \frac{2}{\sqrt{e}}\omega_E \exp(-1/\lambda), \tag{4.25}$$

and with including the renormalization factor is defined as follows

$$\Delta_0 = \frac{2}{\sqrt{e}}\omega_E \exp(-(1+\lambda)/\lambda). \tag{4.26}$$

The blue line is the BCS approximation, the red line shows the Eliashberg result and the green line represents the numerical result which are in good agreement as $\lambda \to 0$.

2. Finite-temperature limit

In the finite-temperature limit ($T > 0$ or $\omega_E \ll T$), the thermal fluctuations destroy pairing in the low-frequency limit. Here, we write the Bose function as

$$N(\omega_E) \approx \frac{1}{1 + \beta\omega_E - 1} \approx \frac{1}{\beta\omega_E} \approx \frac{T}{\omega_E}, \tag{4.27}$$

and the Fermi function becomes

$$f(\omega_E \pm z) \sim f(\pm z), \tag{4.28}$$

At non zero temperature limit, the solution of the gap function and renormalization function can be obtained using numerical iterations. The low frequency behavior of gap function and renormalization

[a]

[b]

[c]

[d]

51
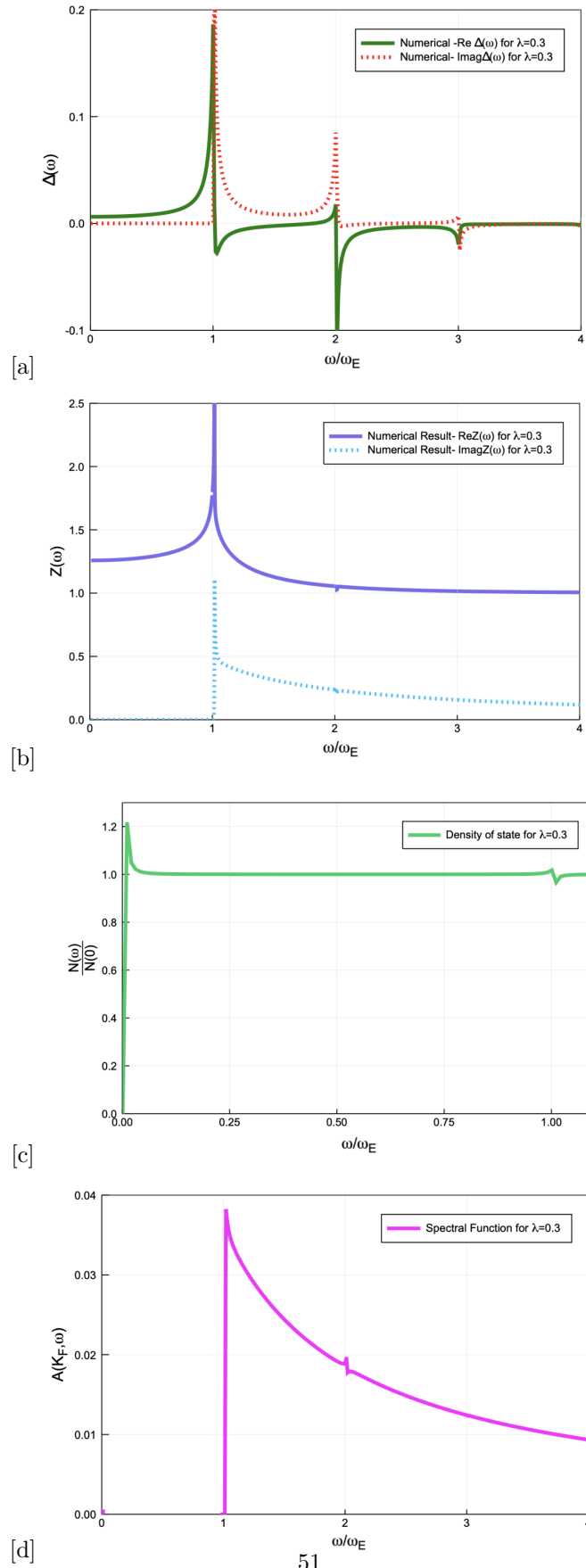
Figure 14. [a] A plot of $\Delta(\omega)$ in units of ω_E versus ω/ω_E. [b] A plot of $Z(\omega)$ versus ω/ω_E. [c] $N(\omega)/N(0)$ versus ω/ω_E. [d] $A(K_F, \omega)$ versus ω/ω_E at $t = T/T_c = 0.01$ for $\lambda = 0.3$ and $\omega_E = 1.0$ meV.
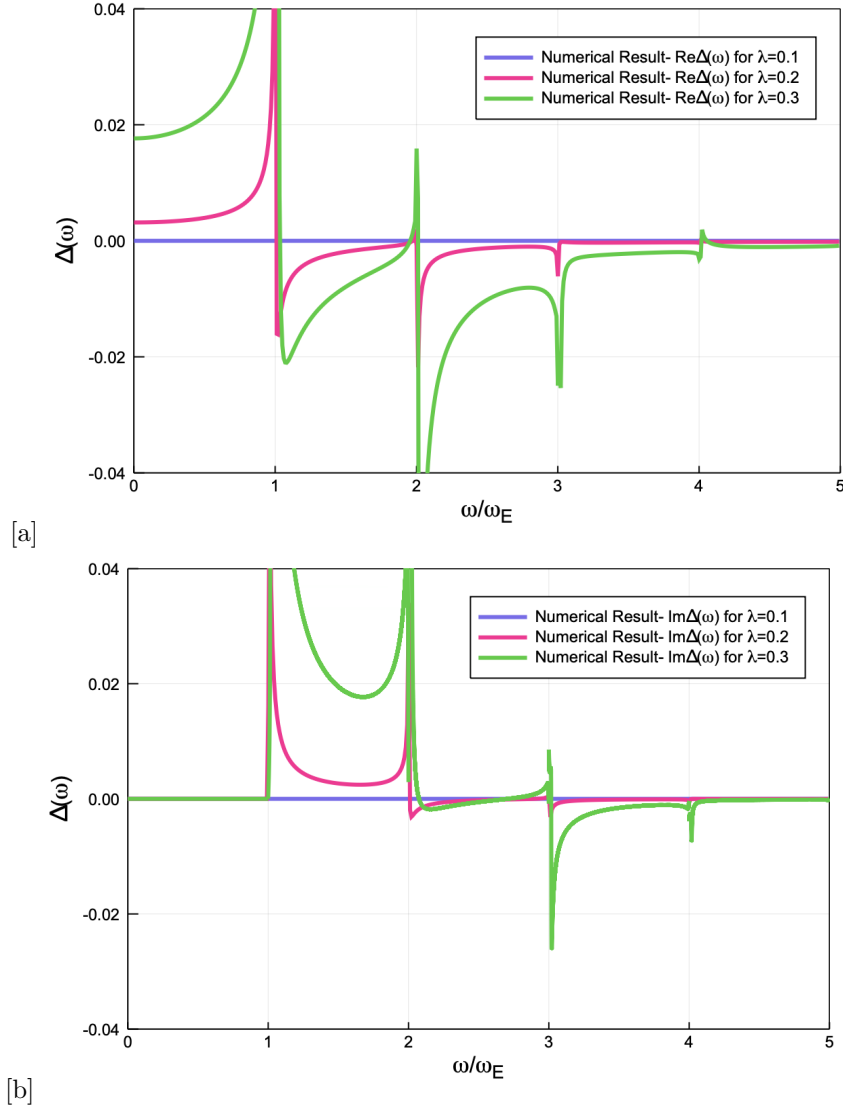
Figure 15. [a] The plot of the real part of $\Delta(\omega)$ in units of ω_E versus ω/ω_E for $\lambda = 0.1$, $\lambda = 0.2$ and $\lambda = 0.3$ at $T = 0.2T_c$.[b] The plot of the imaginary part of $\Delta(\omega)/\Delta(\omega_1)$ versus ω/ω_E for $\lambda = 0.1$, $\lambda = 0.2$ and $\lambda = 0.3$ including the renormalization factor in both cases at $T = 0.2T_c$.

function at any non zero temperature limit lead to [16]

$$
\begin{aligned}
\mathrm{Re}\Delta(\omega) &\propto \omega^2, \\
\mathrm{Im}\Delta(\omega) &\propto \omega, \\
\mathrm{Re}Z(\omega) &= d(T), \\
\mathrm{Im}Z(\omega) &= 1/\omega.
\end{aligned}
\tag{4.29}
$$

which illustrates "gapless" superconductivity at finite temperature [16]. Although in the weak-coupling limit, the gapless superconductivity is not observable. Using the identities

$$
N(\omega_E) + f(\omega_E - z) = \frac{[1 + N(\omega_E)][1 - f(z - \omega_E)]}{[1 - f(z)]}.
\tag{4.30}
$$

[a]

[b]
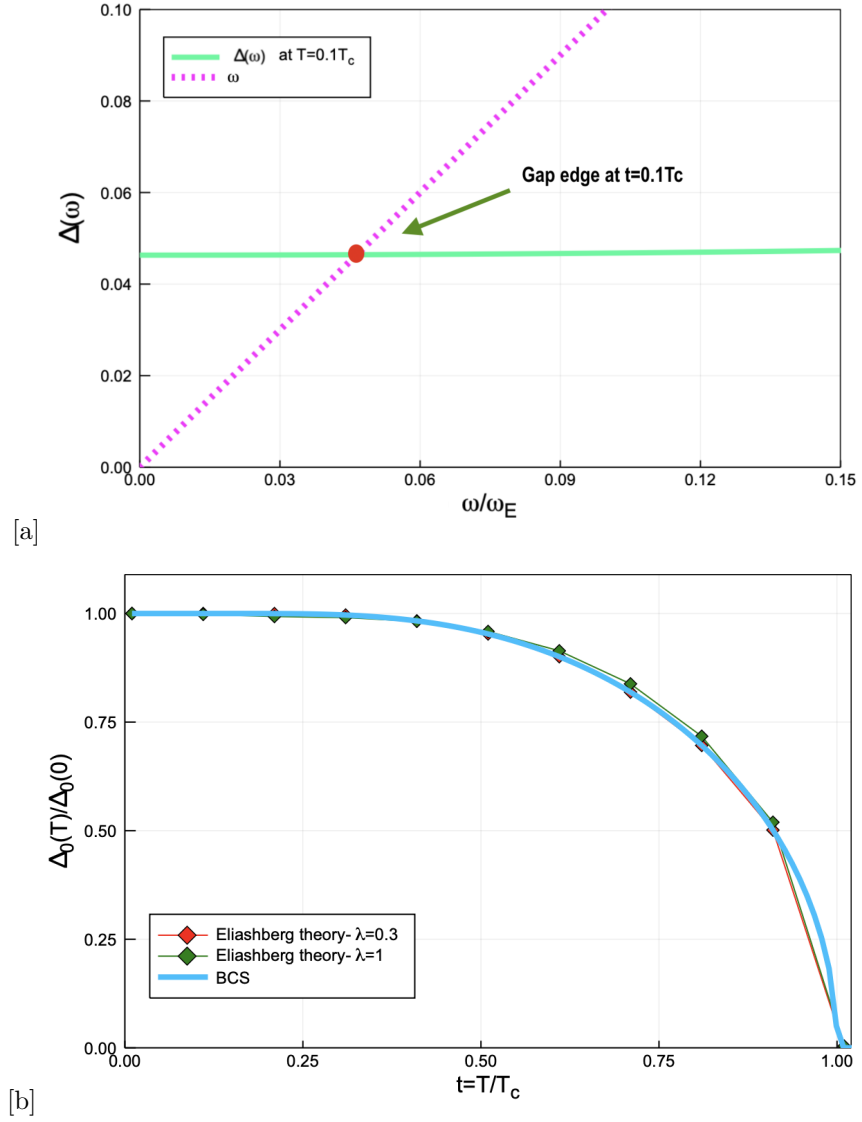
Figure 16. [a] A plot of the intersection of the curves of gap function $\Delta(\omega)$ in units of ω_E and ω on the real axis for $\lambda = 0.3$ at $T = 0.1T_c$. [b] A plot of $\Delta_0(T)/\Delta_0(0)$ versus T/T_c of BCS and Eliashberg theories.

$$N(\omega_E) + f(\omega_E + z) = \frac{N(\omega_E)[1 - f(z + \omega_E)]}{[1 - f(z)]}. \tag{4.31}$$
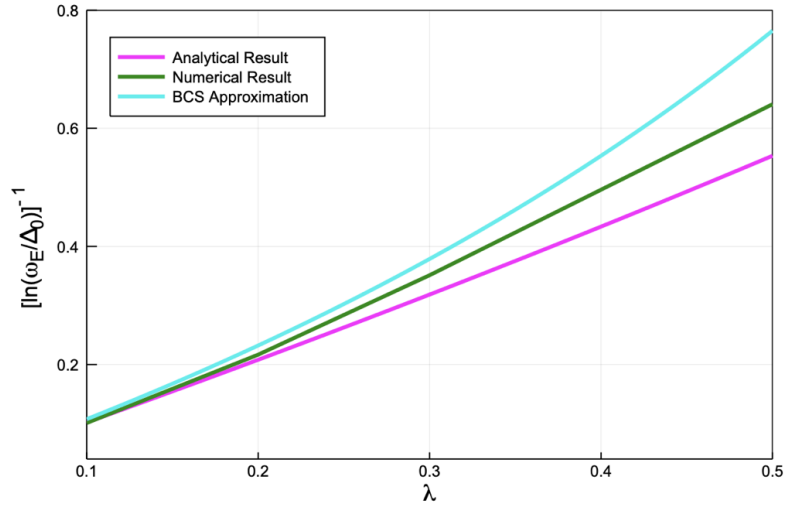
[a]
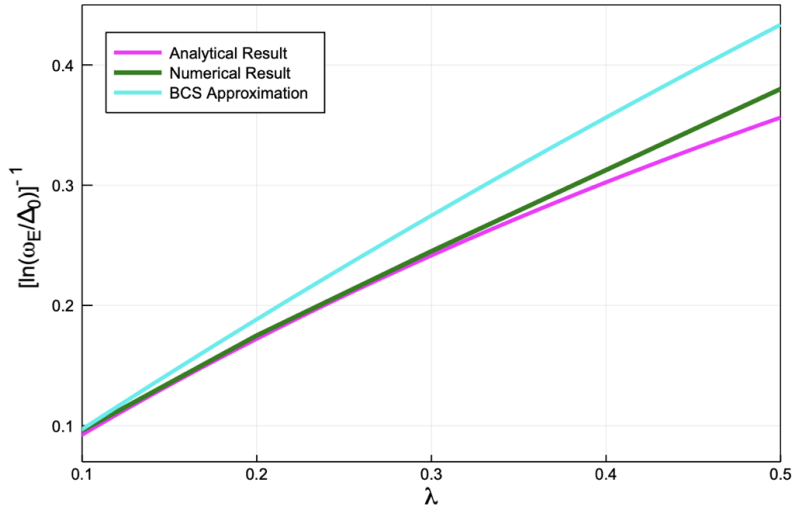
[b]

Figure 17. [a] A plot of $1/[\ln(\omega_E/\Delta_0)]$ versus λ without including the renormalization function. [b] A plot of the $1/[\ln(\omega_E/\Delta_0)]$ versus λ with including the renormalization function.

one can write

$$Z(z)\Delta(z) = \pi T \sum_{-\infty}^{\infty} \lambda(z - i\omega_m) \frac{\omega_m}{\sqrt{\omega_m^2 + \Delta_m^2}}$$

$$+ \frac{i\pi A(\omega_E)}{[1 - f(z)]} \{[1 + N(\omega_E)] \frac{\Delta(z - \omega_E)}{\sqrt{(z - \omega_E)^2 - \Delta^2(z - \omega_E)}}$$

$$+ N(\omega_E)[1 - f(\omega_E + z)] \frac{\Delta(z + \omega_E)}{\sqrt{(z + \omega_E)^2 - \Delta^2(z + \omega_E)}}\}. \tag{4.32}$$

$$Z(z) = 1 + \frac{i\pi T}{z} \sum_{-\infty}^{\infty} \lambda(z - i\omega_m) \frac{\omega_m}{\sqrt{\omega_m^2 + \Delta_m^2}}$$

$$+ \frac{i\pi A(\omega_E)}{[1 - f(z)]} \{[1 + N(\omega_E)][1 - f(z - \omega_E)] \frac{(z - \omega_E)}{\sqrt{(z - \omega_E)^2 - \Delta^2(z - \omega_E)}}$$

$$+ N(\omega_E)[1 - f(\omega_E + z)] \frac{(z + \omega_E)}{\sqrt{(z + \omega_E)^2 - \Delta^2(z + \omega_E)}}\}. \tag{4.33}$$

The second terms in both Eq.(4.32) and Eq.(4.33) are the result of quasi-particle scattering with emission and absorption of a phonon [32]. In Fig.(18) and (19) we plot the gap, renormalization function, density of states and spectral function at finite-temperature $T = 0.9Tc$ for $\lambda = 1$ and $\lambda = 0.3$. In order to plot the gap function and renormalization function we have used the contribution of all the terms in Eq.(4.11) and Eq.(4.12) over the frequency range. For $\lambda = 1$, close to the critical temperature, the structure is still sharp. We observe the structures at $\Delta_0(T = 0.9T_c) + n\omega_E$ and $-\Delta_0(T = 0.9T_c) + n\omega_E$ in the finite-temperature limit [33]. In the finite-temperature limit, the gap at zero frequency has an imaginary part but the real part of the gap at zero frequency approaches zero for $\lambda = 1$.

In Fig.(20a) the real axis result for $\lambda = 0.1$ is depicted, showing the real (green) and imaginary (red) parts of $\Delta(\omega)$ in units of ω_E as a function of $\bar{\omega}$, for various temperatures. In this plot we consider the gap function versus frequency at $T = 0.2T_c$, $T = 0.4T_c$, $T = 0.6T_c$ and $T = 0.8T_c$. As $t = T/T_c$ increases from 0.2 to 0.9, the curves are ordered from the largest to the smallest amount [31]. Furthermore, in Fig.(20b) we show the plot of $\Delta(\omega)/\Delta(\omega \approx 0)$ versus ω/ω_E below the critical temperature. All the four green curves, which are the real part of the gap at various temperatures overlap. In addition, all the red curves, which are the imaginary part of the gap function, will overlap which indicates that in the weak-coupling limit the real frequency axis gap equation is temperature independent below T_c. Therefore,

$$\frac{\Delta(\omega; T, \lambda)}{\Delta(\omega_1; T, \lambda)} = f(\omega, \lambda). \tag{4.34}$$

Also, we plot $\Delta(\omega)/\Delta(\omega \approx 0)$ versus ω/ω_E in Fig.(21) for $\lambda = 0.1, 0.2$ and 0.3 at $T = 0.2T_c, 0.4T_c, 0.6T_c$ and $T = 0.8T_c$. All of the curves related to gap function in the weak coupling limits will overlap for temperatures below T_c. Here, $\Delta(\bar{\omega} \approx 0)$ means the low-frequency ($\omega \approx 0$) gap function. In Fig.(22a) and (22b) we plot the numerical result for the real and imaginary parts of the normalized gap equation at a low temperature $T = 0.2T_c$ and $T = T_c$ for the weak coupling limit [31]. Both the real and imaginary parts of the gap are universal functions of frequency and are temperature independent. For $\lambda = 0.3$, the imaginary part of the gap function at $\omega < \omega_E$ is due to the fact that $T_c = 0.009932\omega_E$ and non-negligible.

[a]

[b]

[c]

[d]
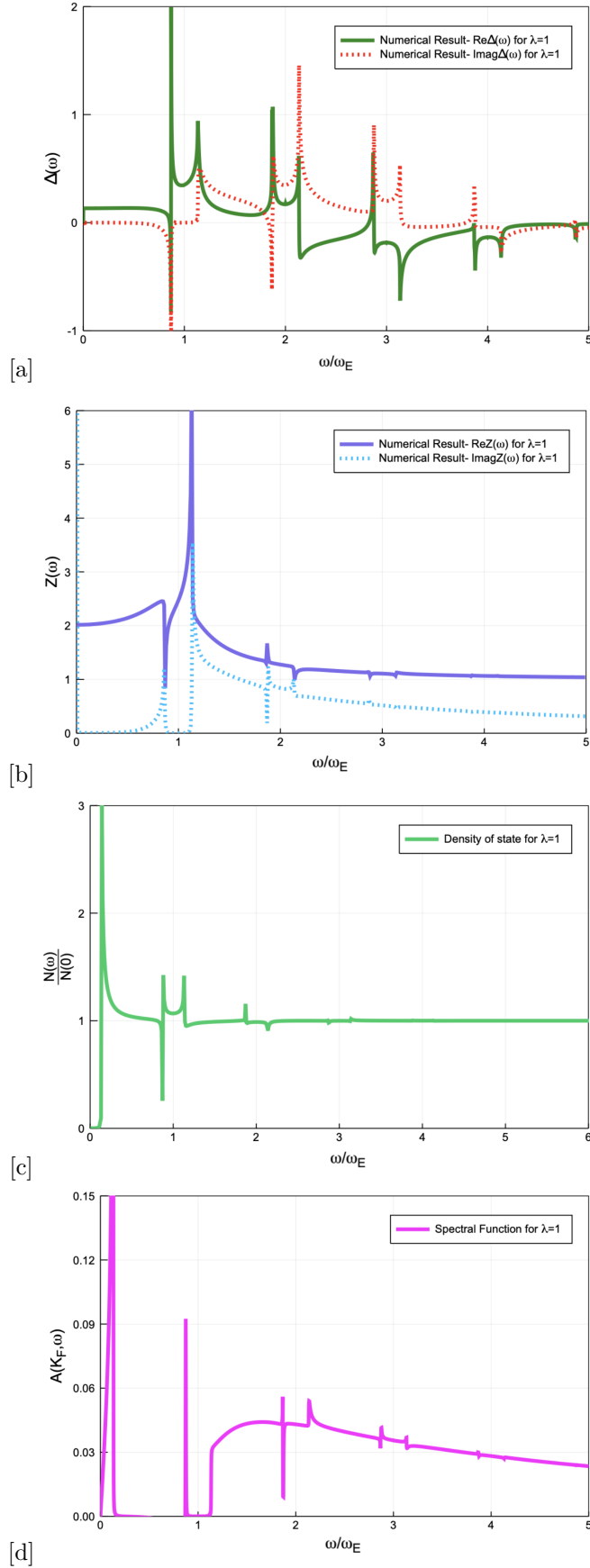
Figure 18. [a] A plot of $\Delta(\omega)$ in units of ω_E versus ω/ω_E. [b] A plot of $Z(\omega)$ versus ω/ω_E. [c] $N(\omega)/N(0)$ versus ω/ω_E. [d] $A(K_F, \omega)$ versus ω/ω_E at $t = T/T_c = 0.9$ for $\lambda = 1$ and $\omega_E = 1.0$ meV.

[a]

[b]

[c]

[d]

57
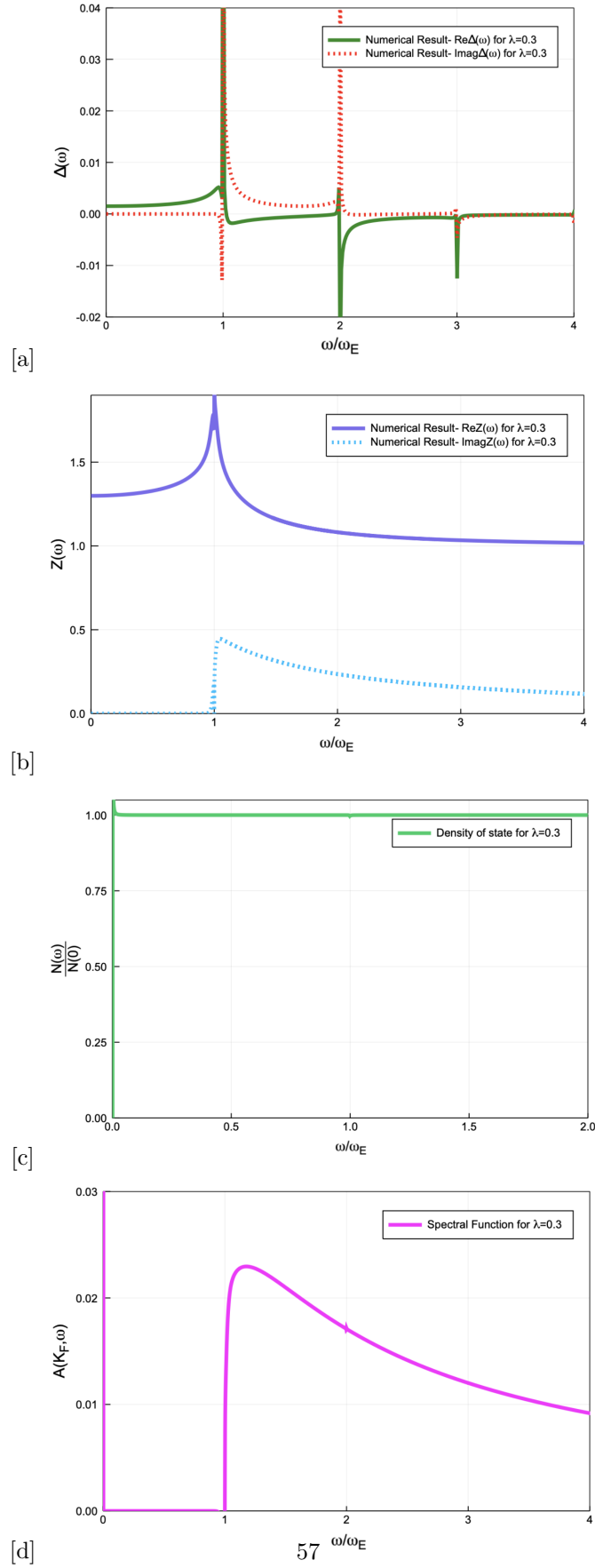
Figure 19. [a] A plot of $\Delta(\omega)$ in units of ω_E versus ω/ω_E. [b] A plot of $Z(\omega)$ versus ω/ω_E. [c] $N(\omega)/N(0)$ versus ω/ω_E. [d] $A(K_F, \omega)$ versus ω/ω_E at $t = T/T_c = 0.9$ for $\lambda = 0.3$ and $\omega_E = 1$ meV.
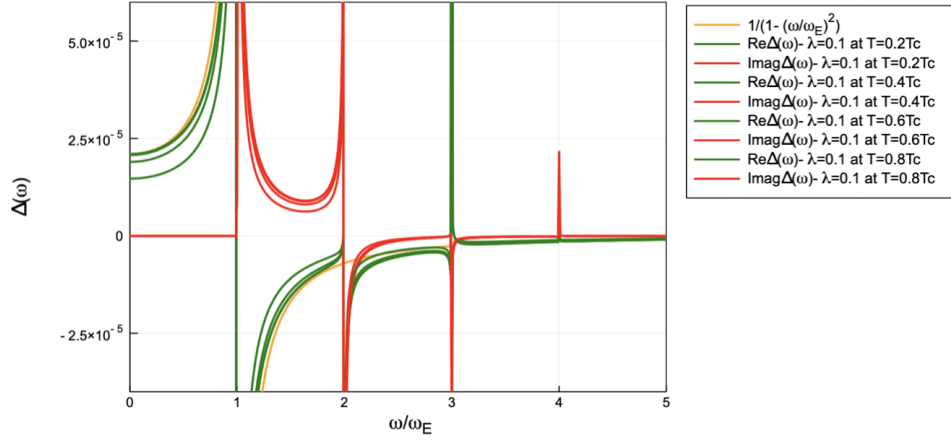
[a]
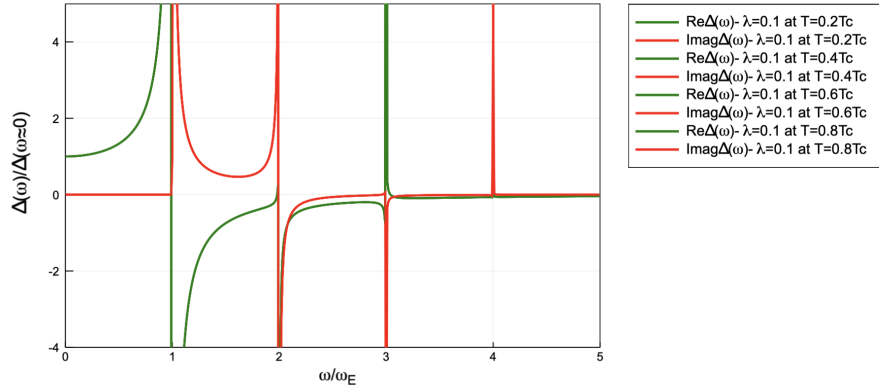
[b]

Figure 20. [a] A plot of $\Delta(\omega)$ in units of ω_E versus ω/ω_E below critical temperature for $\lambda = 0.1$ (the orange curve represents $1/(1 - \bar{\omega}^2)$, where all the curves are trending toward the orange curve). [b] A plot of $\Delta(\omega)/\Delta(\omega \approx 0)$ ($\Delta(\bar{\omega} \approx 0)$ means the low-frequency ($\omega \approx 0$) gap function.) versus ω/ω_E below critical temperature for $\lambda = 0.1$. Here, four curves related to the gap function at various temperatures ($T = 0.2T_c, 0.4T_c, 0.6T_c$ and $T = 0.8T_c$) overlap. In both plots we included the renormalization factor.
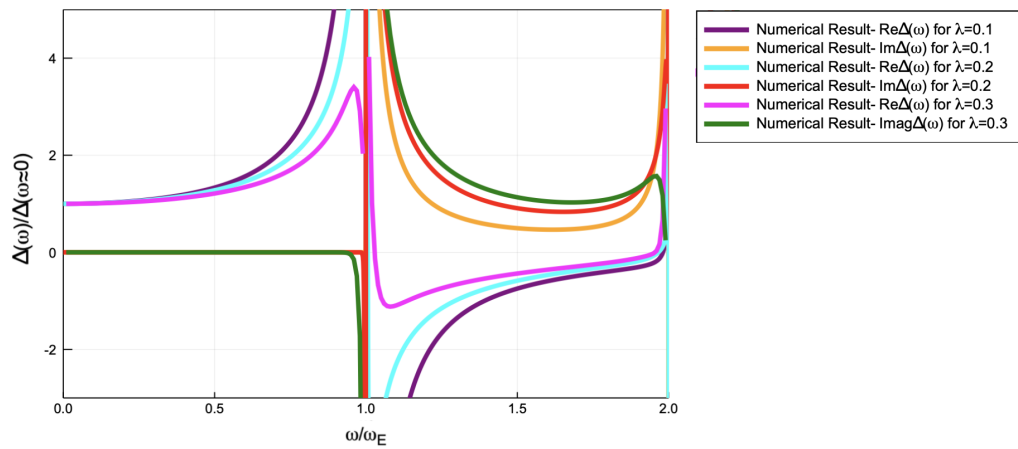
Figure 21. A plot of the the real and imaginary part of $\Delta(\omega)/\Delta(\omega \approx 0)$ versus ω/ω_E below critical temperature ($T = 0.2T_c, 0.4T_c, 0.6T_c \ T = 0.8T_c$) for $\lambda = 0.1, 0, 2$ and $\lambda = 0.3$. All of the four curves overlap which is an indicator of the fact that below T_c the real-frequency axis gap function is temperature independent.
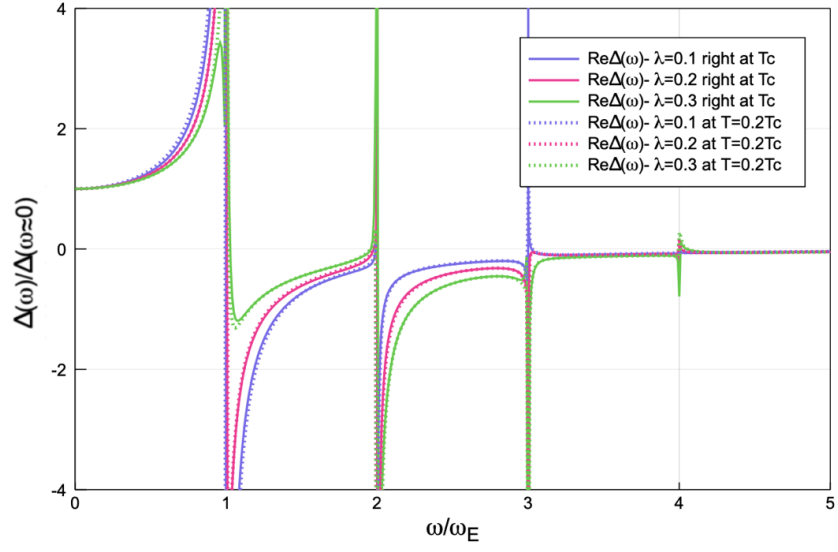
[a]
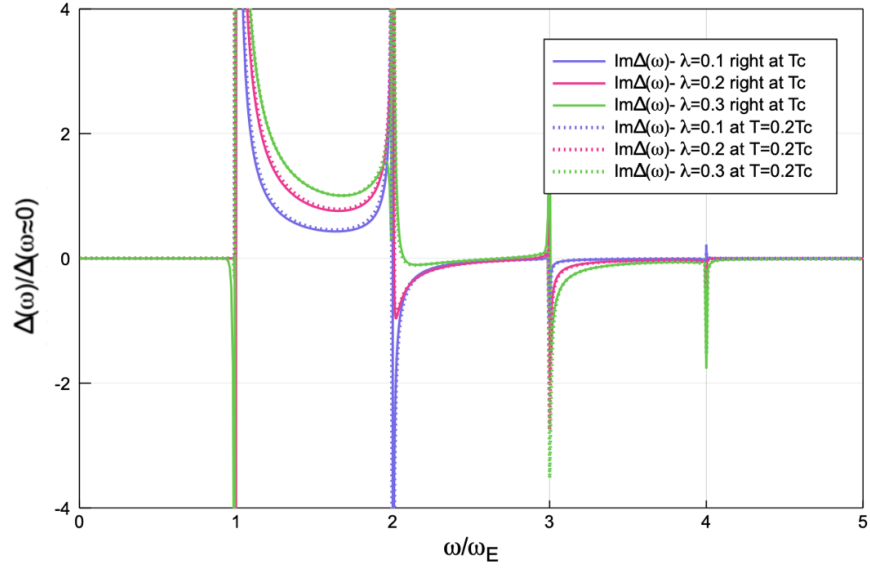
[b]

Figure 22. [a] A plot of the real part of the $\Delta(\omega)/\Delta(\omega \approx 0)$ versus ω/ω_E at $T = 0.2T_c$ and $T = T_c$ for $\lambda = 0.1$, $\lambda = 0.2$ and $\lambda = 0.3$. [b] A plot of the imaginary part of the $\Delta(\omega)/\Delta(\omega \approx 0)$ versus ω/ω_E at $T = 0.2T_c$ and $T = T_c$ for $\lambda = 0.1$, $\lambda = 0.2$ and $\lambda = 0.3$. For the three coupling strength the gap at $T = 0.2T_c$ and $T = T_c$ are indistinguishable.

C. Full comparison between numerical and analytical calculations

The gap function and renormalization function on the real frequency axis are

$$
\begin{aligned}
Z(z)\Delta(z) =&\pi T \sum_{m=-\infty}^{\infty} \lambda(z - i\omega_m)\frac{\Delta(i\omega_m)}{\sqrt{\omega_m^2 + \Delta^2(i\omega_m)}} \\
&+ i\pi A\left[[N(\omega_E) + f(\omega_E - z)]\frac{\Delta(z - \omega_E)}{\sqrt{(z - \omega_E)^2 - \Delta^2(z - \omega_E)^2}}\right] \\
&+ i\pi A\left[[N(\omega_E) + f(\omega_E + z)]\frac{\Delta(z + \omega_E)}{\sqrt{(z + \omega_E)^2 - \Delta^2(z + \omega_E)^2}}\right].
\end{aligned}
\tag{4.35}
$$

$$
\begin{aligned}
Z(z) =&1 + \frac{i\pi T}{z} \sum_{m=-\infty}^{\infty} \lambda(z - i\omega_m)\frac{\omega_m}{\sqrt{\omega_m^2 + \Delta^2(i\omega_m)}} \\
&+ \frac{i\pi A}{z}\left[[N(\omega_E) + f(\omega_E - z)]\frac{(z - \omega_E)}{\sqrt{(z - \omega_E)^2 - \Delta^2(z - \omega_E)^2}}\right] \\
&+ \frac{i\pi A}{z}\left[[N(\omega_E) + f(\omega_E + z)]\frac{(z + \omega_E)}{\sqrt{(z + \omega_E)^2 - \Delta^2(z + \omega_E)^2}}\right],
\end{aligned}
\tag{4.36}
$$

where $z \equiv \omega + i\delta$ and δ is an infinitesimal positive value, which tells us that analytical continuation is solved above the real frequency axis. On the other hand, the analytical approximation for the gap function on the real frequency axis with the renormalization factor included at T_c is given by

$$
\begin{aligned}
\Delta(\bar{\omega}) =&\frac{1}{1 + (-i\bar{\omega} + \delta)^2} \frac{\left[1 + \lambda\left(\frac{3}{2} - g_1(\bar{\omega})\right)\right]}{\left[1 + \frac{\lambda}{2\bar{\omega}}\ln\left|\frac{1+\bar{\omega}}{1-\bar{\omega}}\right|\right]} \\
=&\frac{1}{2}\left(\frac{1}{1 - i(-i\bar{\omega} + \delta)} + \frac{1}{1 + i(-i\bar{\omega} + \delta)}\right) \frac{\left[1 + \lambda\left(\frac{3}{2} - g_1(\bar{\omega})\right)\right]}{\left[1 + \frac{\lambda}{2\bar{\omega}}\ln\left|\frac{1+\bar{\omega}}{1-\bar{\omega}}\right|\right]} \\
=&\frac{1}{2}\left[\mathcal{P}\left(\frac{1}{1-\bar{\omega}} + \frac{1}{1+\bar{\omega}}\right) + i\pi\left(\delta(1 - \bar{\omega}) - \delta(1 + \bar{\omega})\right)\right] \frac{\left[1 + \lambda\left(\frac{3}{2} - g_1(\bar{\omega})\right)\right]}{\left[1 + \frac{\lambda}{2\bar{\omega}}\ln\left|\frac{1+\bar{\omega}}{1-\bar{\omega}}\right|\right]},
\end{aligned}
\tag{4.37}
$$

where $\mathcal{P}$ is the Cauchy principle value and $g_1(\bar{\omega})$ is obtained in Eq.(3.101). Also, the asymptotic gap equation on the real axis with $Z(\bar{\omega}) = 1$ is given as

$$
\Delta(\bar{\omega}) = \frac{1}{2}\left[\mathcal{P}\left(\frac{1}{1-\bar{\omega}} + \frac{1}{1+\bar{\omega}}\right) + i\pi\left(\delta(1 - \bar{\omega}) - \delta(1 + \bar{\omega})\right)\right]\left[1 + \lambda\left(\frac{1}{2} - g_1(\bar{\omega})\right)\right].
\tag{4.38}
$$

In Fig.(23a) and (23b) we plot real and imaginary part of $\Delta(\omega)/\Delta(\omega \approx 0)$ versus $\bar{\omega}$ for $\lambda = 0.1$, $\lambda = 0.2$ and $\lambda = 0.3$ at the critical temperature [31]. Here, $\Delta(\bar{\omega} \approx 0)$ means the low-frequency $\omega \approx 0$. To obtain the gap function at the critical temperature, we linearize the gap function by setting $\Delta(\bar{\omega})$ to zero in the denominators of Eq.(4.35) and (4.36). In the weak-coupling limit, the critical temperature is very small, therefore the Bose function is still zero and the Fermi function is a step function in the above equations. Since the energy scale is of the order of ω_E then we are able to see resonances at multiple Einstein phonon frequency. Higher peaks depend on higher powers of λ, in other word, the successive peaks decrease in height with increasing λ.

Now, in order to make a meaningful comparison between the analytical approximation and numerical results using Eq.(4.35) and (4.36), we plot $\Delta(\bar{\omega})[1 - \bar{\omega}^2]$ versus ω/ω_E with renormalization function in
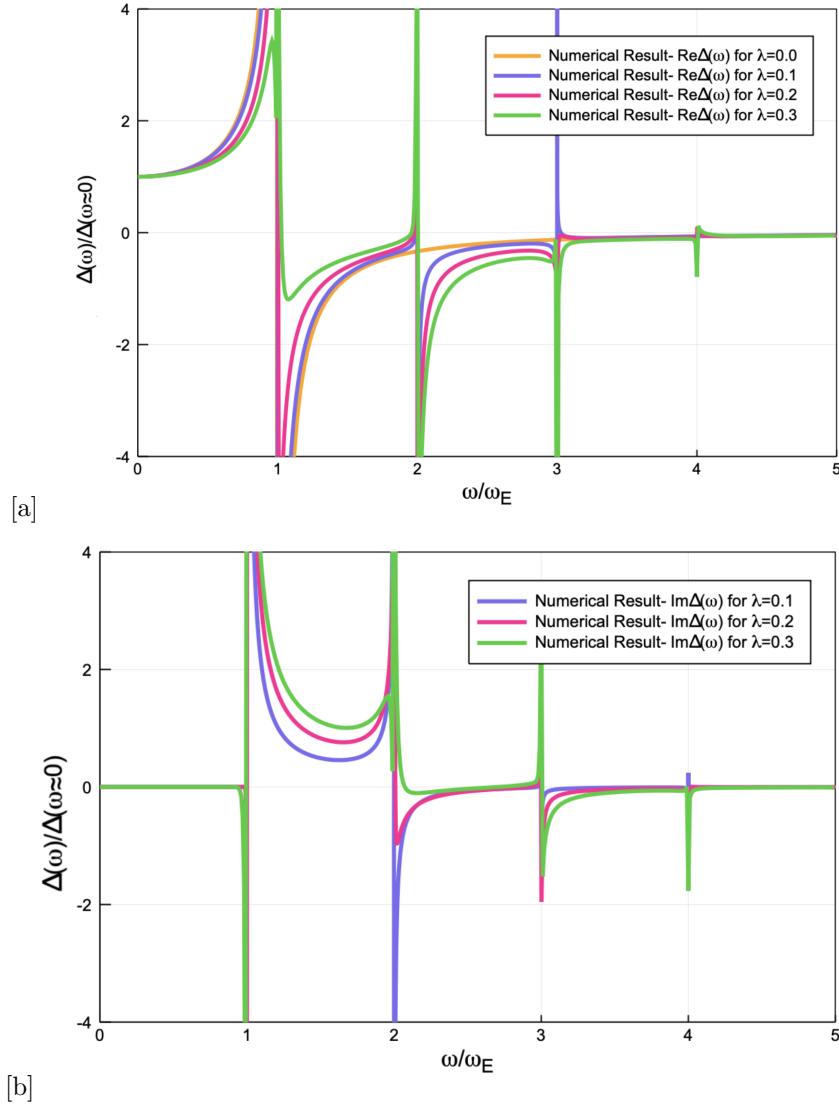
Figure 23. [a] A plot of the real part of $\Delta(\omega)/\Delta(\omega \approx 0)$ versus $\bar{\omega}$ for $\lambda = 0.1$, $\lambda = 0.2$ and $\lambda = 0.3$ at the critical temperature, ($\Delta(\omega \approx 0)$ means low-frequency gap function). [b] A plot of the imaginary part of $\Delta(\omega)/\Delta(\omega \approx 0)$ versus $\bar{\omega}$ for $\lambda = 0.1$, $\lambda = 0.2$ and $\lambda = 0.3$ at the critical temperature. In both plots we have included the renormalization factor.

Fig.(24a) and without renormalization factor in Fig.(24b). One might notice that at $(\omega/\omega_E = \bar{\omega}) = 1$, $(1 - \bar{\omega}^2)\mathcal{P}\left(\frac{1}{1-\bar{\omega}}\right) \equiv 0$, where $\mathcal{P}$ is the Cauchy principle value. Also, $(1 - \bar{\omega}^2)\left[\delta(1 - \bar{\omega}) - \delta(1 + \bar{\omega})\right] = 0$ because $x\delta(x) = 0$. We observe a deviation between numerical and analytical approximation for $\bar{\omega} > 1$ in Fig.(24a).

Now, if we add $i\pi A\left[[N(\omega_E) + f(\omega_E - z)]\frac{\Delta(z-\omega_E)}{|(z-\omega_E)|}\right]$ term to the analytical results of Eq.(4.37) and (4.38) for $\bar{\omega} > 1$ we observe a better agreement between the numerical and analytical approximation in the weak-coupling limit as depicted in Fig.(25). Comparing Fig.(24a) with Fig.(25a) we realize that adding $i\pi A\left[[N(\omega_E) + f(\omega_E - z)]\frac{\Delta(z-\omega_E)}{|(z-\omega_E)|}\right]$ term to the analytical approximation results for $\bar{\omega} > 1$ shows

62
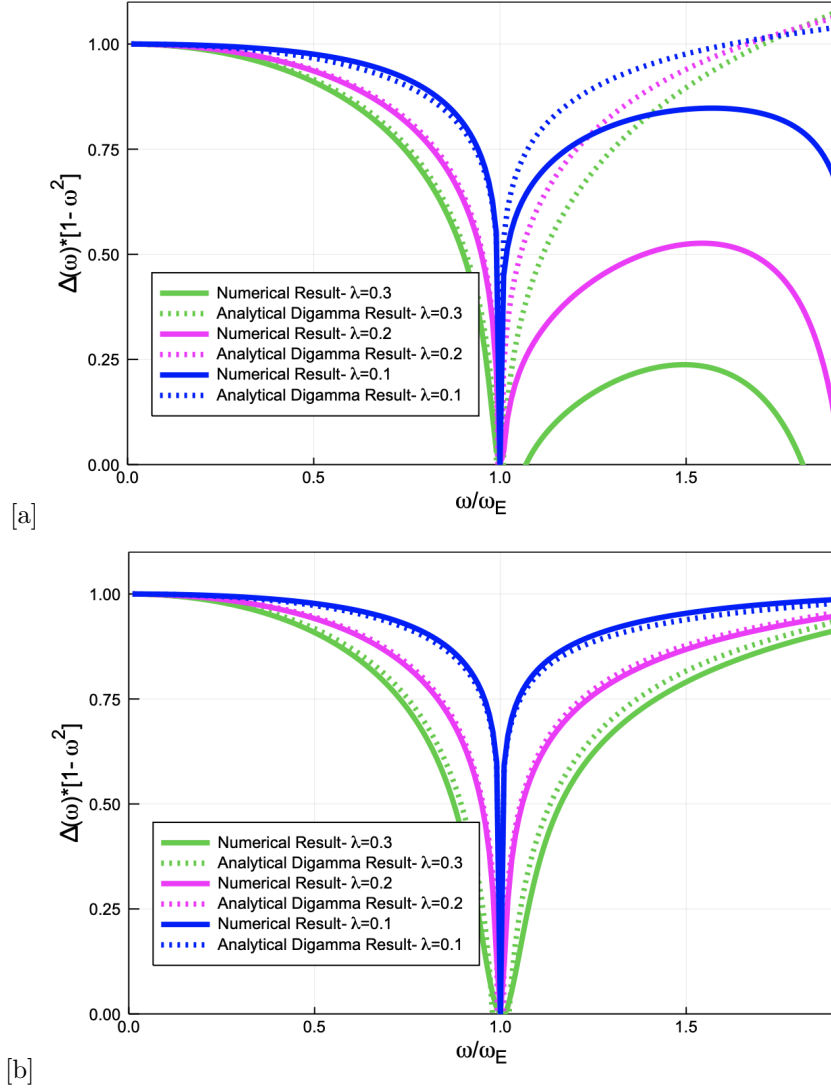
Figure 24. [a] The plot of numerical result for $\Delta[1-\bar{\omega}^2]$ in units of $\Delta(\omega \approx 0)$ versus ω/ω_E including the renormalization factor. [b] The plot of analytical digamma result for $\Delta[1-\bar{\omega}^2]$ in units of $\Delta(\omega \approx 0)$ versus ω/ω_E not including the renormalization factor for $\lambda = 0.1, 0.2$ and 0.3 at the critical temperature. In both figures only the inhomogeneous terms are included in the calculation of the gap function.

a better agreement. In addition, we plot the real and imaginary part of $\Delta(\omega)/\Delta(\omega \approx 0)$ versus ω/ω_E in Fig.(26) for $\lambda = 0.1$, $\lambda = 0.2$ and $\lambda = 0.3$ at the critical temperature using both the numerical and analytical approximation results to show their agreement [31]. As is shown in this figure, for the case of $\lambda = 0.3$ the deviation between the numerical and asymptotic approximation is only discernible in the vicinity of ω_E. The frequency at which a noticeable discrepancy exist is of the magnitude of T_c which is small. In this chapter we have showed the real frequency axis quantities and described special features like the temperature independent result.
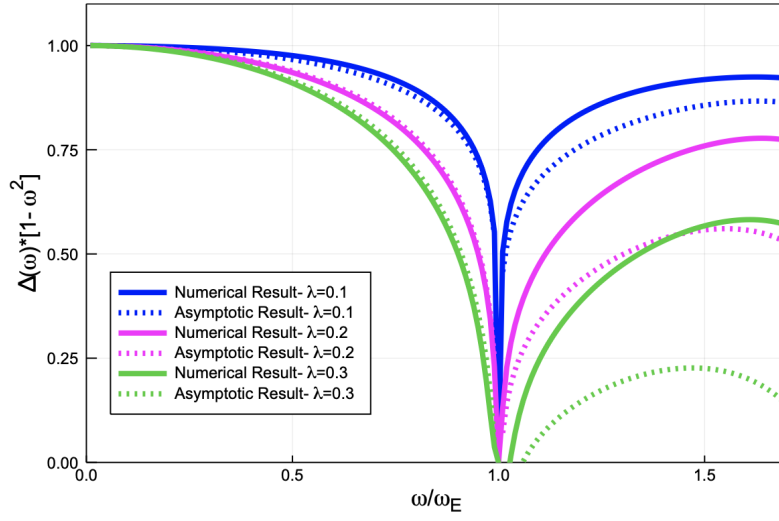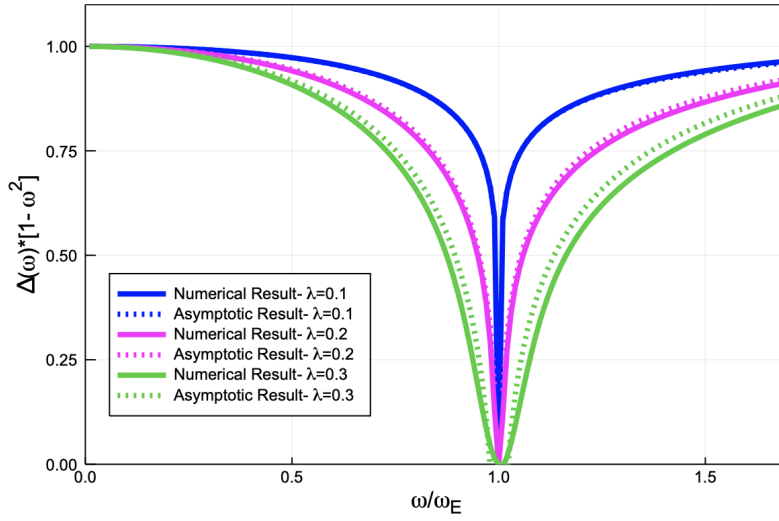
Figure 25. [a] The plot of numerical result for $\Delta[1 - \bar{\omega}^2]$ in units of $\Delta(\omega \approx 0)$ versus ω/ω_E including the renormalization factor. [b] The plot of analytical digamma result for $\Delta[1 - \bar{\omega}^2]$ in units of $\Delta(\omega \approx 0)$ versus ω/ω_E not including the renormalization factor. In both figures the homogeneous terms in the gap function are added to the analytical approximation result to obtain a better agreement.
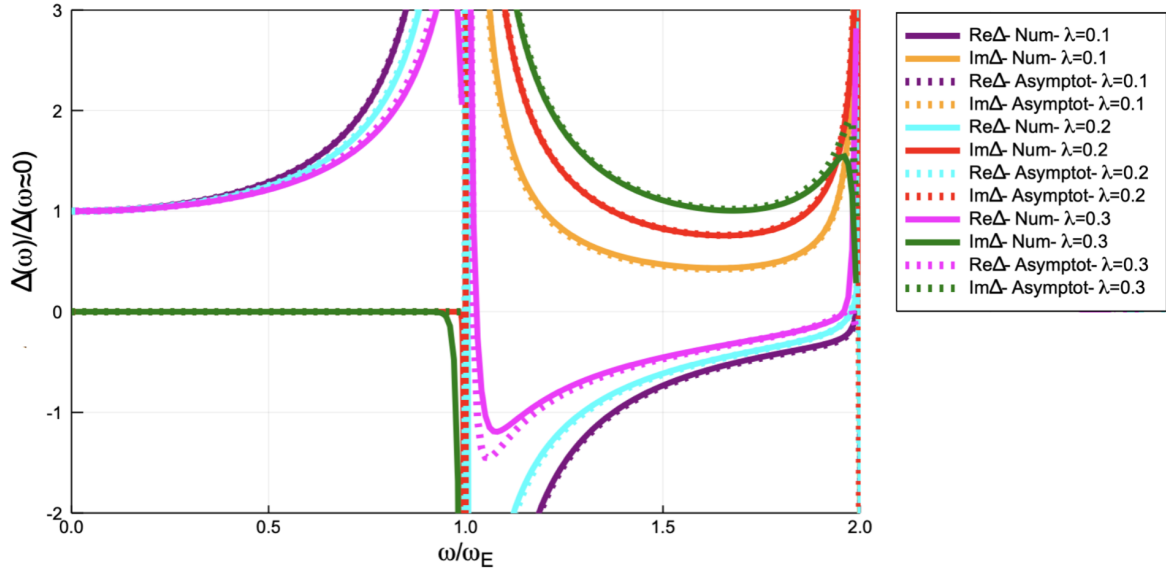
Figure 26. A plot of the the real and imaginary part of $\Delta(\omega)/\Delta(\omega \approx 0)$ versus ω/ω_E at the critical temperature for $\lambda = 0.1$, $\lambda = 0.2$ and $\lambda = 0.3$ which show that the numerical calculation and the asymptotic approximation solutions for the gap function on the real axis are in good agreement. In this plot the dotted line shows the asymptotic result and the solid line is the numerical calculations.

V. THERMODYNAMIC PROPERTIES OF SUPERCONDUCTORS

A. Free energy

The thermodynamic characteristics of superconductors are calculated from the free energy. Computing the free energy from perturbation theory is computationally demanding since it converges very slowly. However, the Bardeen-Stephen formula [37] is a nice approach to easily capture the thermal properties. In 1964, Bardeen and Stephen obtained the free-energy difference between superconducting and normal states using the Eliashberg statement for the total free energy. Utilizing the Bardeen-Stephen formula is numerically efficient since it converges very fast [6]. One finds the derivative of the free-energy and performs the Matsubara summation to obtain the thermodynamic features of superconductors such as the heat capacity, and critical magnetic field. The free energy difference is then given by

$$\frac{\Delta F}{N(0)} = -\pi T \sum_{i\omega_m} \left(\sqrt{\omega_m^2 + \Delta^2(\omega_m)} - |\omega_m| \right) \left(Z_S(\omega_m) - Z_N(\omega_m) \frac{|\omega_m|}{\sqrt{\omega_m^2 + \Delta^2(\omega_m)}} \right), \qquad (5.1)$$

where $Z_S(\omega_m)$ and $Z_N(\omega_m)$ are the renormalization functions in the superconducting state ($\Delta \neq 0$) and the normal state ($\Delta = 0$) respectively. Here, $\Delta(i\omega_m)$ is the frequency-dependent gap function in the Eliashberg theory. However, in the BCS theory, the gap function is frequency independent. In order to obtain the normal-state renormalization function, $\Delta(i\omega_m)$ is set to zero in denominator of the self-consistent renormalization function equation. Furthermore, we set $Z_S(i\omega_m)$ and $Z_N(i\omega_m)$ to unity for simplicity. Thus, one can write [13]

$$\frac{\Delta F}{N(0)} = -\pi T \sum_{i\omega_m} \left(\sqrt{\omega_m^2 + \Delta^2(\omega_m)} - |\omega_m| \right) \left(1 - \frac{|\omega_m|}{\sqrt{\omega_m^2 + \Delta^2(\omega_m)}} \right). \qquad (5.2)$$

1. Zero-temperature limit

In the zero-temperature limit, we apply the prescription:

$$T \sum_{m=-\infty}^{+\infty} \to \int_{-\infty}^{+\infty} \frac{d\omega}{2\pi}.$$

The Bardeen-Stephen formula for the free energy difference becomes

$$\frac{\Delta F}{N(0)} = -\frac{1}{2} \int_{-\infty}^{\infty} d\omega \left(\sqrt{\omega^2 + \Delta^2} - |\omega| \right) \left(1 - \frac{|\omega|}{\sqrt{\omega^2 + \Delta^2}} \right). \qquad (5.3)$$

---

[13]The appropriate free energy units for the BCS and Eliashberg theories are considered in Appendix (E).

The next step is to normalize the gap function and frequencies by ω_E to obtain

$$\frac{\Delta \bar{F}}{\bar{N}(0)} = -\frac{1}{2} \int_{-\infty}^{\infty} d\bar{\omega} \left(\sqrt{\bar{\omega}^2 + \bar{\Delta}^2} - |\bar{\omega}| \right) \left(1 - \frac{|\bar{\omega}|}{\sqrt{\bar{\omega}^2 + \bar{\Delta}^2}} \right),$$

$$\approx -\frac{1}{2} \int_{-\infty}^{\infty} d\bar{\omega} \left(\sqrt{\bar{\omega}^2 + \left(\frac{\bar{\Delta}_0}{1+\bar{\omega}^2} \right)^2} - |\bar{\omega}| \right) \left(1 - \frac{|\bar{\omega}|}{\sqrt{\bar{\omega}^2 + \left(\frac{\bar{\Delta}_0}{1+\bar{\omega}^2} \right)^2}} \right),$$

$$\approx -\frac{1}{2} \int_{-\infty}^{\infty} d\bar{\omega} \left(\sqrt{\bar{\omega}^2 + \bar{\Delta}_0^2} - |\bar{\omega}| \right) \left(1 - \frac{|\bar{\omega}|}{\sqrt{\bar{\omega}^2 + \bar{\Delta}_0^2}} \right),$$

$$= -\int_0^{\infty} d\bar{\omega} \left(\sqrt{\bar{\omega}^2 + \bar{\Delta}_0^2} - 2|\bar{\omega}| + \frac{\bar{\omega}^2}{\sqrt{\bar{\omega}^2 + \bar{\Delta}_0^2}} \right). \tag{5.4}$$

The first integral can be simplified to

$$\int d\bar{\omega} \sqrt{\bar{\omega}^2 + \bar{\Delta}_0^2} = \int d\bar{\omega} \sqrt{\bar{\omega}^2 + \bar{\Delta}_0^2} \frac{d}{d\bar{\omega}} \bar{\omega} = \bar{\omega} \sqrt{\bar{\omega}^2 + \bar{\Delta}_0^2} - \int d\bar{\omega} \frac{\bar{\omega}^2}{\sqrt{\bar{\omega}^2 + \bar{\Delta}_0^2}}. \tag{5.5}$$

Thus, the free energy is now

$$\frac{\Delta \bar{F}}{\bar{N}(0)} = -\lim_{L \to \infty} \left(\bar{\omega} \sqrt{\bar{\omega}^2 + \bar{\Delta}_0^2} - \bar{\omega}^2 \right) |_{\bar{\omega}=0}^{\bar{\omega}=L} = -\frac{\bar{\Delta}_0^2}{2}. \tag{5.6}$$

Using the previous result for $\bar{\Delta}_0$, namely,

$$\bar{\Delta}_0 = \frac{1}{\sqrt{\exp(1)}} \left[2 \exp \left(-\frac{1}{\lambda} \right) \right], \tag{5.7}$$

we find that the free-energy becomes

$$\frac{\Delta \bar{F}}{\bar{N}(0)} = \frac{1}{\exp(1)} \left[-\frac{1}{2} \Delta_{\text{BCS}}^2 (T=0, \lambda \to 0) \right]. \tag{5.8}$$

The free-energy difference accordingly gets a correction, this time proportional to $1/\exp(1)$.

2. $T \to T_c$ limit

In the $T \to T_c$ limit, $\Delta \ll T_c$, the free energy can be expanded in powers of Δ:

$$\frac{\Delta F}{N(0)} = -\pi T \sum_{i\omega_m} (\sqrt{\omega_m^2 + \Delta^2} - |\omega_m|) \left(1 - \frac{|\omega_m|}{\sqrt{\omega_m^2 + \Delta^2}} \right),$$

$$\frac{\Delta F}{N(0)} \to -\frac{\pi T_c}{4} \sum_{i\omega_m} \frac{\Delta^4}{|\omega_m|^3}. \tag{5.9}$$

In the weak-coupling limit below the critical temperature we write the gap function as follows:

$$\Delta(i\omega_m, T) = \frac{\Delta_0(T)}{1 + \bar{\omega}_m^2}. \tag{5.10}$$

67

The small frequencies are the most dominant contribution to the sum, thus

$$\frac{\Delta F}{N(0)} \approx -\frac{\pi T_c}{2} \sum_{i\omega_m} \frac{\Delta_0^4(T)}{\omega_m^3}. \tag{5.11}$$

In the weak-coupling limit of the Eliashberg theory, the temperature dependence of the gap edge is the same as the BCS theory, which is

$$\Delta_0(T) = \pi \sqrt{\frac{8}{7\zeta(3)}} T_c \sqrt{1 - \frac{T}{T_c}}. \tag{5.12}$$

Substituting the gap edge in the free-energy difference gives

$$\begin{aligned}
\frac{\Delta F}{N(0)} &= -\frac{\pi T_c}{4(\pi T_c)^3} \left(T_c \pi \sqrt{\frac{8}{7\zeta(3)}} \right)^4 \left(1 - \frac{T}{T_c} \right)^2 \sum_{m=0}^{\infty} \frac{2}{(2m+1)^3}, \\
&= -\frac{\pi^2 T_c^2}{2} \left(\frac{8}{7\zeta(3)} \right)^2 \left(1 - \frac{T}{T_c} \right)^2 \frac{7\zeta(3)}{8}.
\end{aligned} \tag{5.13}$$

B. Heat Capacity

The heat capacity at constant volume is

$$\Delta C = -T \left(\frac{\partial^2 \Delta F}{\partial T^2} \right) = -N(0) T_c t \frac{\partial^2}{\partial^2 t} \left(\frac{\Delta F}{N(0) T_c^2} \right).$$

and the heat capacity ratio is defined as

$$R = \frac{\Delta C}{C_N(T_c)}. \tag{5.14}$$

The normal-state value for $C_N(T_c)$ is

$$C_N(T_c) = \frac{2\pi^2 Z}{3} N(0) T_c, \tag{5.15}$$

where the renormalization factor Z is $1 + \lambda$. The heat capacity in the superconducting phase is $C_S \equiv \Delta C + C_N$. Normalizing C_S by $C_N(T_c)$, we can write it as follows

$$\begin{aligned}
\frac{C_S(T)}{C_N(T_c)} &= \frac{\Delta C}{C_N(T_c)} + \frac{C_N(T)}{C_N(T_c)} \\
&= -\frac{1}{\frac{2\pi^2 Z}{3} N(0) T_c} N(0) T_c t \frac{\partial^2}{\partial t^2} \left(\frac{\Delta F}{N(0) T_c^2} \right) + \frac{T}{T_c} \\
&= -\frac{3}{2\pi^2} t \frac{\partial^2}{\partial t^2} \left(\frac{\Delta F}{N(0) T_c^2} \right) + t.
\end{aligned} \tag{5.16}$$

Here, we plot $C_S(T)/C_N(T_c)$ versus T/T_c for both the BCS and Eliashberg theories in Fig.(27). In this plot, $Z_S(i\omega_m)$ and $Z_N(i\omega_m)$ are set to unity. At the critical temperature, there exists a discontinuity and C_S is greater than C_N. The ratio of the heat capacity in the BCS and weak-coupling Eliashberg theories, for the particular case $\lambda = 0.3$, shows very good agreement between the two theories. However, for $\lambda = 1$, we observe a deviation from the BCS result.

In Fig.(28) we plot $C_S(T)/C_N(T_c)$ versus the reduced temperature. In this graph both $Z_S(i\omega_m)$ and
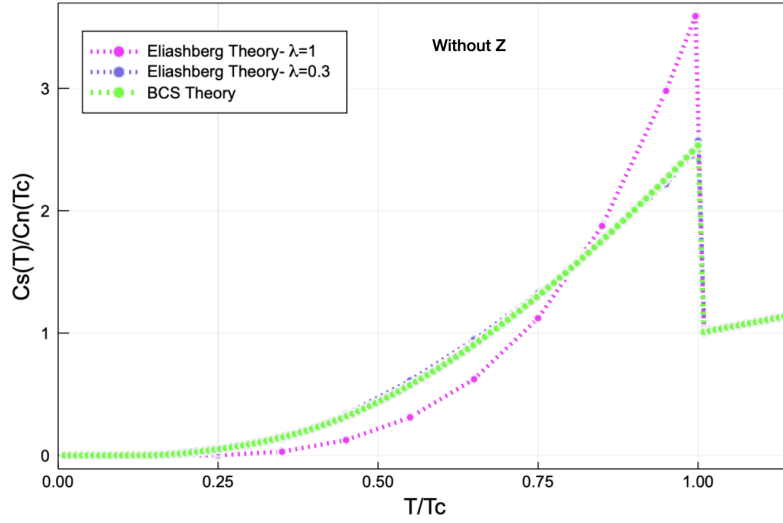
Figure 27. A plot of $C_S(T)/C_N(T_c)$ versus the reduced temperature, using the frequency dependent gap equation of Eliashberg theory in the Bardeen-Stephen formula for $\lambda = 1$ and $\lambda = 0.3$ in comparison to the BCS theory. In this plot the superconducting and normal state renormalization functions are set to unity.
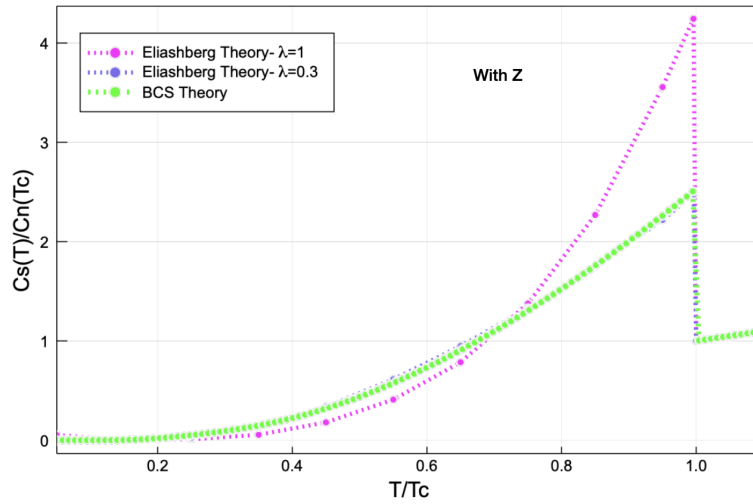
Figure 28. A plot of $C_S(T)/C_N(T_c)$ versus the reduced temperature, using the frequency dependent gap equation of Eliashberg theory in the Bardeen-Stephen formula for $\lambda = 1$ and $\lambda = 0.3$ in comparison to the BCS theory. In this plot the superconducting and normal state renormalization functions are included.

$Z_N(i\omega_m)$ are included. As a result, there is no discernible difference between the weak-coupling Eliashberg theory and the BCS result. The change in the heat capacity, normalized by the normal state value at

$T = T_c$, $C_N = \frac{2\pi^2}{3} Z N(0) T_c$ is

$$\frac{\Delta C}{C_N(T_c)} = -\frac{\partial^2 \Delta F}{\partial T^2}$$

$$= \frac{3}{2\pi^2} \frac{\pi^2 T_c^2}{2} \frac{8}{7\zeta(3)} \left(1 - \frac{T}{T_c}\right)^2 \frac{\partial^2}{\partial T^2} \left(1 - \frac{T}{T_c}\right)^2 .$$

(5.17)

Simplifying the above equation, the ratio becomes

$$\frac{\Delta C}{C_N(T_c)} = \frac{12}{7\zeta(3)} = 1.43.$$

(5.18)

In the BCS theory, this value is the universal result. The normalized change in the heat capacity for the Eliashberg theory is equal to that of its BCS counterpart.

$$\left(\frac{\Delta C}{C_N(T_c)}\right)_{\text{Eliashberg}} = \left(\frac{\Delta C}{C_N(T_c)}\right)_{\text{BCS}}.$$

(5.19)

The ratio of the heat capacity in both BCS and Eliashberg theories are equal at the critical temperature. Since we are considering the weak-coupling limit, the critical temperature is very small and it is similar to the zero-temperature limit. Hence, this is why the normalized heat capacity ratios for both BCS and Eliashberg theories agree for all temperatures.

C.   Critical Magnetic field

The critical field can be defined as follows

$$H_c = \sqrt{-8\pi \Delta F},$$

(5.20)

where the free-energy difference is obtained from Bardeen-Stephen formula. In the BCS theory, the critical magnetic field can be obtained in these two limit [6]:

$$\frac{H_c^{\text{BCS}}(T \to 0)}{H_c^{\text{BCS}}(0)} \simeq 1 - 1.06 \left(\frac{T}{T_c}\right)^2 .$$

(5.21)

where

$$H_c^2(0)/8\pi = N(0)\Delta_0^2/2.$$

(5.22)

In the zero-temperature limit, the product of the zero-temperature gap function Δ_0 which is the binding energy for the cooper pairs and the number of cooper pairs $(N(0)\Delta_0)/2$ provide us with the condensation energy [1, 38].

It is shown from Fig.(29) that near $T = 0$, the critical magnetic field goes as $1 - (\exp(0.5772)^2/3)(T/T_c)^2$, which is close to $1 - (T/T_c)^2$ [22]. Near T_c, the critical magnetic field is defined as

$$\frac{H_c^{\text{BCS}}(T \to T_c)}{H_c^{\text{BCS}}(0)} \simeq 1.74 \left(1 - \frac{T}{T_c}\right).$$

(5.23)

Figure (30) depicts the normalized critical field versus the reduced temperature comparing both Eliashberg and BCS theories for the case when $Z_S(i\omega_m)$ and $Z_N(i\omega_m)$ are included.
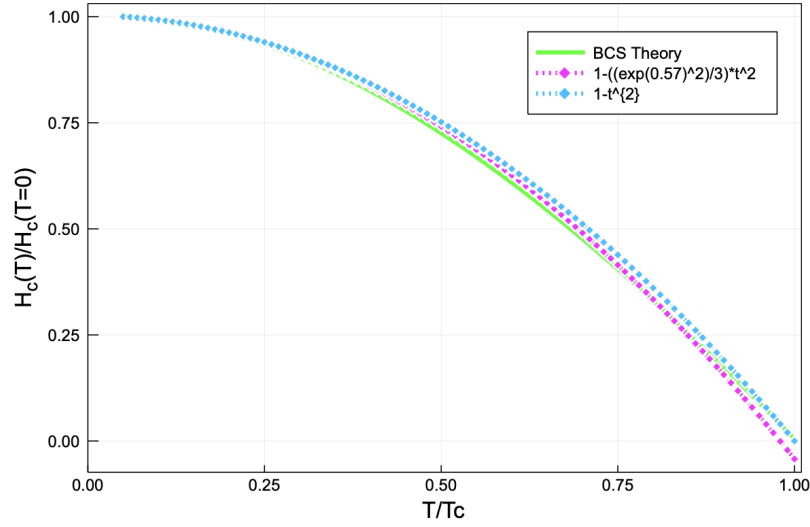
Figure 29. A plot of the critical magnetic field versus the reduced temperature comparing the BCS theory which is normalized by $H_c(T = 0)$ with $1 - (\exp^2{(0.5772)}/3)t^2$ and $1 - t^2$. Near $T = 0$, the critical field goes as $1 - (\exp{(0.5772)}^2/3)t^2$, which is close to $1 - t^2$. Here, $T/T_c = t$.
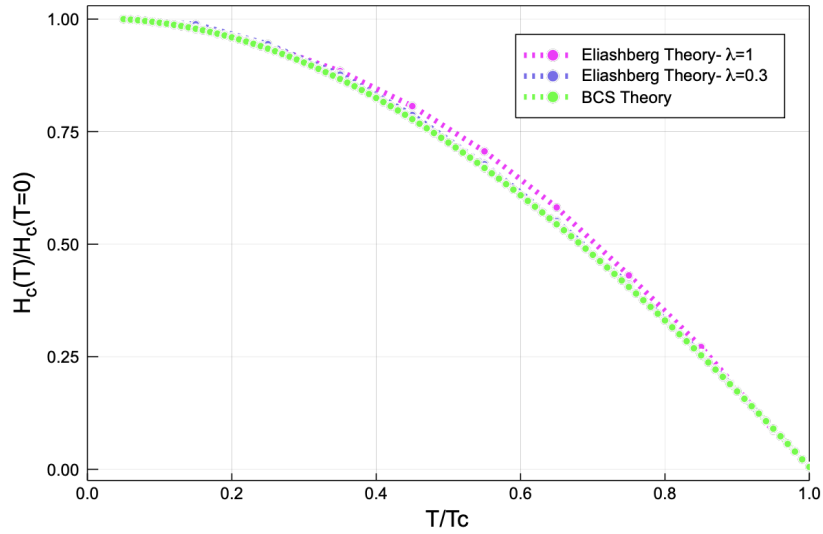
Figure 30. A plot of the normalized critical magnetic field versus reduced temperature, using the frequency-dependent gap equation of Eliashberg theory in the Bardeen-Stephen formula for $\lambda = 1$ and $\lambda = 0.3$ in comparison to the BCS theory. In this plot $Z_S(i\omega_m)$ and $Z_N(i\omega_m)$ are included.

VI.   CONCLUSION

In this thesis, we have studied the complex gap and renormalization functions, in the context of Eliashberg theory on the real frequency axis and in the weak-coupling limit. Mapping from the imaginary axis to the real axis can be obtained by evaluating an analytic function $G(\mathbf{k}, i\omega_n)$ in the upper half of the complex plane using $i\omega_n \to \omega + i\delta$, where δ is an infinitesimal positive quantity.

We have applied the Marsiglio, Schossomann, and Carbotte method for solving the Eliashberg equations on the real frequency axis, which are applicable at all temperatures.

In chapter two, we derived the full equation of motion for the Green's function in order to obtain the Eliashberg equations and treat the problem with an instantaneous interaction. In chapter three, we solved the gap and renormalization functions, both on the imaginary and real frequency axes. Chapter four provides a synopsis of all the numerical results obtained. In chapter five, some of the thermodynamical characteristics of the superconductivity are computed.

On the imaginary frequency axis we used the standard approximation to achieve a self-consistent equation for the order parameter. We determined the critical temperature using the linearized form of the Eliashberg gap equation on the imaginary axis for the weak-coupling electron-phonon interaction. Furthermore, we have used the non-linear Eliashberg functions on the imaginary axis to study the full temperature dependence of the gap equation.

We have presented the zero-temperature and finite-temperature limits, on the real frequency axis, of the gap, renormalization function, the density of states, and spectral function in both the strong and weak-coupling limits. This enables us to understand the structures due to multi-boson emission using the numerical results.

We have calculated the gap and renormalization functions analytically using digamma expressions for expanding the summations in the gap and renormalization functions to the first order in λ which provide quantitatively acceptable result in comparison with the numerical results at the critical temperature. As the coupling becomes weaker, there is better agreement between the analytical and numerical evaluations performed on the real frequency axis.

The asymptotic behavior of the gap function for large ω_n on the imaginary frequency axis is $1/\omega_n^2$ including the renormalization factor and $1/\omega_n$ without the renormalization function. The gap function on the Matsubara frequency axis is the real part of an analytic function. Therefore, it has no terms dependent on $i\omega_n$ alone (it also depends on the conjugate $-i\omega_n$). As a result, the analytical continuation of the real part of an analytic function can give different behaviour because the real part of an analytic function is itself non-analytic. The $g_1(\bar{\omega})$ function on the real axis was calculated in the vicinity of $\bar{\omega} = 1$, and its value was found to be $\log(\bar{\omega}_E) - \psi(1/2)$, in the limit of large $\bar{\omega}_E$.

In the weak-coupling Eliashberg theory, we determined the gap edge Δ_0 on the real axis. There is a pre-factor $1/\sqrt{e}$ difference with the BCS theory, and this is also seen in calculation of T_c. However, the gap ratio remains a universal result.

We have considered the gap edge $\Delta_0(T)/\Delta_0(T=0)$ as a function of temperature to verify that for both weak-coupling BCS and Eliashberg theories there exists the same universal result as $\lambda \to 0$.

In addition, the free energy difference in the normal and superconducting state utilizing Eliashberg calculation is different from the BCS theory by a factor of $1/(\sqrt{e})^2$. Furtheremore, in the weak coupling limit, the heat capacity ratio of both BCS and Eliashberg theories are identical at all temperatures.

REFERENCES

[1] G. Rickayzen, *Theory of superconductivity*, Interscience monographs and texts in physics and astronomy, Vol. 14 (Interscience Publishers, 1965).

[2] E. Maxwell, Physical Review **78**, 477 (1950).

[3] C. Reynolds, B. Serin, and L. Nesbitt, Physical Review **84**, 691 (1951).

[4] J. R. Schrieffer, *Theory of superconductivity* (CRC Press, 2018).

[5] R. Parks, *Superconductivity: Part 1 (In Two Parts)*, Superconductivity (Taylor & Francis, 1969).

[6] G. Grimvall, *The electron-phonon interaction in metals*, Selected topics in solid state physics (North-Holland Pub. Co. : sole distributors for the U.S.A. and Canada, Elsevier North-Holland, 1981).

[7] P. B. Allen and B. Mitrović, in *Solid state physics*, Vol. 37 (Elsevier, 1983) pp. 1–92.

[8] A. Migdal, Sov. Phys. JETP **7**, 996 (1958).

[9] Y. Nambu, Physical Review **117**, 648 (1960).

[10] G. Eliashberg, Sov. Phys. JETP **11**, 696 (1960).

[11] V. Ambegaokar and L. Tewordt, Physical Review **134**, A805 (1964).

[12] D. Scalapino, Y. Wada, and J. Swihart, Physical Review Letters **14**, 102 (1965).

[13] W. McMillan, Physical Review **167**, 331 (1968).

[14] P. B. Allen and R. Dynes, Physical Review B **12**, 905 (1975).

[15] P. Morel and P. Anderson, Physical Review **125**, 1263 (1962).

[16] A. Karakozov, E. Maksimov, and S. Mashkov, Zh. Eksp. Teor. Fiz **68**, 1937 (1975).

[17] F. Marsiglio, M. Schossmann, and J. Carbotte, Physical Review B **37**, 4965 (1988).

[18] F. Marsiglio and J. P. Carbotte, Superconductivity , 73–162.

[19] G. A. Ummarino, Emergent Phenomena in Correlated Matter: Autumn School Organized by the Forschungszentrum Jülich and the German Research School for Simulation Sciences at Forschungszentrum Jülich 23-27 September 2013; Lecture Notes of the Autumn School Correlated Electrons 2013 **3** (2013).

[20] H. Vidberg and J. Serene, Journal of Low Temperature Physics **29**, 179 (1977).

[21] F. Marsiglio, Physical Review B **98**, 024523 (2018).

[22] A. Abrikosov, L. Gorkov, and I. E. Dzyaloshinskii, Dover, New-York (1975).

[23] B. Mitrović and J. Carbotte, Canadian journal of physics **61**, 784 (1983).

[24] A. L. Fetter and J. D. Walecka, *Quantum Theory of Many-Particle Systems* (McGraw-Hill, Boston, 1971).

[25] A. Larkin and A. Varlamov, *Theory of fluctuations in superconductors* (Clarendon Press, 2005).

[26] P. Coleman, *Introduction to many-body physics* (Cambridge University Press, 2015).

[27] P. Henrici, *Applied and Computational Complex analysis*, Vol. 3 (1923).

[28] M. Abramowitz and I. A. Stegun, *Handbook of mathematical functions: with formulas, graphs, and mathematical tables*, Vol. 55 (Courier Corporation, 1965).

[29] F. W. Olver, D. W. Lozier, R. F. Boisvert, and C. W. Clark, *NIST handbook of mathematical functions hardback and CD-ROM* (Cambridge university press, 2010).

[30] T. J. I. Bromwich, *Elementary Integrals: a Short Table* (1911).

[31] S. Mirabi, R. Boyack, and F. Marsiglio, Phys. Rev. B **101**, 064506 (2020).

[32] F. Marsiglio, *Eliashberg Theory and the High Tc Oxides*, Ph.D. thesis, Mc Master University (1988).

[33] F. Marsiglio and J. Carbotte, Physical Review B **43**, 5355 (1991).

[34] F. Marsiglio, "Eliashberg theory: a short review," (2019), arXiv:1911.05065 [cond-mat.supr-con].

[35] X. Zheng and D. Walmsley, Physical Review B **77**, 104510 (2008).

[36] C. Leavens, Physical Review B **29**, 5178 (1984).

[37] J. Bardeen and M. Stephen, Physical Review **136**, A1485 (1964).

[38] T. Tsuneto, "References and bibliography," in *Superconductivity and Superfluidity*, edited by M. Nakahara (Cambridge University Press, 1998) p. 198–206.

[39] H. Bruus, K. Flensberg, and O. U. Press, *Many-Body Quantum Theory in Condensed Matter Physics: An Introduction*, Oxford Graduate Texts (OUP Oxford, 2004).

[40] E. T. Whittaker and G. N. Watson, *A Course of Modern Analysis*, 4th ed., Cambridge Mathematical Library (Cambridge University Press, 1996).

[41] G. N. Watson, *A treatise on the theory of Bessel functions* (Cambridge university press, 1995).

[42] M. Tinkham, *Introduction to superconductivity* (Courier Corporation, 2004).

Appendix A: Equation of motion for the Green's functions

1. The single-particle Green's function

The equation of motion for the single-particle Green's function is [1]

$$-\left(\frac{\partial}{\partial\tau_1}+\xi_\mathbf{k}\right)G_\uparrow(\mathbf{k},\tau_1-\tau_2)=\delta(\tau_1-\tau_2)-\sum_{\mathbf{k}'}\left|g_{\mathbf{k}-\mathbf{k}'}\right|^2\int_0^\beta d\tau'D(\mathbf{k}-\mathbf{k}',\tau_1-\tau')$$
$$\times\{G(\mathbf{k}\uparrow\tau',\mathbf{k}'\uparrow\tau_1;\mathbf{k}\uparrow\tau_2,\mathbf{k}'\uparrow\tau')+G(-\mathbf{k}'\downarrow\tau',\mathbf{k}'\uparrow\tau_1;\mathbf{k}\uparrow\tau_2,-\mathbf{k}\downarrow\tau')\}. \tag{A.1}$$

We define the two-particle correlation function as

$$G(\alpha_1\tau_1,\alpha_2\tau_2;\alpha_3\tau_3,\alpha_4\tau_4)=G(\alpha_1,\tau_1-\tau_3)G(\alpha_2,\tau_2-\tau_4)\delta_{\alpha_1\alpha_3}\delta_{\alpha_2\alpha_4}-G(\alpha_1,\tau_1-\tau_4)G(\alpha_2,\tau_2-\tau_3)\delta_{\alpha_1\alpha_4}\delta_{\alpha_2\alpha_3}$$
$$+C(\alpha_1\tau_1,\alpha_2\tau_2;\alpha_3\tau_3,\alpha_4\tau_4). \tag{A.2}$$

Therefore,

$$G(\mathbf{k}\uparrow\tau',\mathbf{k}'\uparrow\tau_1;\mathbf{k}\uparrow\tau_2,\mathbf{k}'\uparrow\tau')=G_\uparrow(\mathbf{k},\tau'-\tau_2)G_\uparrow(\mathbf{k}',\tau_1-\tau')\delta_{\mathbf{k},\mathbf{k}}\delta_{\mathbf{k}',\mathbf{k}'}$$
$$-G_\uparrow(\mathbf{k},0)G_\uparrow(\mathbf{k}',\tau_1-\tau_2)\delta_{-\mathbf{k}',-\mathbf{k}}\delta_{\mathbf{k}',\mathbf{k}}+C(\mathbf{k}\uparrow\tau',\mathbf{k}'\uparrow\tau_1;\mathbf{k}\uparrow\tau_2,\mathbf{k}'\uparrow\tau'). \tag{A.3}$$

The last term of the above equation is zero because the second-order correlation function with parallel spin does not contribute. Similarly,

$$G(-\mathbf{k}'\downarrow\tau',\mathbf{k}'\uparrow\tau_1;\mathbf{k}\uparrow\tau_2,-\mathbf{k}\downarrow\tau')=0-G_\downarrow(\mathbf{k}',0)G_\uparrow(\mathbf{k}',\tau_1-\tau_2)\delta_{-\mathbf{k}',-\mathbf{k}}\delta_{\mathbf{k}',\mathbf{k}}$$
$$+C(-\mathbf{k}'\downarrow\tau',\mathbf{k}'\uparrow\tau_1;\mathbf{k}\uparrow\tau_2,-\mathbf{k}\downarrow\tau'). \tag{A.4}$$

Notice that $D(\mathbf{k}'-\mathbf{k},\tau-\tau')\delta_{\mathbf{k},\mathbf{k}'}=D(0,\tau-\tau')=0$; this removes the terms containing a Green's function at zero time argument [22, 24]. Substituting Eq.(A.3) and Eq.(A.4) in Eq.(A.1) we obtain

$$-\left(\frac{\partial}{\partial\tau_1}+\xi_\mathbf{k}\right)G_\uparrow(\mathbf{k},\tau_1-\tau_2)=\delta(\tau_1-\tau_2)+\sum_{\mathbf{k}'}\left|g_{\mathbf{k}-\mathbf{k}'}\right|^2\int_0^\beta d\tau'D(\mathbf{k}-\mathbf{k}',\tau_1-\tau')\times$$
$$\{G_\uparrow(\mathbf{k},\tau'-\tau_2)G_\uparrow(\mathbf{k}',\tau_1-\tau')+C(-\mathbf{k}'\downarrow\tau',\mathbf{k}'\uparrow\tau_1;\mathbf{k}\uparrow\tau_2,-\mathbf{k}\downarrow\tau')\}$$
$$+\mid g_0\mid^2\int d\tau'D(0,\tau-\tau')\{-G_\uparrow(\mathbf{k},0)G_\uparrow(\mathbf{k},\tau_1-\tau_2)-G_\downarrow(-\mathbf{k},0)G_\uparrow(\mathbf{k},\tau_1-\tau_2)\}. \tag{A.5}$$

After simplification one obtains

$$-\left(\frac{\partial}{\partial\tau_1}+\xi_\mathbf{k}\right)G_\uparrow(\mathbf{k},\tau_1-\tau_2)=\delta(\tau_1-\tau_2)-\sum_{\mathbf{k}'}\left|g_{\mathbf{k}-\mathbf{k}'}\right|^2\int_0^\beta d\tau'D(\mathbf{k}-\mathbf{k}',\tau_1-\tau')\times$$
$$\{G_\uparrow(\mathbf{k},\tau'-\tau_2)G_\uparrow(\mathbf{k}',\tau_1-\tau')+C(-\mathbf{k}'\downarrow\tau',\mathbf{k}'\uparrow\tau_1;\mathbf{k}\uparrow\tau_2,-\mathbf{k}\downarrow\tau')\}. \tag{A.6}$$

2. Two-particle Green's function

The two-particle Green's function equation is defined as [1]

$$G(\mathbf{k}_1\boldsymbol{\sigma}_1\tau_1,\mathbf{k}_2\boldsymbol{\sigma}_2\tau_2,\mathbf{k}_3\boldsymbol{\sigma}_3\tau_3,\mathbf{k}_4\boldsymbol{\sigma}_4\tau_4)\equiv\langle T_\tau c_{\mathbf{k}_1\boldsymbol{\sigma}_1}(\tau_1)c_{\mathbf{k}_2\boldsymbol{\sigma}_2}(\tau_2)c_{\mathbf{k}_4\boldsymbol{\sigma}_4}^\dagger(\tau_4)c_{\mathbf{k}_3\boldsymbol{\sigma}_3}^\dagger(\tau_3)\rangle. \tag{A.7}$$

Isolating the τ_1 dependence, one finds

$$
\begin{aligned}
G(\mathbf{k}_1\boldsymbol{\sigma}_1\tau_1, \mathbf{k}_2\boldsymbol{\sigma}_2\tau_2, \mathbf{k}_3\boldsymbol{\sigma}_3\tau_3, \mathbf{k}_4\boldsymbol{\sigma}_4\tau_4) =& \theta(\tau_1 - \tau_3)\langle T_\tau c_{\mathbf{k}_1\boldsymbol{\sigma}_1}(\tau_1) c^\dagger_{\mathbf{k}_3\boldsymbol{\sigma}_3}(\tau_3) c_{\mathbf{k}_2\boldsymbol{\sigma}_2}(\tau_2) c^\dagger_{\mathbf{k}_4\boldsymbol{\sigma}_4}(\tau_4)\rangle, \\
& - \theta(\tau_3 - \tau_1)\langle T_\tau c^\dagger_{\mathbf{k}_3\boldsymbol{\sigma}_3}(\tau_3) c_{\mathbf{k}_1\boldsymbol{\sigma}_1}(\tau_1) c_{\mathbf{k}_2\boldsymbol{\sigma}_2}(\tau_2) c^\dagger_{\mathbf{k}_4\boldsymbol{\sigma}_4}(\tau_4)\rangle \\
& - \theta(\tau_1 - \tau_4)\langle T_\tau c_{\mathbf{k}_1\boldsymbol{\sigma}_1}(\tau_1) c^\dagger_{\mathbf{k}_4\boldsymbol{\sigma}_4}(\tau_4) c_{\mathbf{k}_2\boldsymbol{\sigma}_2}(\tau_2) c^\dagger_{\mathbf{k}_3\boldsymbol{\sigma}_3}(\tau_3)\rangle \\
& + \theta(\tau_4 - \tau_1)\langle T_\tau c^\dagger_{\mathbf{k}_4\boldsymbol{\sigma}_4}(\tau_4) c_{\mathbf{k}_1\boldsymbol{\sigma}_1}(\tau_1) c_{\mathbf{k}_2\boldsymbol{\sigma}_2}(\tau_2) c^\dagger_{\mathbf{k}_3\boldsymbol{\sigma}_3}(\tau_3)\rangle. \quad \text{(A.8)}
\end{aligned}
$$

Here, T_τ is the time ordering operator. The time derivative of G with respect to τ_1 is

$$
\begin{aligned}
\frac{\partial}{\partial \tau_1} G(\mathbf{k}_1\boldsymbol{\sigma}_1\tau_1, \mathbf{k}_2\boldsymbol{\sigma}_2\tau_2; \mathbf{k}_3\boldsymbol{\sigma}_3\tau_3, \mathbf{k}_4\boldsymbol{\sigma}_4\tau_4) =& \delta(\tau_1 - \tau_3)\langle T_\tau \{c_{\mathbf{k}_1\boldsymbol{\sigma}_1}(\tau_1), c^\dagger_{\mathbf{k}_3\boldsymbol{\sigma}_3}(\tau_3)\} c_{\mathbf{k}_2\boldsymbol{\sigma}_2}(\tau_2) c^\dagger_{\mathbf{k}_4\boldsymbol{\sigma}_4}(\tau_4)\rangle, \\
& - \delta(\tau_1 - \tau_4)\langle T_\tau \{c_{\mathbf{k}_1\boldsymbol{\sigma}_1}(\tau_1), c^\dagger_{\mathbf{k}_4\boldsymbol{\sigma}_4}(\tau_4)\} c_{\mathbf{k}_2\boldsymbol{\sigma}_2}(\tau_2) c^\dagger_{\mathbf{k}_3\boldsymbol{\sigma}_3}(\tau_3)\rangle, \\
& + \langle T[H, c_{\mathbf{k}_1\boldsymbol{\sigma}_1}(\tau_1)] c_{\mathbf{k}_2\boldsymbol{\sigma}_2}(\tau_2) c^\dagger_{\mathbf{k}_4\boldsymbol{\sigma}_4}(\tau_4) c^\dagger_{\mathbf{k}_3\boldsymbol{\sigma}_3}(\tau_3)\rangle. \quad \text{(A.9)}
\end{aligned}
$$

The commutator in the third term of Eq.(A.9) is given in Eq.(2.10).

$$
\begin{aligned}
\frac{\partial}{\partial \tau_1} G(\mathbf{k}_1\boldsymbol{\sigma}_1\tau_1, \mathbf{k}_2\boldsymbol{\sigma}_2\tau_2; \mathbf{k}_3\boldsymbol{\sigma}_3\tau_3, \mathbf{k}_4\boldsymbol{\sigma}_4\tau_4) =& \delta(\tau_1 - \tau_3)\delta_{\mathbf{k}_1, \mathbf{k}_3}\langle T_\tau c_{\mathbf{k}_2\boldsymbol{\sigma}_2}(\tau_2) c^\dagger_{\mathbf{k}_4\boldsymbol{\sigma}_4}(\tau_4)\rangle, \\
& - \delta(\tau_1 - \tau_4)\delta_{\mathbf{k}_1, \mathbf{k}_4}\langle T_\tau c_{\mathbf{k}_2\boldsymbol{\sigma}_2}(\tau_2) c^\dagger_{\mathbf{k}_3\boldsymbol{\sigma}_3}(\tau_3)\rangle, \\
& - \xi_{\mathbf{k}_1}\langle T_\tau c_{\mathbf{k}_1\boldsymbol{\sigma}_1}(\tau_1) c_{\mathbf{k}_2\boldsymbol{\sigma}_2}(\tau_2) c^\dagger_{\mathbf{k}_4\boldsymbol{\sigma}_4}(\tau_4) c^\dagger_{\mathbf{k}_3\boldsymbol{\sigma}_3}(\tau_3)\rangle, \\
& - \sum_{\mathbf{k}'} g_{\mathbf{k}_1 - \mathbf{k}'}\langle T_\tau (b^\dagger_{\mathbf{k}_1, \mathbf{k}'} + b_{\mathbf{k}', \mathbf{k}_1}) \\
& \times c_{\mathbf{k}_1\boldsymbol{\sigma}_1}(\tau_1) c_{\mathbf{k}_2\boldsymbol{\sigma}_2}(\tau_2) c^\dagger_{\mathbf{k}_4\boldsymbol{\sigma}_4}(\tau_4) c^\dagger_{\mathbf{k}_3\boldsymbol{\sigma}_3}(\tau_3)\rangle. \quad \text{(A.10)}
\end{aligned}
$$

Therefore,

$$
\begin{aligned}
\left(\frac{\partial}{\partial \tau_1} + \xi_{\mathbf{k}_1}\right) G(\mathbf{k}_1\boldsymbol{\sigma}_1\tau_1, \mathbf{k}_2\boldsymbol{\sigma}_2\tau_2; \mathbf{k}_3\boldsymbol{\sigma}_3\tau_3, \mathbf{k}_4\boldsymbol{\sigma}_4\tau_4) =& - \delta(\tau_1 - \tau_3)G_{\boldsymbol{\sigma}_2}(\mathbf{k}_2, \tau_2 - \tau_4)\delta_{\mathbf{k}_1, \mathbf{k}_3}\delta_{\mathbf{k}_2, \mathbf{k}_4}\delta_{\boldsymbol{\sigma}_1\boldsymbol{\sigma}_3}\delta_{\boldsymbol{\sigma}_2\boldsymbol{\sigma}_4}, \\
& + \delta(\tau_1 - \tau_4)G_{\boldsymbol{\sigma}_2}(\mathbf{k}_2, \tau_2 - \tau_3)\delta_{\mathbf{k}_1, \mathbf{k}_4}\delta_{\mathbf{k}_2, \mathbf{k}_3}\delta_{\boldsymbol{\sigma}_1\boldsymbol{\sigma}_4}\delta_{\boldsymbol{\sigma}_2\boldsymbol{\sigma}_3}, \\
& - \sum_{\mathbf{k}'} g_{\mathbf{k}_1 - \mathbf{k}'}\langle T_\tau (b^\dagger_{\mathbf{k}_1, \mathbf{k}'} + b_{\mathbf{k}', \mathbf{k}_1}) \\
& \times c_{\mathbf{k}'\boldsymbol{\sigma}_1}(\tau_1) c_{\mathbf{k}_2\boldsymbol{\sigma}_2}(\tau_2) c^\dagger_{\mathbf{k}_4\boldsymbol{\sigma}_4}(\tau_4) c^\dagger_{\mathbf{k}_3\boldsymbol{\sigma}_3}(\tau_3)\rangle. \quad \text{(A.11)}
\end{aligned}
$$

where

$$
\langle T_\tau [b^\dagger_{\mathbf{k}, \mathbf{k}'}(\tau) + b_{\mathbf{k}', \mathbf{k}}(\tau)]\rangle = -g_{\mathbf{k}' - \mathbf{k}} \int d\tau' D(\mathbf{k} - \mathbf{k}', \tau - \tau')\langle c^\dagger_{\mathbf{k}'\uparrow}(\tau') c_{\mathbf{k}\uparrow}(\tau') + c^\dagger_{-\mathbf{k}\downarrow}(\tau') c_{-\mathbf{k}'\downarrow}(\tau')\rangle. \quad \text{(A.12)}
$$

3. Three-particle Green's function

The three-particle Green's function is defined as follows [1]

$$
\begin{aligned}
G_3(\alpha_1\tau_1, \alpha_2\tau_2, \alpha_3\tau_3; \alpha_4\tau_4, \alpha_5\tau_5, \alpha_6\tau_6) =\ & G(\alpha_1, \tau_1 - \tau_4)G(\alpha_2, \tau_2 - \tau_5)G(\alpha_3, \tau_3 - \tau_6)\delta_{\alpha_1\alpha_4}\delta_{\alpha_2\alpha_5}\delta_{\alpha_3\alpha_6} \\
& - G(\alpha_1, \tau_1 - \tau_4)G(\alpha_2, \tau_2 - \tau_6)G(\alpha_3, \tau_3 - \tau_5)\delta_{\alpha_1\alpha_4}\delta_{\alpha_2\alpha_6}\delta_{\alpha_3\alpha_5} \\
& + G(\alpha_1, \tau_1 - \tau_5)G(\alpha_2, \tau_2 - \tau_6)G(\alpha_3, \tau_3 - \tau_4)\delta_{\alpha_1\alpha_5}\delta_{\alpha_2\alpha_6}\delta_{\alpha_3\alpha_4} \\
& - G(\alpha_1, \tau_1 - \tau_5)G(\alpha_2, \tau_2 - \tau_4)G(\alpha_3, \tau_3 - \tau_6)\delta_{\alpha_1\alpha_5}\delta_{\alpha_2\alpha_4}\delta_{\alpha_3\alpha_6} \\
& + G(\alpha_1, \tau_1 - \tau_6)G(\alpha_2, \tau_2 - \tau_4)G(\alpha_3, \tau_3 - \tau_5)\delta_{\alpha_1\alpha_6}\delta_{\alpha_2\alpha_4}\delta_{\alpha_3\alpha_5} \\
& - G(\alpha_1, \tau_1 - \tau_6)G(\alpha_2, \tau_2 - \tau_5)G(\alpha_3, \tau_3 - \tau_4)\delta_{\alpha_1\alpha_6}\delta_{\alpha_2\alpha_5}\delta_{\alpha_3\alpha_4} \\
& + \frac{1}{2}G(\alpha_1, \tau_1 - \tau_4)C(\alpha_2\tau_2, \alpha_3\tau_3; \alpha_5\tau_5, \alpha_6\tau_6)\delta_{\alpha_1\alpha_4} \\
& - \frac{1}{2}G(\alpha_1, \tau_1 - \tau_4)C(\alpha_2\tau_2, \alpha_3\tau_3; \alpha_6\tau_6, \alpha_5\tau_5)\delta_{\alpha_1\alpha_4} \\
& + \frac{1}{2}G(\alpha_1, \tau_1 - \tau_5)C(\alpha_2\tau_2, \alpha_3\tau_3; \alpha_6\tau_6, \alpha_4\tau_4)\delta_{\alpha_1\alpha_5} \\
& - \frac{1}{2}G(\alpha_1, \tau_1 - \tau_5)C(\alpha_2\tau_2, \alpha_3\tau_3; \alpha_4\tau_4, \alpha_6\tau_6)\delta_{\alpha_1\alpha_5} \\
& + \frac{1}{2}G(\alpha_1, \tau_1 - \tau_6)C(\alpha_2\tau_2, \alpha_3\tau_3; \alpha_4\tau_4, \alpha_5\tau_5)\delta_{\alpha_1\alpha_6} \\
& - \frac{1}{2}G(\alpha_1, \tau_1 - \tau_6)C(\alpha_2\tau_2, \alpha_3\tau_3; \alpha_5\tau_5, \alpha_4\tau_4)\delta_{\alpha_1\alpha_6} \\
& + C(\alpha_1\tau_1, \alpha_2\tau_2, \alpha_3\tau_3; \alpha_4\tau_4, \alpha_5\tau_5, \alpha_6\tau_6)
\end{aligned}
\tag{A.13}
$$

The two-particle Green's function equation of motion is

$$
\begin{aligned}
G(\mathbf{k}_1 \uparrow \tau_1, -\mathbf{k}_1 \downarrow \tau_2; \mathbf{k}_2 \uparrow \tau_3, -\mathbf{k}_2 \downarrow \tau_4) =\ & C(\mathbf{k}_1 \uparrow \tau_1, -\mathbf{k}_1 \downarrow \tau_2; \mathbf{k}_2 \uparrow \tau_3, -\mathbf{k}_2 \downarrow \tau_4) \\
& + G_\uparrow(\mathbf{k}_1, \tau_1 - \tau_3)G_\downarrow(-\mathbf{k}_1, \tau_2 - \tau_4)\delta_{\mathbf{k}_1,\mathbf{k}_2}\delta_{-\mathbf{k}_1,-\mathbf{k}_2}.
\end{aligned}
\tag{A.14}
$$

The time derivative of the above equation with respect to τ_1 is written as

$$
\begin{aligned}
& \left(\frac{\partial}{\partial\tau_1} + \xi_{\mathbf{k}_1}\right) C(\mathbf{k}_1 \uparrow \tau_1, -\mathbf{k}_1 \downarrow \tau_2; \mathbf{k}_2 \uparrow \tau_3, -\mathbf{k}_2 \downarrow \tau_4) \\
=\ & \left(\frac{\partial}{\partial\tau_1} + \xi_{\mathbf{k}_1}\right) G(\mathbf{k}_1 \uparrow \tau_1, -\mathbf{k}_1 \downarrow \tau_2; \mathbf{k}_2 \uparrow \tau_3, -\mathbf{k}_2 \downarrow \tau_4) \\
& - \left(\frac{\partial}{\partial\tau_1} + \xi_{\mathbf{k}_1}\right) G_\uparrow(\mathbf{k}_1, \tau_1 - \tau_3)G_\downarrow(-\mathbf{k}_1, \tau_2 - \tau_4)\delta_{\mathbf{k}_1,\mathbf{k}_2}\delta_{-\mathbf{k}_1,-\mathbf{k}_2}.
\end{aligned}
\tag{A.15}
$$

Then, we expand the second term in Eq.(A.15) to obtain

$$
\begin{aligned}
& \left(\frac{\partial}{\partial\tau_1} + \xi_{\mathbf{k}_1}\right) C(\mathbf{k}_1 \uparrow \tau_1, -\mathbf{k}_1 \downarrow \tau_2; \mathbf{k}_2 \uparrow \tau_3, -\mathbf{k}_2 \downarrow \tau_4) \\
=\ & \left(\frac{\partial}{\partial\tau_1} + \xi_{\mathbf{k}_1}\right) G(\mathbf{k}_1 \uparrow \tau_1, -\mathbf{k}_1 \downarrow \tau_2, \mathbf{k}_2 \uparrow \tau_3, -\mathbf{k}_2 \downarrow \tau_4) \\
& - G_\downarrow(-\mathbf{k}_1, \tau_2 - \tau_4)\delta_{\mathbf{k}_1,\mathbf{k}_2}\delta_{-\mathbf{k}_1,-\mathbf{k}_2} \left(\frac{\partial}{\partial\tau_1} + \xi_{\mathbf{k}_1}\right) G_\uparrow(\mathbf{k}_1, \tau_1 - \tau_3) \\
& - G_\uparrow(\mathbf{k}_1, \tau_1 - \tau_3)\delta_{\mathbf{k}_1,\mathbf{k}_2}\delta_{-\mathbf{k}_1,-\mathbf{k}_2} \left(\frac{\partial}{\partial\tau_1} + \xi_{\mathbf{k}_1}\right) G_\downarrow(-\mathbf{k}_1, \tau_2 - \tau_4).
\end{aligned}
\tag{A.16}
$$

To calculate the second term in the above equation we can use

$$-\left(\frac{\partial}{\partial\tau_1}+\xi_{\mathbf{k}_1}\right)G_\uparrow(\mathbf{k}_1,\tau_1-\tau_3)$$

$$=\delta(\tau_1-\tau_3)+\sum_{\mathbf{k}'}\left|g_{\mathbf{k}_1-\mathbf{k}'}\right|^2\int_0^\beta d\tau'D(\mathbf{k}_1-\mathbf{k}',\tau_1-\tau')\times$$

$$[G_\uparrow(\mathbf{k}',\tau_1-\tau')G_\uparrow(\mathbf{k}_1,\tau'-\tau_3)+C(-\mathbf{k}'\downarrow\tau',\mathbf{k}'\uparrow\tau_1;\mathbf{k}_1\uparrow\tau_3,-\mathbf{k}_1\downarrow\tau')]. \tag{A.17}$$

Also, we can replace the first term in Eq.(A.15) with

$$\left(\frac{\partial}{\partial\tau_1}+\xi_{\mathbf{k}_1}\right)G(\mathbf{k}_1\uparrow\tau_1,-\mathbf{k}_1\downarrow\tau_2;\mathbf{k}_2\uparrow\tau_3,-\mathbf{k}_2\downarrow\tau_4)$$

$$=-\delta(\tau_1-\tau_3)G_\downarrow(-\mathbf{k}_1,\tau_2-\tau_4)\delta_{\mathbf{k}_1,\mathbf{k}_2}$$

$$+\sum_{\mathbf{k}'}\left|g_{\mathbf{k}_1-\mathbf{k}'}\right|^2\int d\tau'D(\mathbf{k}_1-\mathbf{k}',\tau_1-\tau')\times$$

$$\left[G(\mathbf{k}'\uparrow\tau_1,\mathbf{k}_1\uparrow\tau',-\mathbf{k}_1\downarrow\tau_2;\mathbf{k}'\uparrow\tau',\mathbf{k}_2\uparrow\tau_3,-\mathbf{k}_2\downarrow\tau_4)\right.$$

$$\left.+G(-\mathbf{k}_1\downarrow\tau_2,\mathbf{k}'\uparrow\tau_1,-\mathbf{k}'\downarrow\tau';-\mathbf{k}_1\downarrow\tau',\mathbf{k}_2\uparrow\tau_3,-\mathbf{k}_2\downarrow\tau_4)\right]. \tag{A.18}$$

Substituting Eq.(A.17) and Eq.(A.18) in Eq.(A.16) one obtains

$$\left(\frac{\partial}{\partial\tau_1}+\xi_{\mathbf{k}_1}\right)C(\mathbf{k}_1\uparrow\tau_1,-\mathbf{k}_1\downarrow\tau_2;\mathbf{k}_2\uparrow\tau_3,-\mathbf{k}_2\downarrow\tau_4)$$

$$=-\sum_{\mathbf{k}'}\left|g_{\mathbf{k}_1-\mathbf{k}'}\right|^2\int d\tau'D(\mathbf{k}_1-\mathbf{k}',\tau_1-\tau')\times$$

$$\{G_\uparrow(\mathbf{k}',\tau_1-\tau')C(\mathbf{k}_1\uparrow\tau',-\mathbf{k}_1\downarrow\tau_2;\mathbf{k}_2\uparrow\tau_3,-\mathbf{k}_2\downarrow\tau_4)$$

$$+G_\downarrow(-\mathbf{k}_1,\tau_2-\tau')C(\mathbf{k}'\uparrow\tau_1,-\mathbf{k}'\downarrow\tau';\mathbf{k}_2\uparrow\tau_3,-\mathbf{k}_2\downarrow\tau_4)\}. \tag{A.19}$$

Appendix B: Nambu's Green function method

The theory of normal metals breaks down below the superconducting transition temperature, and Nambu's formalism is helpful in diagonalizing the Hamiltonian. The Nambu's formalisim is defined by Nambu's spinors as a two component electron-field operators $\psi_{\mathbf{k}}(\tau)$ and $\psi_{\mathbf{k}}^\dagger(\tau)$ with imaginary time τ as follows:

$$\psi_k(\tau)=\begin{pmatrix}c_{\mathbf{k}\uparrow}(\tau)\\c_{-\mathbf{k}\downarrow}^\dagger(\tau)\end{pmatrix}, \tag{B.1}$$

and

$$\psi_{\mathbf{k}}^\dagger(\tau)=\begin{pmatrix}c_{\mathbf{k}\uparrow}^\dagger(\tau) & c_{-\mathbf{k}\downarrow}(\tau)\end{pmatrix}. \tag{B.2}$$

The nambu Green's function is written as a matrix applying the spinors. The Pauli matrices in Nambu space are shown by τ. The thermodynamic electron Green's function is defined as

$$G(\mathbf{k},\tau)=-\langle T\psi_{\mathbf{k}}(\tau)\psi_{\mathbf{k}}^\dagger(0)\rangle=\begin{pmatrix}G_{\uparrow\uparrow}(\mathbf{k},\tau) & F_{\downarrow\uparrow}^\dagger(\mathbf{k},\tau)\\F_{\downarrow\uparrow}(\mathbf{k},\tau) & G_{\downarrow\downarrow}^\dagger(-\mathbf{k},\tau)\end{pmatrix}, \tag{B.3}$$

where G_{11} and G_{22} are the normal Green's function and G_{12} and G_{21} are the anomalous Green's function. The equation of motion is

$$\partial_\tau G(\mathbf{k}, \tau) = -\delta \begin{pmatrix} 1 & 0 \\ 0 & 1 \end{pmatrix} - \begin{pmatrix} \xi_\mathbf{k} & -\Delta_\mathbf{k} \\ -\Delta_\mathbf{k}^\dagger & -\xi_\mathbf{k} \end{pmatrix} G(\mathbf{k}, \tau). \tag{B.4}$$

By Fourier transformation and matrix inversion one obtains

$$\partial_\tau G(\mathbf{k}, i\omega_k) = \frac{1}{(i\omega_k)^2 - E_k^2} \begin{pmatrix} i\omega_k + \xi_\mathbf{k} & -\Delta_\mathbf{k} \\ -\Delta_\mathbf{k}^\dagger & i\omega_k - \xi_\mathbf{k} \end{pmatrix}, \tag{B.5}$$

where $E_\mathbf{k} = \sqrt{\xi_\mathbf{k}^2 + \Delta_\mathbf{k}^2}$ [5, 9, 39].

Appendix C: Properties of the gamma and digamma functions

1. Euler gamma function

The definition of Gamma function is [40]

$$\Gamma(z) = \int_0^\infty t^{z-1} e^{-t} dt. \tag{C.1}$$

Here, Γ is defined for all complex $z \in \mathbb{C}$ excluding negative integer values of z.

2. Digamma function

The definition of digamma function is [40]

$$\psi(z) = \frac{d \log \Gamma(z)}{dz}, \tag{C.2}$$

where the Γ function obeys the identity

$$\Gamma(z+1) = z\Gamma(z). \tag{C.3}$$

Several useful asymptotic expressions for the digmma function are shown here. For the large argument of $z \gg 1$,

$$\psi(z) \approx \ln z - \frac{1}{2z} - \frac{1}{12z^2}, \tag{C.4}$$

$$\psi\left(\frac{1}{2} + z\right) \approx \ln z + \frac{1}{24z^2}. \tag{C.5}$$

Furthermore, the functional relation can be written as

$$\psi(1+z) - \psi(z) = \frac{1}{z}, \tag{C.6}$$

$$\psi(1-z) - \psi(z) = \pi \cot(\pi z), \tag{C.7}$$

$$\psi\left(\frac{1}{2}+iz\right) - \psi\left(\frac{1}{2}-iz\right) = \pi i \tanh \pi z, \tag{C.8}$$

$$\psi\left(\frac{1}{2}-z\right) - \psi\left(\frac{1}{2}+z\right) = -\pi \tan \pi z, \tag{C.9}$$

$$-\psi(1) = \gamma = 0.577216.., \tag{C.10}$$

where $\gamma \approx 0.577216$ is the Euler-Mascheroni constant.

$$\psi\left(\frac{1}{2}\right) = -2\log(2) - \gamma, \tag{C.11}$$

The digamma summation relation is

$$\sum_{m=0}^{N} \frac{1}{a+m} = \psi(a+N+1) - \psi(a). \tag{C.12}$$

From this equation it then follows

$$\sum_{m=0}^{\infty}\left(\frac{1}{m+a} - \frac{1}{m+b}\right) = \lim_{N\to\infty}[\psi(a+N+1) - \psi(a) - \psi(b+N+1) + \psi(b)],$$
$$= \psi(b) - \psi(a). \tag{C.13}$$

Appendix D: Properties of BCS theory

1.   Zero-temperature gap function

In this subsection, we obtain information about the dependence of the magnitude of the gap in the excitation spectrum [24]. In BCS theory, $\Delta(\mathbf{k}, i\omega_n)$ is replaced with $\Delta(\mathbf{k})$. Hence, the gap function and phonon propagator are independent of frequency. Then, Eq.(2.47) can be written as

$$\Delta(\mathbf{k}) = \sum_{\mathbf{k}'}\left|g_{\mathbf{k}-\mathbf{k}'}\right|^2 D(\mathbf{k} - \mathbf{k}')\Delta(\mathbf{k}')\sum_{n'}\frac{1}{\omega_{n'}^2 + \xi_{\mathbf{k}'}^2 + \Delta_{\mathbf{k}'}},$$
$$= \frac{\beta}{2}\sum_{\mathbf{k}'}\left|g_{\mathbf{k}-\mathbf{k}'}\right|^2 D(\mathbf{k} - \mathbf{k}')\Delta(\mathbf{k}')\frac{\tanh(\frac{1}{2}\beta(\xi'^2 + \Delta'^2)^{1/2})}{(\xi'^2 + \Delta'^2)^{1/2}}, \tag{D.1}$$

where $E_{\mathbf{k}} = \sqrt{(\epsilon_{\mathbf{k}} - \mu)^2 + \Delta(\mathbf{k})^2}$ is the quasi-particle energy in the superconducting state. This is shown in Fig.(D.1). We assume $\mid g_{\mathbf{k}-\mathbf{k}'}\mid^2 D(\mathbf{k} - \mathbf{k}')$ as the form of the interaction. The BCS gap equation is

$$\Delta(\mathbf{k}) = \frac{\beta}{2}\sum_{\mathbf{k}'}V_{\mathbf{k},\mathbf{k}'}\Delta(\mathbf{k}')\frac{\tanh(\frac{1}{2}\beta E_{\mathbf{k}})}{2E_{\mathbf{k}}}, \tag{D.2}$$

where $V_{\mathbf{k},\mathbf{k}'}$ is the pairing interaction and we assume $V_{\mathbf{k},\mathbf{k}'} = -|V|$. Here, V is a positive constant. We convert Eq.(D.2) into an integration over ξ by making the replacement

$$\sum_{\mathbf{k}'} \to N(\epsilon_F)\int d\xi$$
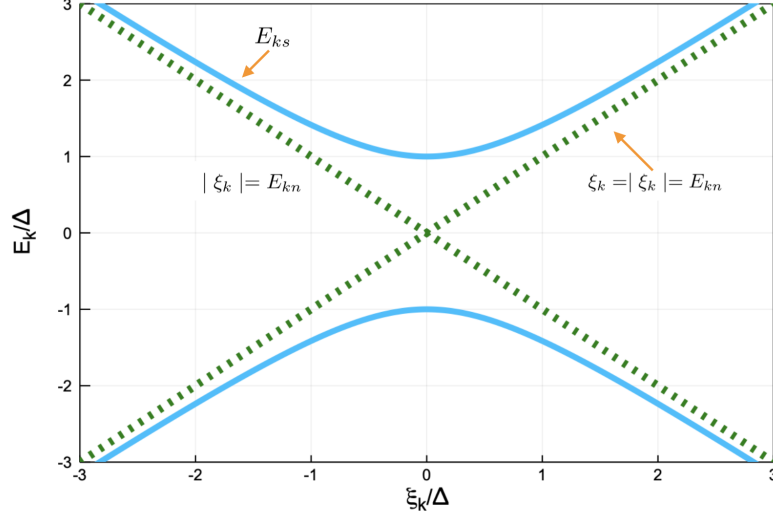
Figure D.1. The plot of the excitation spectrum in the superconducting and normal states.

The density of state is approximated by a constant around the Fermi surface.

$$\frac{1}{\lambda} = \int_0^{\omega_D} \frac{d\xi}{E} \left(1 - \frac{2}{\exp(\beta E) + 1}\right). \tag{D.3}$$

where $\lambda \equiv N(\epsilon_F)|V|$. We first consider the $T = 0$ case

$$\frac{1}{\lambda} = 2\int_0^{\omega_D} \frac{d\xi}{\sqrt{\xi^2 + \Delta^2}}. \tag{D.4}$$

We write

$$\frac{1}{\lambda} = 2\int_{|\Delta|}^{\omega_D + (\omega_D^2 + \Delta^2)^{1/2}} \frac{dy}{2y} = \log\left(\frac{\omega_D + (\omega_D^2 + \Delta_0^2)^{1/2}}{\Delta_0}\right). \tag{D.5}$$

In the weak coupling limit, $\omega_D \gg \Delta_0$, so this becomes

$$\frac{1}{\lambda} = \log\left(\frac{2\omega_D}{\Delta_0}\right). \tag{D.6}$$

Therefore, the zero temperature gap is given by

$$\Delta_0 = 2\omega_D \exp\left(-\frac{1}{\lambda}\right), \tag{D.7}$$

which is shown in Fig.(D.2). The energy gap Δ_0 depends on the eletron-phonon coupling λ and the Debye energy. In order to have strong superconductivity with a high transition temperature, strong electron-phonon coupling with a large Debye frequency is one possible mechanism. The zero-temperature gap in BCS theory is

$$\frac{2\Delta_0}{k_B T_c} = 3.53. \tag{D.8}$$

80
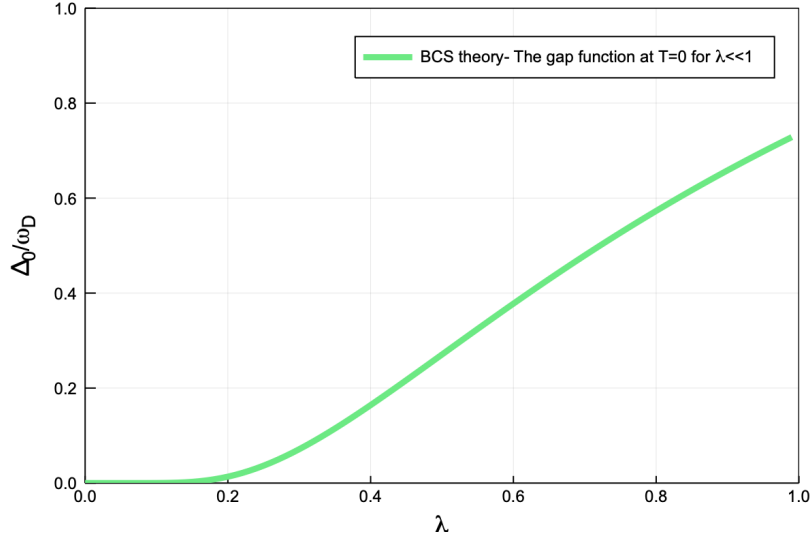
Figure D.2. In the BCS theory, superconductivity is suppressed exponentially at $\lambda \ll 1$.

For many superconductors this value is valid. However, for the strong coupling superconductors this ratio is 4.3 and 4.6 for Pb and Hg respectively [5].

2. Gap function close to T_c

Now we consider the finite temperature case [22]

$$\frac{1}{\lambda} = 2 \int_0^{\omega_D} \frac{d\xi}{2E} \left(1 - \frac{2}{\exp(\beta E) + 1} \right). \tag{D.9}$$

In the second integral we extend the range of integration as follows:

$$\begin{aligned}
\frac{1}{\lambda} &= 2 \int_0^{\omega_D} \frac{d\xi}{\sqrt{\xi^2 + \Delta^2}} - 2 \int_\Delta^\infty \frac{\frac{dE}{\xi}}{\exp(\beta E) + 1} \\
&= \log\left(\frac{\omega_D + \sqrt{\omega_D^2 + \Delta^2}}{\Delta} \right) - 2 \int_1^\infty \frac{dx}{\sqrt{x^2 - 1}} \exp(-\beta \Delta x) \sum_{n=0}^\infty (-1)^n \exp(-n\beta \Delta x) \\
&= \log\left(\frac{\omega_D + \sqrt{\omega_D^2 + \Delta^2}}{\Delta} \right) - 2 \sum_{n=1}^\infty (-1)^{n+1} \int_1^\infty dx \frac{e^{-n\beta \Delta x}}{\sqrt{x^2 - 1}}. \tag{D.10}
\end{aligned}$$

In the weak-coupling limit $\omega_D \gg \Delta$, one writes

$$\frac{1}{\lambda} = \log\left(\frac{2\omega_D}{\Delta_0} \frac{\Delta_0}{\Delta} \right) - 2 \sum_{n=1}^\infty (-1)^{n+1} K_0\left(\frac{n\Delta}{T}. \right) \tag{D.11}$$

$$\log\left(\frac{\Delta_0}{\Delta} \right) = 2 \sum_{n=1}^\infty (-1)^{n+1} K_0\left(\frac{n\Delta}{T} \right). \tag{D.12}$$

81

Now solving for the gap function we obtain

$$\Delta = \Delta_0 - \sqrt{2\pi T\Delta_0}\left(1 - \frac{T}{8\Delta_0}\right)e^{-\Delta_0/T}. \tag{D.13}$$

The νth order modified Bessel function of the second order can be calculated as [14]

$$K_\nu(z) = \frac{\Gamma(1/2)(z/2)^\nu}{\Gamma(\nu+1/2)}\int_1^\infty dt\,\exp(-zt)(t^2-1)^{\nu-1/2}. \tag{D.16}$$

Utilizing this result the gap function is

$$1/\lambda = \log\left(\frac{\omega_D + \sqrt{\omega_D^2 + \Delta^2}}{\Delta}\right) - 2\sum_{n=1}^\infty (-1)^{n+1}K_0\left(\frac{n\Delta}{T}\right). \tag{D.17}$$

In the weak-coupling limit $\omega_D \gg \Delta$,

$$\frac{1}{\lambda} = \log\left(\frac{2\omega_D}{\Delta_0}\frac{\Delta_0}{\Delta}\right) - 2\sum_{n=1}^\infty (-1)^{n+1}K_0\left(\frac{n\Delta}{T}\right). \tag{D.18}$$

Solving for the gap function we get

$$\Delta = \Delta_0 - \sqrt{2\pi T\Delta_0}\left(1 - \frac{T}{8\Delta_0}\right)e^{-\Delta_0/T}. \tag{D.19}$$

The temperature dependent gap equation near the transition temperature can be calculated as follows [22]:

$$\frac{1}{\lambda} \approx T\sum_{\omega_n}\int_{-\omega_D}^{\omega_D}\frac{d\xi}{(\omega_n^2+\xi^2)}\left[1 - \frac{\Delta^2}{(\omega_n^2+\xi^2)} + \frac{\Delta^4}{(\omega_n^2+\xi^2)^2}\right]. \tag{D.20}$$

After calculating the integration in Eq.(D.20) we obtain

$$\frac{1}{\lambda} = T\sum_{\omega_n}\frac{\pi}{|\omega_n|} - T\Delta^2\sum_{\omega_n}\frac{\pi}{2|\omega_n|^3} + T\Delta^4\sum_{\omega_n}\frac{3\pi}{8|\omega_n|^5}. \tag{D.21}$$

Substituting $\omega_n = \pi T(2n+1)$ in the above equation, we obtain

$$\frac{1}{\lambda} = \sum_{n=0}^N\frac{1}{n+1/2} - \left(\frac{\Delta}{\pi T}\right)^2\sum_{n=0}^N\frac{1}{(2n+1)^3} + \frac{3}{4}\left(\frac{\Delta}{\pi T}\right)^4\sum_{n=0}^N\frac{1}{(2n+1)^5}. \tag{D.22}$$

The summation in the first term of Eq.(D.22) can be easily done using digamma functions. In the asymptotic limit, $z \to \infty$, $\psi(z) \to \log z$. Now, we consider the critical temperature solution in the BCS theory. At transition temperature, the gap vanishes ($\Delta = 0$), then $E_\mathbf{k} = \xi_\mathbf{k}$. We compute

---

[14]When $T \ll \Delta$, the asymptotic expansion for the νth order modified Bessel functions for the second kind can be written as [41] :

$$K_\nu(z) \sim \left(\frac{\pi}{2z}\right)^{1/2}e^{-z}\left[1 + \frac{4\nu^2 - 1^2}{1!8z} + \frac{(4\nu^2-1)(4\nu^2-3^2)}{2!(8z)^2} + \dots\right], \tag{D.14}$$

So that,

$$K_0(z) \sim \left(\frac{\pi}{2z}\right)^{1/2}e^{-z}\left[1 - \frac{1^2}{1!8z} + \frac{1^2.3^2}{2!(8z)^2} + \dots\right]. \tag{D.15}$$

$$\frac{1}{\lambda} = T \sum_{\omega_n} \int_{\infty}^{\infty} \frac{d\xi}{\omega_n^2 + \xi_{\mathbf{k}}^2} = T\pi \sum_{\omega_n} \frac{1}{|\omega_n|},$$

$$= 2\pi T \sum_{n=0}^{N} \frac{1}{2\pi T(n + 1/2)} = T \sum_{n=0}^{N} \frac{1}{(n + 1/2)}. \tag{D.23}$$

We use the property of digamma function to write the critical-temperature result as follows:

$$k_B T_c = \frac{2\hbar\omega_D \exp(\gamma)}{\pi} \exp\left(-1/\lambda\right). \tag{D.24}$$

Applying the $T = T_c$ result, we obtain

$$\log\left(\frac{2\omega_D e^\gamma}{T_c}\right) = \log\left(\frac{2\omega_D e^\gamma}{T}\right) - \frac{\Delta^2}{(\pi T)^2} \sum_{n=0}^{\infty} \frac{1}{(2n+1)^3} + \frac{3\Delta^4}{4(\pi T)^4} \sum_{n=0}^{\infty} \frac{1}{(2n+1)^5}. \tag{D.25}$$

The second and third summations can be solved using the Riemann-zeta function [41]

$$\log\left(\frac{T}{T_c}\right) = -\frac{\Delta^2}{(\pi T)^2} \sum_{n=0}^{\infty} \frac{1}{(2n+1)^3} + \frac{3\Delta^4}{4(\pi T)^4} \sum_{n=0}^{\infty} \frac{1}{(2n+1)^5},$$

$$= -\frac{7\zeta(3)}{8} \left(\frac{\Delta}{\pi T}\right)^2 + \frac{93\zeta(5)}{128} \left(\frac{\Delta}{\pi T}\right)^4. \tag{D.26}$$

Furthermore,

$$\sum_{n=0}^{\infty} \frac{1}{(2n+1)^z} = \left(\frac{2^z - 1}{2^z}\right) \zeta(z). \tag{D.27}$$

where

$$\zeta(z) = \sum_{n=0}^{\infty} \frac{1}{(n+1)^z}.$$

Solving for the gap equation close to the critical-temperature we obtain

$$\Delta(T) = \pi T_c \sqrt{\frac{8}{7\zeta(3)}} \sqrt{\frac{T_c - T}{T_c}}. \tag{D.28}$$

The finite-temperature gap function can be written as

$$\frac{1}{\lambda} = \int d\xi \frac{\tanh\left(\left(\frac{\Delta_0}{2T_c}/\frac{T}{T_c}\right)\sqrt{(\frac{\xi}{\Delta_0})^2 + (\frac{\Delta}{\Delta_0})^2}\right)}{\Delta_0 \sqrt{(\frac{\xi}{\Delta_0})^2 + (\frac{\Delta}{\Delta_0})^2}}, \tag{D.29}$$

and the zero temperature gap function is

$$\frac{1}{\lambda} = \int d\xi \frac{1}{\Delta_0 \sqrt{(\frac{\xi}{\Delta_0})^2 + 1}}, \tag{D.30}$$

If we subtract the finite-temperature BCS energy gap from the zero-temperature gap function, it becomes

83

$$1 - \left[\left(\sqrt{(2\pi\Delta_0 T)} \exp(-\Delta_0/T) \right) / \Delta_0 \right]$$

$$1.74 \left(1 - \frac{T}{T_c} \right)^{1/2}$$
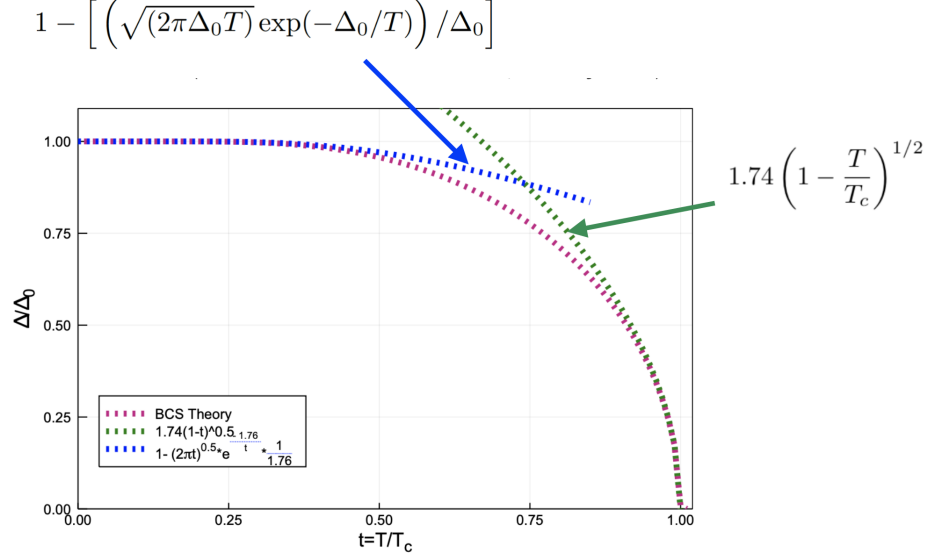
Figure D.3. Reduced gap function versus the reduced temperature using BCS theory.

$$\int_0^\infty dx \left[\frac{\tanh\left(\left(\frac{\Delta_0}{2T_c} / \frac{T}{T_c} \right) \sqrt{x^2 + (\Delta/\Delta_0)^2} \right)}{\sqrt{x^2 + (\Delta/\Delta_0)^2}} - \frac{1}{\sqrt{x^2 + 1}} \right] = 0. \tag{D.31}$$

We set $\xi = x/\Delta_0$, and substitute $2\Delta_0/k_B T_c = 3.53$ in Eq.(D.31). Figure.(D.3) represents Δ/Δ_0 vs. T/T_c. The red dotted curve shows the behavior of the energy gap, which is a universal function of T/T_c. The gap function decreases from 1 at $T = 0$, so the hyperbolic tangent becomes unity, which means that the energy gap is constant until the quasi-particles become thermally excited. Near T_c, the gap drops to zero [42]. This integral converges to zero very fast at higher energies.

Appendix E: Units of Free energy

The free energy difference is

$$\frac{\Delta F}{N(0)} = -2\pi T \sum_{m=0}^{\infty} \left(\sqrt{\omega_m^2 + \tilde{\Delta}^2(i\omega_m)} - \omega_m \right) \left(1 - \frac{\omega_m}{\sqrt{\omega_m^2 + \tilde{\Delta}^2(i\omega_m)}} \right), \tag{E.1}$$

Here, $\tilde{\Delta} = \Delta\alpha$.

$$\frac{\Delta F}{N(0)} = -2\pi T \sum_{m=0}^{\infty} \left(\sqrt{\omega_m^2 + \Delta^2(i\omega_m)\alpha^2} - \omega_m \right) \left(1 - \frac{\omega_m}{\sqrt{\omega_m^2 + \Delta^2(i\omega_m)\alpha^2}} \right)$$

$$= -2\pi T \alpha \sum_{m=0}^{\infty} \left(\sqrt{\left(\omega_m/\alpha\right)^2 + \Delta^2(i\omega_m)} - \frac{\omega_m}{\alpha} \right) \left(1 - \frac{\omega_m/\alpha}{\sqrt{\left(\omega_m/\alpha\right)^2 + \Delta^2(i\omega_m)}} \right)$$

$$= -2\pi T \alpha \sum_{m=0}^{\infty} \left(\sqrt{\left[(2m+1)\pi \frac{T}{T_c}\frac{T_c}{\alpha}\right]^2 + \Delta^2(i\omega_m)} - (2m+1)\pi\frac{T}{T_c}\frac{T_c}{\alpha} \right)$$

$$\times \left(1 - (2m+1)\frac{T}{T_c}\frac{T_c}{\alpha} \frac{1}{\sqrt{\left(2m+1)\pi \frac{T}{T_c}\frac{T_c}{\alpha}\right)^2 + \Delta^2(i\omega_m)}} \right). \tag{E.2}$$

Now if we set

$$\frac{T_c}{\alpha} = \frac{T_c}{\omega_E},$$

and

$$\bar{\omega}_m = \pi t (2m+1) T_c / \omega_E.$$

$$\frac{\Delta F}{N(0)T_c^2} = -2\pi \frac{\omega_E}{T_c} t \sum_{m=0}^{\infty} \left(\sqrt{\left(\pi t(2m+1)T_c/\omega_E\right)^2 + \Delta^2(i\omega_m)} - \frac{(\pi t(2m+1)T_c)}{\omega_E} \right)$$

$$\times \left(1 - \frac{(\pi t(2m+1)T_c)/\omega_E}{\sqrt{\left((\pi t(2m+1)T_c)/\omega_E\right)^2 + \Delta^2(i\omega_m)}} \right).$$

This equation is used in obtaining the Eliashberg result. If we are interested in BCS theory, we set $\alpha = \Delta_0$, where $\Delta_0 = \pi \exp(-\gamma) T_c$. Thus,

$$\frac{T_c}{\alpha} = \frac{T_c}{\pi \exp(-\gamma)T_c} = \frac{\exp(\gamma)}{\pi} \approx \frac{1}{1.76}. \tag{E.3}$$

Then, we obtain

$$\frac{\Delta F}{N(0)T_c^2} = -(2\pi \times 1.76)t \sum_{m=0}^{\infty} \left(\sqrt{\left(\pi t(2m+1)/1.76\right)^2 + \Delta^2(i\omega_m)} - \frac{(\pi t(2m+1))}{1.76} \right)$$

$$\times \left(1 - \frac{(\pi t(2m+1))/\omega_E}{\sqrt{\left((\pi t(2m+1))/1.76\right)^2 + \Delta^2(i\omega_m)}} \right). \tag{E.4}$$